

VU Research Portal

Risk Modeling and Treatment Planning: a Breast Cancer Case

Chen, W.

2016

document version

Publisher's PDF, also known as Version of record

[Link to publication in VU Research Portal](#)

citation for published version (APA)

Chen, W. (2016). *Risk Modeling and Treatment Planning: a Breast Cancer Case*. [PhD-Thesis – Research external, graduation internal, Vrije Universiteit Amsterdam].

General rights

Copyright and moral rights for the publications made accessible in the public portal are retained by the authors and/or other copyright owners and it is a condition of accessing publications that users recognise and abide by the legal requirements associated with these rights.

- Users may download and print one copy of any publication from the public portal for the purpose of private study or research.
- You may not further distribute the material or use it for any profit-making activity or commercial gain
- You may freely distribute the URL identifying the publication in the public portal

Take down policy

If you believe that this document breaches copyright please contact us providing details, and we will remove access to the work immediately and investigate your claim.

E-mail address:

vuresearchportal.ub@vu.nl

VRIJE UNIVERSITEIT

Risk Modeling and Treatment Planning: a Breast Cancer Case

ACADEMISCH PROEFSCHRIFT

ter verkrijging van de graad Doctor aan
de Vrije Universiteit Amsterdam,
op gezag van de rector magnificus
prof.dr. V. Subramaniam,
in het openbaar te verdedigen
ten overstaan van de promotiecommissie
van de Faculteit der Geneeskunde
op maandag 20 juni 2016 om 9.45 uur
in de aula van de universiteit,
De Boelelaan 1105

door

Wei Chen

geboren te Shenyang, China

promotoren: prof.dr. M. Verheij
 prof.dr. G.M.M. Bartelink

copromotoren: dr.ir. J.-J. Sonke
 dr. K.G.A. Gilhuijs

promotiecommissie:

prof.dr. B.J. Slotman

prof.dr. L.J. Boersma

prof.dr.ir. A.L.A.J. Dekker

prof.dr. C.R.N. Rasch

prof.dr. M.J van de Vijver

The studies described in this thesis were financially supported by CTMM (Centre for Translational Molecular Medicine, www.ctmm.nl), Project Breast Care, No. 03O-104.

The printing of this thesis was sponsored by
Netherlands Cancer Institute



Cover Design: Raula, raula517@gmail.com

Printing: REPRO, repro@vu.nl

ISBN: 978-90-5383-197-7

Copyright © 2016, Wei Chen

All rights reserved. Copyright of the individual chapters belongs to the publisher of the journal listed at the beginning of each respective chapter. No part of this publication may be reproduced, stored in a retrieval system, or transmitted in any form or by any means, electronic, mechanical, photocopying, recording or otherwise, without the prior permission from the copyright owner.

Risk Modeling and Treatment Planning: a Breast Cancer Case

Wei Chen

In Memory of My Parents

Table of contents

Chapter 1	Introduction	2
-----------	--------------	---

Part I Surgical Impact on Risk

Chapter 2	Analysis of deformations between in-vivo and ex-vivo tissue around invasive breast cancer	10
-----------	---	----

Chapter 3	Impact of negative margin width on local recurrence in breast conserving therapy	20
-----------	--	----

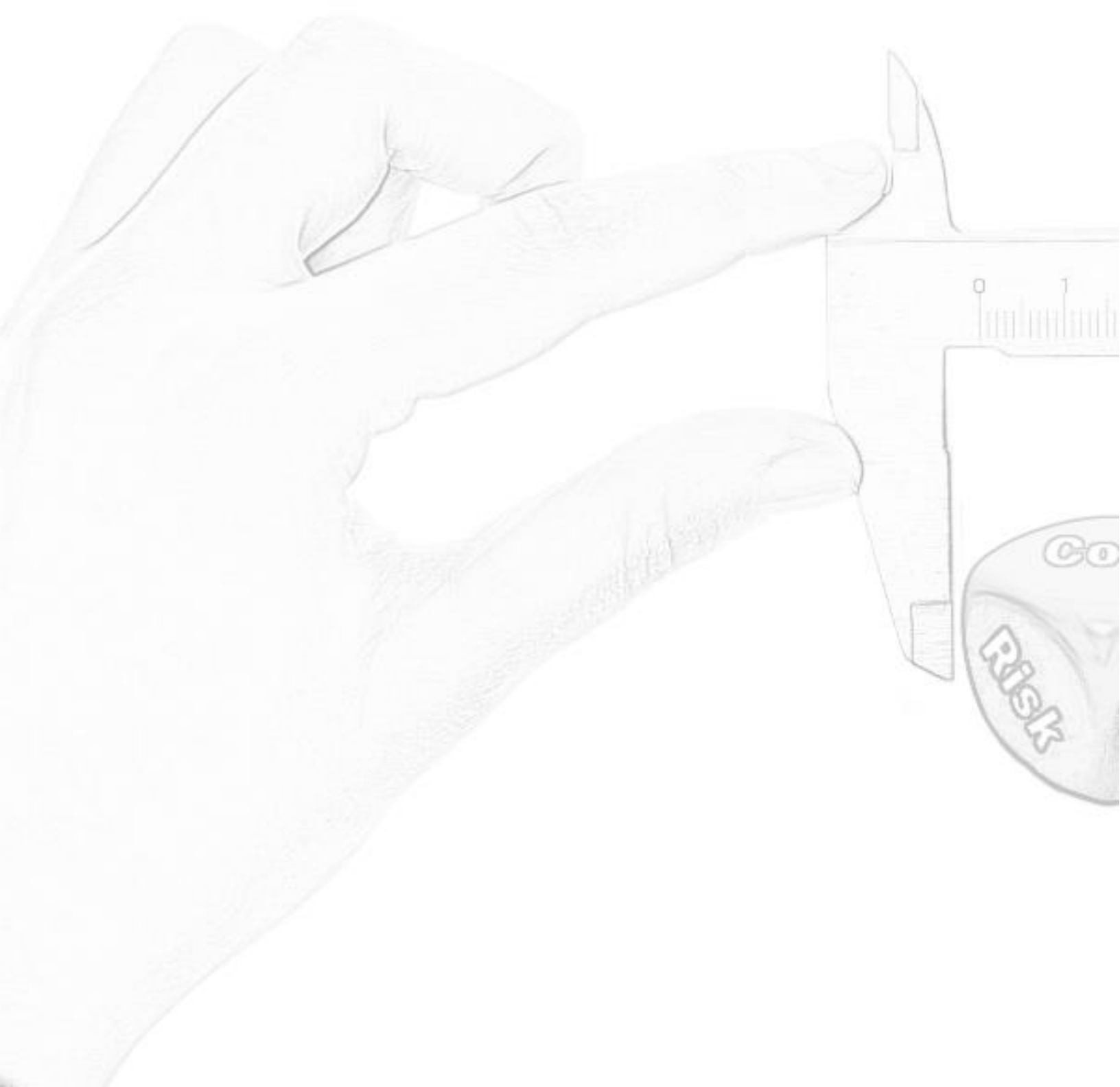
Part II Risk Modeling Framework

Chapter 4	A simulation framework for modeling tumor control probability in breast conserving therapy	40
-----------	--	----

Chapter 5	The effect of age in breast conserving therapy: a retrospective analysis on pathology and clinical outcome data	64
-----------	---	----

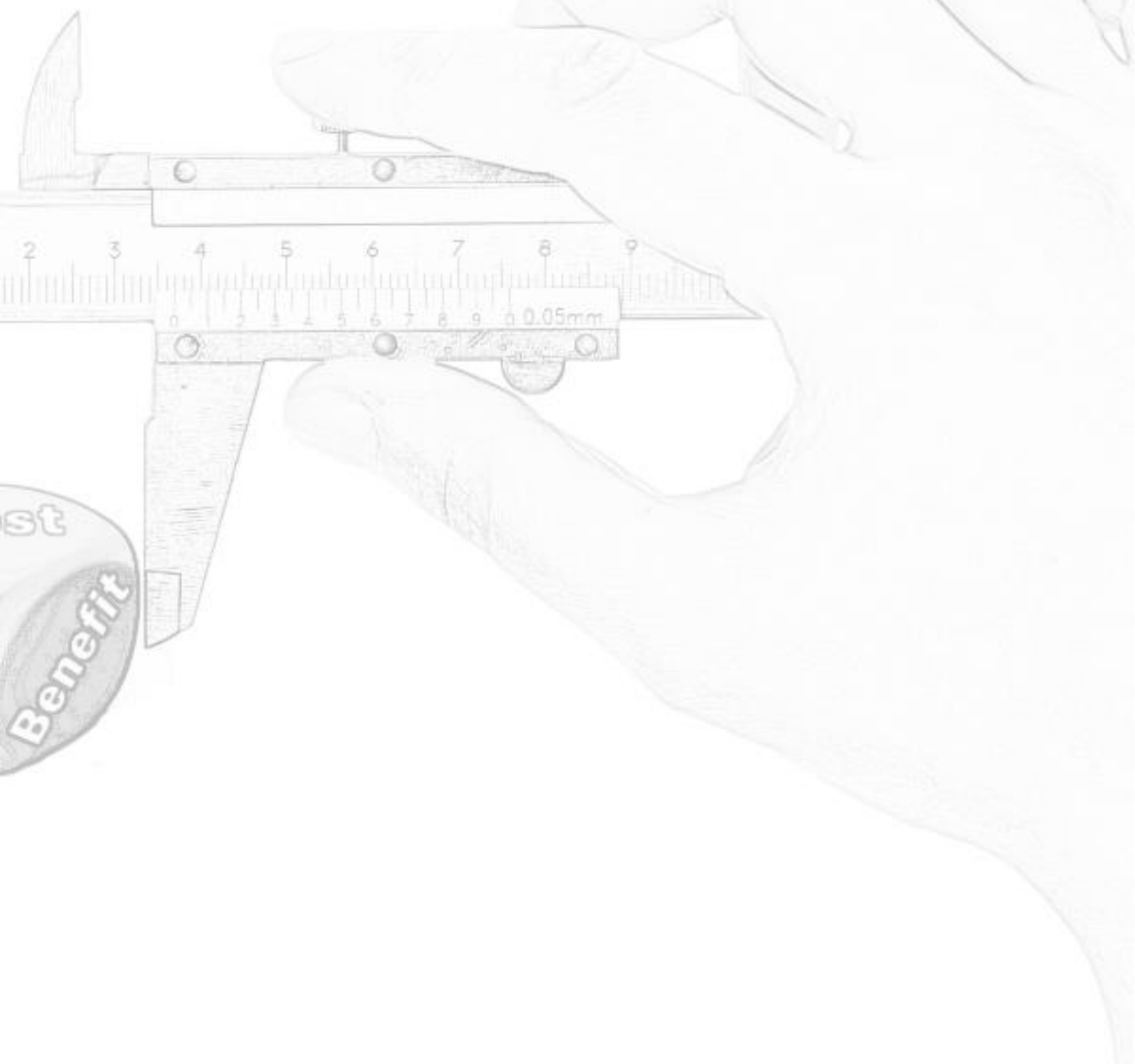
Part III Treatment Planning

Chapter 6	Towards dose-painting for microscopic disease: application to breast-conserving therapy	90
Chapter 7	Discussion	112
	Summary	124
	List of abbreviation	126
	List of publications	128
	Acknowledgement	130
	Curriculum Vitae	133



Chapter 1

Introduction



Chapter 1

Breast cancer is the most common type of cancer among women, accounting for nearly 1 in 3 cancers [1]. It is also the most common cause of cancer-related mortality among women, accounting for approximately 411,000 deaths each year [2], which is approximately 15% of all cancer-related deaths [3]. The lifetime risk of developing breast cancer is as high as 1 in 8 women in some Western countries [4] and a 5-year prevalence of approximately 4.4 million cases worldwide [1]. In 2013 alone, an estimated 232,340 new cases of invasive breast cancer were expected to be diagnosed among women in US, as well as an estimated 64,640 additional cases of in situ breast cancer. That year, approximately 39,620 US women were expected to die from breast cancer. Only lung cancer accounts for more cancer deaths in women [5].

The standard of care nowadays for early-stage breast cancer includes whole breast irradiation in case a breast conserving strategy is applicable [6]. The purpose of the irradiation is to minimize the risk of loco-regional failure and thus ultimately improve disease-specific survival while aiming to minimize side effects to the heart or lungs or cosmetics. This strategy includes irradiating the mammary gland and in node-positive patients also loco-regional lymph nodes with doses around 50 Gy in about 25 fractions delivered as daily treatment 5 days per week for 5 weeks. Several large trials have demonstrated this as a safe procedure with local failure rates of 0.5–1% per year of follow-up and acceptable side effects and cosmetics [7]. In a meta-analysis study, it was reported that radiotherapy to the conserved breast halves the rate at which the disease recurs and reduces the breast cancer death rate by about a sixth. These proportional benefits vary little between different groups of women [7].

Nevertheless, radiotherapy for early stage breast cancer can decrease breast cancer mortality but increase other mortality, mainly from heart disease and lung cancer [8]. The mean cardiac dose from irradiation of a left-sided breast cancer can be two or three times than for a right-sided breast cancer. The mean dose to the ipsilateral (i.e., on the same side as the breast cancer) lung can also be two or three times the mean dose to the contralateral lung [9]. Particularly during the 1970s, when typical heart and lung exposure were greater than now, the laterality of an irradiated breast cancer could

Introduction

measurably affect cardiac mortality and mortality from lung cancer decades later. To further improve control and to reduce side effects, boost techniques [10] and accelerated partial breast irradiation (APBI) [11] have been introduced in the clinic. Long-term outcome were compared. Through a systematic analysis, researchers demonstrate the long-term effectiveness and safety of APBI comparable to that of whole-breast irradiation for selected patients with early breast cancer [12]. This also provides the rationale to further optimize the treatment plan for selected patients, instead of applying a standardized treatment on each patient.

Besides, it is also desirable to identify patients at high risk for local recurrence to better guide optimal treatment (probably with high dose) of individual patients [13]. Especially, young age has been associated with a high risk of local recurrence after breast conserving therapy; at present, it is poorly understood what the biological mechanism for this association is. The risk assessment for local recurrence is still primarily based on traditional clinical and histopathologic factors. More studies with the predictors like immunohistochemical markers [14], molecular subtypes [15], and gene expression profiling [16] are emerging. However, because of the variation in different subtypes of breast cancer and variations in the amount of tumor burden remaining after surgery, finding robust predictive profiles is complex [13]. Only when such robust predictors for local recurrence and sensitivity for systemic treatment and radiotherapy are found, better personalized treatment for breast cancer patients will be accomplished.

Thesis Structure

Predicting the outcome of a treatment for an individual patient is important, however, complex. Especially, a classic randomized control trial lasts for 10 years in which researchers can compare the long-term outcome of different treatments. The pressing need of building prediction models for predicting treatment outcome is observed. Therefore, the goals of this thesis are to model the treatment process of breast conserving therapy and to build a prediction model for the treatment outcome. The thesis starts with modeling surgery impact on the treatment outcome. A step further, a general risk modeling framework was developed for breast conserving therapy. The

Chapter 1

framework was then applied for analyzing the difference between younger and older patients and comparing inhomogeneous dose strategy with homogeneous dose strategy. The rest of the thesis consists of six chapters as follows:

Chapter 2: Building the disease spread model is the first step to model the breast cancer treatment. Deformation appears after the breast tissue was surgically removed. This study aims to quantify the deformations in the surgical excision specimen around invasive breast cancers.

Chapter 3: Controversy exists about the impact of the width of negative margins on the risk of local recurrence in breast conserving therapy. This study explains the unexpected observed weak association using a case-control method with simulations.

Chapter 4: Microscopic disease left after tumorectomy is a major cause of local recurrence in breast conserving therapy. However, the effect of microscopic disease and radiation dose on tumor control probability was seldom studied quantitatively. This study presents a risk modeling framework for predicting the local recurrence risk of breast conserving therapy.

Chapter 5: Age is an important prognostic marker of patient outcome after breast conserving therapy; however, it is not clear how age affects the outcome. This study aimed to explore the relationship between age with the cell quantity and the radiosensitivity of microscopic disease in relation to treatment outcome.

Chapter 6: Little knowledge is available on the optimal radiation dose distribution in relation to microscopic disease. Therefore we investigated the effect of inhomogeneous dose distributions on tumor control probability taking into account inhomogeneously distributed tumor cells and setup errors.

Chapter 7: Discussion

Introduction

Reference

- [1] Hortobagyi GN, de la Garza Salazar J, Pritchard K, Amadori D, Haidinger R, Hudis CA, et al. The global breast cancer burden: variations in epidemiology and survival. *Clin Breast Cancer* 2005;6:391–401.
- [2] Parkin DM, Bray F, Ferlay J, Pisani P. Estimating the world cancer burden: Globocan 2000. *Int J Cancer* 2001;94:153–6.
- [3] Shibuya K, Mathers CD, Boschi-Pinto C, Lopez AD, Murray CJ. Global and regional estimates of cancer mortality and incidence by site: II. results for the global burden of disease 2000. *BMC Cancer* 2002;2:1.
- [4] Jemal A, Clegg LX, Ward E, Ries LAG, Wu X, Jamison PM, et al. Annual report to the nation on the status of cancer, 1975-2001, with a special feature regarding survival. *Cancer* 2004;101:3–27.
- [5] DeSantis C, Ma J, Bryan L, Jemal A. Breast cancer statistics, 2013. *CA Cancer J Clin* 2014;64:52–62.
- [6] Bartelink H, Horiot J-C, Poortmans P, Struikmans H, van den Bogaert W, Barillot I, et al. Recurrence rates after treatment of breast cancer with standard radiotherapy with or without additional radiation. *N Engl J Med* 2001;345:1378–87.
- [7] Darby S, McGale P, Correa C, Taylor C, Arriagada R, Clarke M, et al. Effect of radiotherapy after breast-conserving surgery on 10-year recurrence and 15-year breast cancer death: meta-analysis of individual patient data for 10,801 women in 17 randomised trials. *Lancet* 2011;378:1707–16.
- [8] Darby SC, McGale P, Taylor CW, Peto R. Long-term mortality from heart disease and lung cancer after radiotherapy for early breast cancer: prospective cohort study of about 300,000 women in US SEER cancer registries. *Lancet Oncol* 2005;6:557–65.
- [9] Inskip PD, Stovall M, Flannery JT. Lung cancer risk and radiation dose among women treated for breast cancer. *J Natl Cancer Inst* 1994;86:983–8.
- [10] Bartelink H, Horiot J-C, Poortmans PM, Struikmans H, Van den Bogaert W, Fourquet A, et al. Impact of a higher radiation dose on local control and survival in breast-conserving therapy of early breast cancer: 10-year results of the randomized boost versus no boost EORTC 22881-10882 trial. *J Clin Oncol* 2007;25:3259–65.
- [11] Offersen B V., Overgaard M, Kroman N, Overgaard J. Accelerated partial breast irradiation as part of breast conserving therapy of early breast carcinoma: a systematic review. *Radiother Oncol* 2009;90:1–13.
- [12] Smith BD, Arthur DW, Buchholz TA, Haffty BG, Hahn CA, Hardenbergh PH, et al. Accelerated Partial Breast Irradiation Consensus Statement From the American Society for Radiation Oncology (ASTRO). *Int J Radiat Oncol* 2009;74:987–1001.
- [13] van der Leij F, Elkhuizen PHM, Bartelink H, van de Vijver MJ. Predictive factors for local recurrence in breast cancer. *Semin Radiat Oncol* 2012;22:100–7.
- [14] Lakhani SR. The Pathology of Familial Breast Cancer: Predictive Value of

Chapter 1

Immunohistochemical Markers Estrogen Receptor, Progesterone Receptor, HER-2, and p53 in Patients With Mutations in BRCA1 and BRCA2. *J Clin Oncol* 2002;20:2310–8.

- [15] Esteva FJ, Hortobagyi GN. Prognostic molecular markers in early breast cancer. *Breast Cancer Res* 2004;6:109–18.
- [16] van 't Veer LJ, Dai H, van de Vijver MJ, He YD, Hart AAM, Mao M, et al. Gene expression profiling predicts clinical outcome of breast cancer. *Nature* 2002;415:530–6.

Introduction



Part I Surgical Impact on Risk

Chapter 2

Analysis of Deformations between in-vivo and ex-vivo Tissue around Invasive Breast Cancer



Chen, Wei, Joep Stroom, Jan-Jakob Sonke, Harry Bartelink, Annemarie C. Schmitz, and Kenneth G. Gilhuijs. " Analysis of deformations between in-vivo and ex-vivo tissue around invasive breast cancer." *XVI International Conference on the Use of Computers in Radiation Therapy*, Amsterdam, 2010.

Abstract

Correctly accounting for the extent of tumour is critical for successful radiation therapy of breast cancer. Guidelines to establish the extent of CTV margins can be derived from correlation studies between pre-treatment imaging and pathology. However, this correlation may be compromised by deformations between in-vivo and ex-vivo imaging. The aim of this preliminary study was to quantify the deformations in the surgical excision specimen around invasive breast cancers. The study was performed on 7 patients who underwent wide-local excision (WLE) of breast cancer. The MR slices were reconstructed in the direction of the resection plane at pathology. The displacements of corresponding parenchyma structures were quantified in radial directions around the invasive index tumor using the distance transform. The relative tissue deformations were computed from these displacements. The results suggest that a mean tissue deformation of 12% may occur in the CTV.

Introduction

Breast Cancer is the most common cancer and the second leading cause of cancer death in women in Western countries. Classical treatment consists of surgery (for early stages), chemotherapy, radiotherapy or a combination thereof. With continuous improvement of treatment modalities over the years, the 5-year local recurrence rate after breast-conserving therapy (BCT) varies from 3% to 15% with survival rates of approximately 92% [1].

Because the majority of local recurrences occur in the tumor bed [2], residual tumor cells in the proximity of the gross tumor volume (GTV) after treatment are likely one of the main causes for tumor recurrence after BCT. The combination of radiotherapy and surgery aims to treat all cancer-bearing tissues while involving as little healthy surrounding tissues as possible. Hence, it is important to accurately assess the extension of the disease at pre-treatment imaging. Despite recent progress, uncertainties about the achieved margins during surgical excision and the microscopic spread of disease are major factors that limit further reduction of the boost volume. Pathology studies addressing the distribution of microscopic disease around invasive breast cancer are, however, sparse and have mostly focused on patients undergoing mastectomy during the onset of current breast-cancer screening programs [3]. In a more recent study [4], the incidence and distance of microscopic disease around primary breast tumors were assessed in patients undergoing BCT. In these studies, the impact of tissue deformations around the GTV between *in-vivo* imaging and *ex-vivo* pathology was not taken into account. The aim of this preliminary study was to quantify the deformations of breast tissue around the GTV between *in-vivo* MR imaging and *ex-vivo* pathology processing. Consequently, the correlation between pre-treatment imaging and pathology will be corrected.

Material and methods

Patients

Seven patients who underwent BCT for invasive cancer after conventional breast imaging, clinical examination, and contrast-enhanced MRI were included (Table 1).

Table 1: Patient and tumor characteristics.

Patients		
N		7
Age (years)		60 (38-72)
Left Breast with tumor (Right)		4 (3)
Tumors		
Mean tumor diameter (mm)		12.5 (7.3-18.9)
Mass margin appearance		
Irregular		3
Spiculate		1
Smooth		3
Mass margin sharpness		
Sharp		3
Vague		4

Pathology X-ray Images

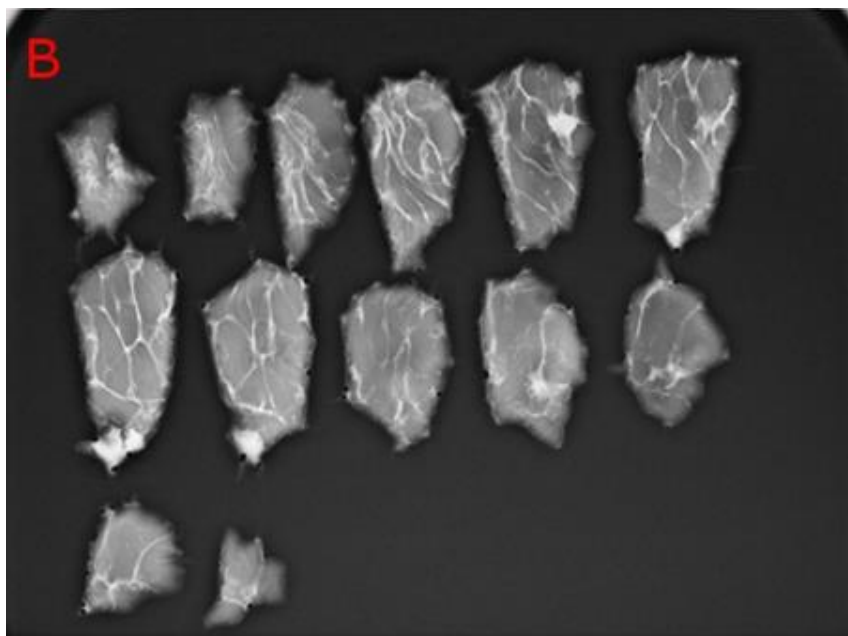
During surgery, the orientation of the excision specimen was marked by sutures and a small skin flap. At pathology, the edges of the specimen were inked with different colors to indicate the original orientation of the specimen in the breast. After inking, the specimens were cooled to -20°C for 20 minutes and sectioned in 4-mm thick slices (Figure 1A). The orientation of slicing was approximately perpendicular to the nipple-to-tumor direction. The slices were sealed in vacuum-locked bags, and digital X-ray images were obtained (Figure 1B).

MR Images

MRI was performed with a 1.5-T scanner (Magnetom, Siemens Medical Systems, Erlangen, Germany) using a coronal fast low-angle shot three-dimensional (FLASH-3D) technique. Both breasts were imaged with the patient in prone orientation, using a dedicated phased-array bilateral breast coil. One series was acquired before and four series after intravenous injection of contrast agent (ProHance, Bracco-Byk Gulden, Konstanz, Germany; 0.1 mmol/kg body weight, at a rate of 2-4 ml/s). The series were acquired at intervals of approximately 120s to achieve theoretically optimal time points to describe contrast uptake in the lesion. The following MRI parameters were used: T1-weighted sequence, repetition time 8.1ms, echo time 4.0ms, reconstructed in-plane matrix 256×256 pixels, isotropic in-plane resolution of 1.35×1.35 mm², 100 slices with thickness 1.35mm, no fat suppression. Subtraction images were reformatted and displayed in three perpendicular planes (coronal, transversal, and sagittal) on a custom build viewing station to examine initial and late enhancement. The largest tumor diameter at MRI was measured on the initial-enhancement images in the coronal, transverse, and sagittal directions.

Figure 1: (A) *Marcoscopic Pathology Slices* (B) *Digital X-ray photograph*





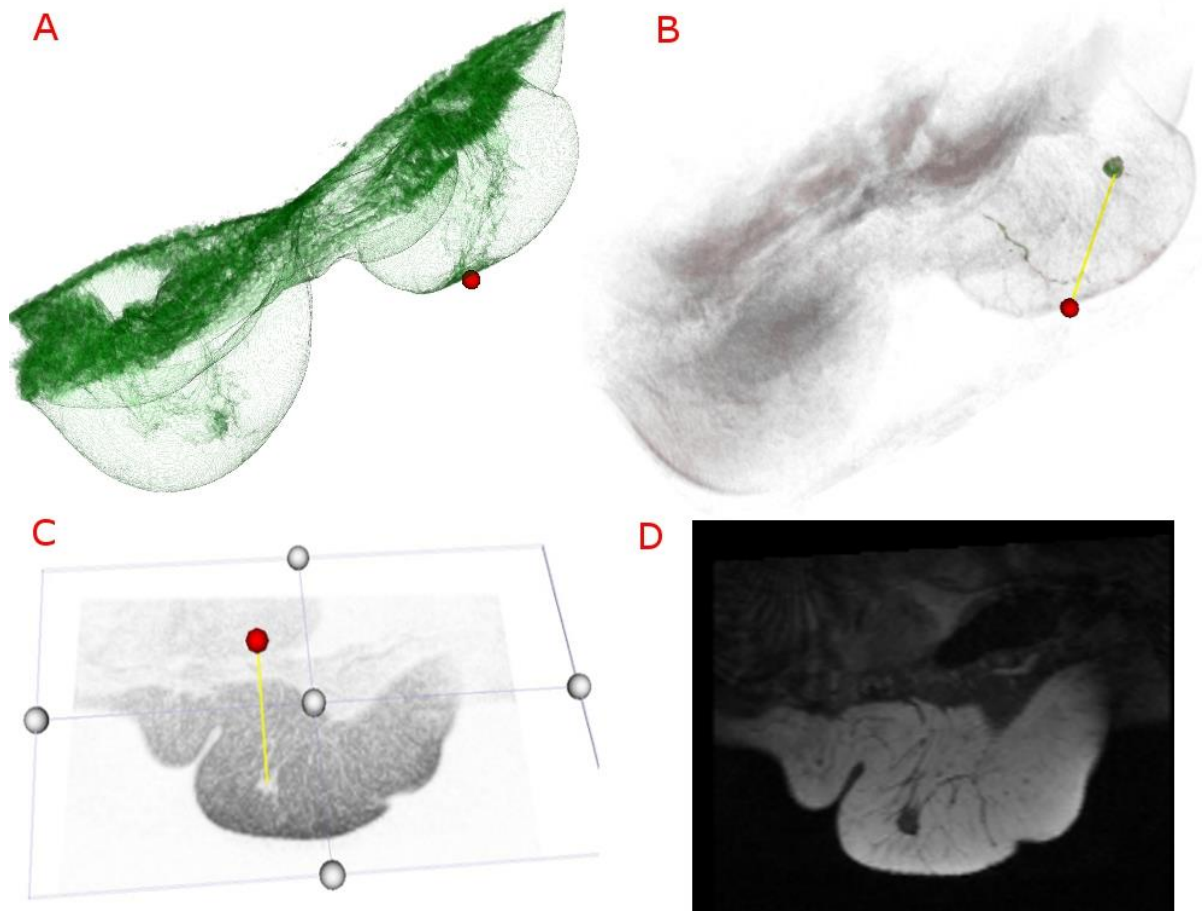
The delineated tumor, its estimated orientation from color coding, and the skin flap in the excision specimen were used as landmarks to determine the orientation of the excised tissue in the MR images. The MRI was subsequently resampled in the pathology slicing direction using the following procedure. First, the location of the nipple was recovered for each breast with tumor (Figure 2A). The orientation of the line connecting the nipple with the centre of gravity in the tumor was subsequently established (Figure 2B). According to the surgical and pathology protocol, this line (yellow) indicates the normal of the pathology slicing planes. The pathology slicing process was computer simulated using the VTK box-widget tool (Figure 2C). Finally, the oblique slice with the largest tumor diameter in the MR images was stored (which we will refer to as the target image), as well as the slices above and below the target image (Figure 2D). The latter MR images were used to verify the estimation of the slicing orientation.

Registration (Deformation Analysis)

The pathology X-ray image with the largest tumor diameter and the MR target image were registered to estimate the relative deformations between them. For this purpose,

we first aligned the index tumor using a rigid alignment procedure. Next, corresponding fiducial structures in the prechyma structure around the index tumor were identified in each image. The distance of fiducial point to GTV in radial directions was calculated using distance map [5] of the binary representation of GTV, and the relative deformation was quantified by the ratio of distances of corresponding fiducial points.

Figure 2: Four steps to obtain MR image slice in the pathology slicing direction.



Results and Discussion

X-ray images of the index tumor and corresponding MR slices are shown for all seven patients in Figure 3. The slices with the largest tumor diameter are shown. The skin and tumor could be identified in all image pairs, indicating that the correct slice pairs were identified. Patient 1 and 7 were skipped from deformation analysis, because no

Chapter 2

corresponding fiducial structures could be identified. The average radial deformation of the structures between the MRI target images and the pathology X-ray images was 1.12 (the minimum 0.79, the maximum 1.61, and std. 0.26). This preliminary result suggests that distances of microscopic disease around the index tumor may be underestimated in pathology studies compared to their counterpart distances inside the patient during prone setup.

Our preliminary study also has some limitations. First, variation in the exact slicing orientation achieved by the pathologists. We made the assumption that pathology slicing is perpendicular to the connected line between nipple and tumor, which is conform the clinical protocols. Another limitation is that the registration is currently performed in 2-D (in the plane with the largest cross section through the tumor). Deformations of the tissue were quantified relative to a prone patient setup (conform the setup during MRI scanning), while typical setup of breast cancer patients during radiotherapy is in supine orientation. In supine setup, the deviations are expected to be smaller, but this issue is topic of current research.

Conclusion

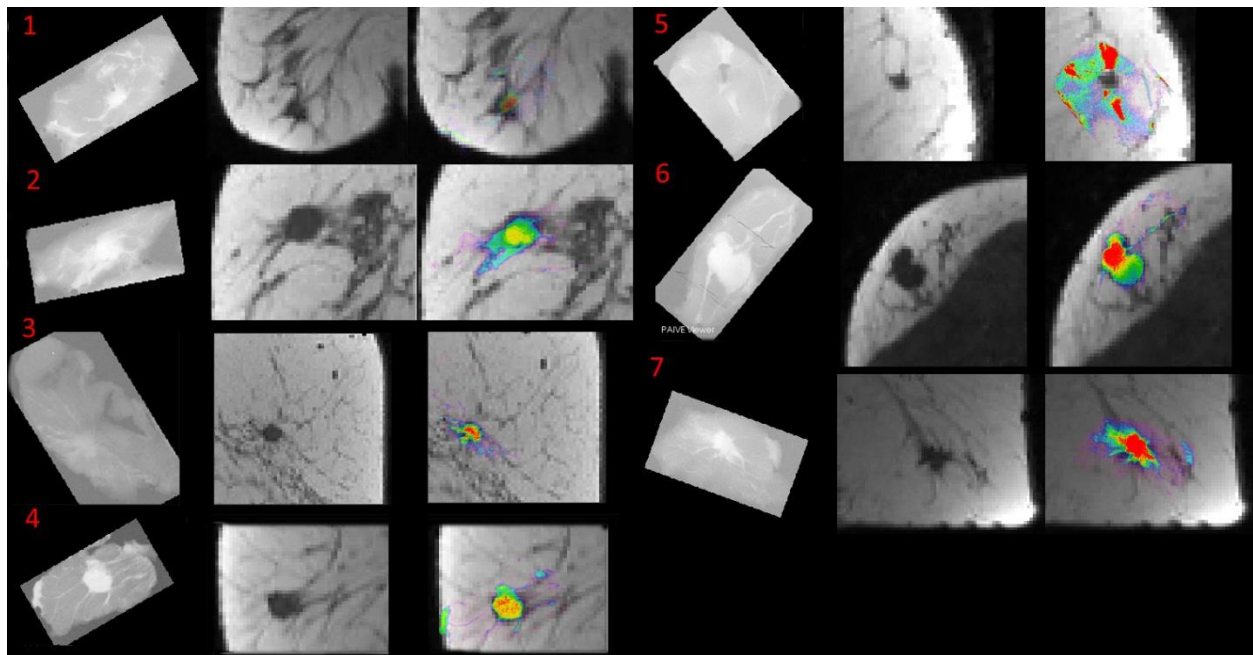
Breast tissue in the proximity of GTV may be compressed by 12% on average between *in-vivo* MR imaging in prone patient orientation and *ex-vivo* pathology evaluation.

References

- [1] Bartelink H, Horiot J C, Poortmans P M, et al. 2007 Impact of a higher radiation dose on local control and survival in breast-conserving therapy of early breast cancer: 10-year results of the randomized boost versus no boost EORTC 22881-10882 trial. *Journal of Clinical Oncology*, 25(22):3259-3265
- [2] Veronesi U, Marubini E, Mariani L, et al. 2001 Radiotherapy after breast-conserving surgery in small breast carcinoma: Long-term results of a randomized trial. *Annals of Oncology* 12:997-1003

- [3] Holland R, Hendriks J H, Vebeek A L, et al. 1990 Extent, distribution and mamographic/ histological correlations of breast ductal carcinoma in situ. *Lancet*, 335:519-522
- [4] Stroom J, Schlieff A, Alderliesten T, Peterse H, Bartelink H and Gilhuijs K 2009 Using histopathology breast cancer data to reduce clinical target volume margins at radiotherapy. *International Journal of Radiation Oncology, Biology, Physics*, 74(3):898-905
- [5] Huttenlocher D, Klanderman G, and Rucklidge W 1993 Comparing images using the hausdorff distance. *IEEE Transactions on Pattern Analysis and Machine Intelligence*, 15(9):850–863

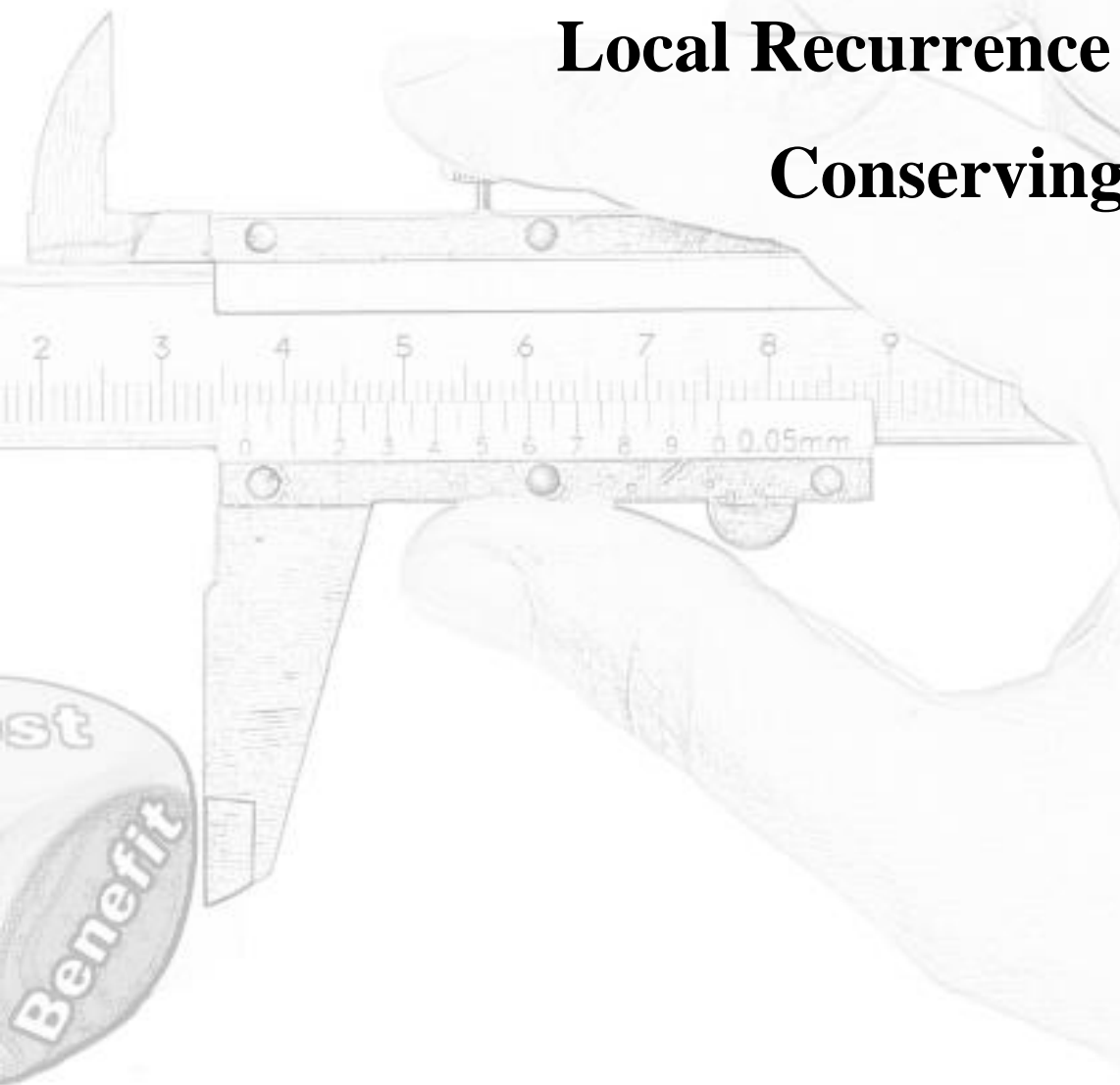
Figure 3: Registration between the pathology X-ray images and the MR images of seven patients in total. The pathology X-ray images are shown in the first and fourth columns. The MR images are shown in the second and fifth columns. The registration overlay images are shown in the third and sixth columns where the pathology X-ray images are overlaid in color.





Chapter 3

Impact of Negative Margin Width on Local Recurrence in Breast Conserving Therapy



Chen, Wei, Joep Stroom, Jan-Jakob Sonke, Harry Bartelink, Annemarie C. Schmitz, and Kenneth G. Gilhuijs. "Impact of negative margin width on local recurrence in breast conserving therapy." *Radiotherapy and Oncology* 104, no. 2 (2012): 148-154.

Abstract

Background and Purpose

This study aims to explain the unexpected weak association between the width of the negative surgical margin and the risk of local recurrence in breast conserving therapy.

Materials and Methods

We utilized a classical tumor-control probability (TCP) model to estimate the risk of local recurrence, considering the heterogeneity of microscopic disease spread observed around the invasive index tumor in a pathology dataset (N=60). The estimated result was compared with the true risk observed in the EORTC boost-versus-no-boost trial (N=1616).

Results

The disease volume beyond any given distance from the edge of the index tumor varied considerably among patients. Adopting this disease volume variation in the TCP model accurately reproduced the local recurrence rate as function of surgical margin width in the boost-versus-no-boost trial (Pearson's correlation coefficients are 0.652 and 0.862, and significant at the 0.05 and 0.01 level for absence and presence of a radiation boost, respectively).

Conclusions

The impact of a negative margin width on local recurrence is limited due to the large variation of microscopic disease that can reach large quantities beyond any given distance from the edge of the index tumor across the patient population of breast-conserving therapy.

Introduction

Breast-conserving therapy (BCT) has become a standard therapeutic option for a large proportion of patients with early-stage invasive breast cancer. In these patients, BCT is typically a preferred treatment over mastectomy, because the survival rates after treatment are comparable, while breast conservation serves cosmetic and psychological benefits [1]. However, radiotherapy also increased long-term mortality from heart disease and lung cancer, as well as severe treatment-induced fibrosis [2,3]. Hence, there is much interest to conform the radiation boost field closer to the expected location and density of tumor cells, but it is currently unknown how to accomplish this.

The European Organization for Research and Treatment of Cancer (EORTC) 22881-10882 trial was designed to investigate the effect of a boost of 16 Gy radiation dose directed to the tumor bed after whole breast irradiation (WBI) of 50 Gy. In the previous multivariate analyses [3-5], an increased risk of local recurrence (LR) was associated with high-grade invasive carcinoma, age at diagnosis younger than 50 years, positive surgical margin and no additional boost, independently. However, the LR risk was not obviously influenced by the width of surgical resection margins (SRMs), if the SRM status is not positive [5]. According to the central pathology review, patients with close (0-2 mm) or negative (>2 mm) margin have similar risk of local recurrence. Comparable results have also been observed in other large trials [6,7]. Conversely, Smitt et al. [8] found that a close SRM is associated with high LR risk. Several pathology tumor load studies [9,10] have also shown that a high quantity of residual tumor cells after breast-conserving surgery (BCS) is correlated with a narrow negative SRM. Although SRM is frequently considered in the planning of RT, an explanation is lacking for these contradictory results on the importance of SRM. Hence, uncertainty exists how to tailor radiotherapy to individual patients after BCS, optimizing local tumor control while preserving cosmetic outcome.

The purpose of this study was to assess the relationship between surgical resection margin and local recurrence rate after BCT. This aim was pursued by adopting the

microscopic disease spread distribution around early-stage invasive breast cancers from a pathology study in a classic tumor control probability (TCP) model, and comparing the result with a case-matched long-term local recurrence rate after BCT in the EORTC boost-versus-no-boost trial.

Materials and Methods

Short Overview of Patients, Study Groups and Statistical Analysis

The study was based on two clinical datasets: the EORTC 22881-10882 boost-vs-no-boost trial (with pathology review) dataset and the Multi-modality Analysis and Radiological Guidance IN breast conServing therapy (MARGINS) dataset. In short (Figure 1), Webb's TCP model [11] was applied to the distribution of microscopic disease spread obtained from the MARGINS dataset, and subsequently used to estimate the treatment outcome of patients with tumors excised with different negative SRM widths, i.e., the smallest distances between the invasive index tumor edge to the surgical resection edge. Next, these estimates were compared with the LR rates in the EORTC dataset. The similarity was measured by the Pearson's correlation coefficient.

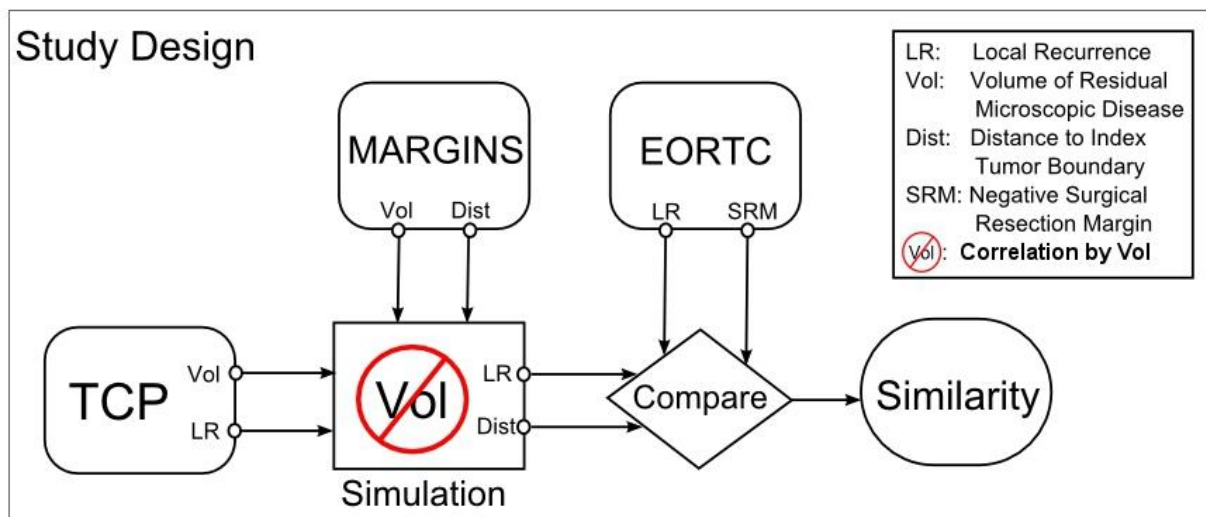
The EORTC dataset

The EORTC dataset with pathology review accrued 1,616 patients from 1989 to 1996 [5]. We used a subset of these data (N=1281) excluding tumors with extensive intraductal component (EIC+) and excluding the cases with SRM width larger than 10 mm. The latter is because we lacked sufficient events to calculate an accurate LR rate for SRM larger than 10 mm (there are only 42 patients with SRM width larger than 10 mm in total). The original objective of this trial was to assess the effect of the boost dose in early-stage breast cancer patients treated with BCT. In short, all patients underwent lumpectomy and axillary lymph node dissection followed by RT. After informed consent, patients after BCS were randomly assigned to receive WBI (total dose of 50 Gy in 5 weeks with a dose per fraction of 2 Gy) with or without a boost of 16 Gy (2 Gy per fraction) to the tumor bed. The surgical margin width (0 mm up to 30 mm), was measured for each patient. Margin status was recognized as positive if invasive tumor

Impact of Negative Margin Width on Local Recurrence in Breast Conserving Therapy

was seen immediately at the inked edge of the resection, close if the margin width was 2 mm or less, and negative if it was greater than 2 mm or if no residual tumor was present.

Figure 1: Overview of our study. The relationship between **Vol** and **LR** is derived from Webb's TCP model and the relationship between **Vol** and **Dist** is extracted from the MARGINS dataset. Both were used in our simulation in order to obtain the correlation between **LR** and **Dist**. The result is finally compared with the observation in the EORTC dataset.



The MARGINS dataset

In 2000, the MARGINS study started at our hospital [10]. Sixty-two patients who did not undergo neo-adjuvant chemo/hormone-therapy and who had no primary DCIS on core biopsies were recruited from MARGINS to undergo additional and more extensive pathology assessment of the tissue after BCS. The wide-local excision (WLE) specimen was subjected to detailed microscopic examination using complete embedding. The type (DCIS, invasive foci, and lymphatic emboli), rate, and quantity of tumor foci were reconstructed at various distances to the edge of invasive index tumor. In the current study, we included all 60 patients without EIC. The incidence and spread of microscopic disease were quantified as a function of distance around the invasive tumor.

To match patient and tumor characteristics between the EORTC dataset and the MARGINS dataset, the following sampling strategy was employed. We first calculated the proportion of patients for two prominent factors that are associated with local recurrence (patient age and histopathological grade [4]) in the MARGINS dataset, and then randomly selected one subset of patients from each treatment arm in the EORTC dataset to match against this proportion. In order to avoid selection bias from a specific subset, we repeated the selection 100 times and computed the average risk of local recurrence from all selections. The final differences between the patient/tumor characteristics in the MARGINS dataset and in the EORTC dataset were examined using the non-parametric Mann-Whitney U test (SPSS v15.0).

Tumor-control probability modeling

Webb's TCP model describes the probability of tumor control (TCP) as a function of the radiosensitivity (α), the volume of tissue containing tumor cells (Vol), the density of tumor cells (ρ) and the total radiation dose (D) considering a homogeneous dose distribution, as follows:

$$TCP = \int f(\alpha) \exp[-\rho Vol \exp(-\alpha D)] d\alpha,$$

where the inter-patient heterogeneity of radiosensitivity is represented by the probability density function $f(\alpha)$. In our study, the radiosensitivity heterogeneity of residual microscopic disease was considered to be normally distributed across the patient population. The cell density of residual microscopic disease (ρ) around the index tumor was obtained on a representative set of 36 digitized microscopy slides from 12 patients using a cell-counting algorithm (Aperio Technologies Inc., US [12]). Two radiation doses (D) were considered in this model, i.e., no-boost (50Gy) and boost (66Gy), representing the two arms in the EORTC trial. Vol was obtained from the MARGINS dataset, and TCP was derived from the EORTC 22881-10882 trial at medium follow-up of 10 years in the previously mentioned subsets of patients. Finally, the parameters α and $f(\alpha)$ in Webb's TCP model were estimated by a Bayesian Inference technique [13].

Monte Carlo simulation

Our procedure to combine the TCP model, the MARGINS dataset, and the EORTC dataset is depicted in Figure 1. The TCP model is correlated with various volumes of microscopic disease (Vol) and used to generate the estimates of local recurrence risk ($LR=1-TCP$). The MARGINS dataset describes the probability of disease volume Vol beyond various distances ($Dist$) from the edge of the index tumor (Vol - $Dist$ relationship). The EORTC dataset includes associations between negative surgical resection margins (SRM) and LR rate. Because the MARGINS dataset describes the incidence of disease beyond distance $Dist$ from the edge of the index tumor and residual microscopic disease in the breast can only occur beyond the surgical resection margin, $Dist$ is directly comparable to SRM (more in the discussion section). Using the optimal radiosensitivity parameters, we estimated the correlation between LR and $Dist$ using Vol as a “bridge” in the Monte Carlo simulation. Next, we compared our estimate (LR - $Dist$ relationship) with the true observations (LR - SRM relationship) in the EORTC trial using the Pearson-Correlation coefficient.

Results

The EORTC dataset

The original EORTC data was stratified according to previously identified risk factors for both treatment arms (Table 1).

The MARGINS dataset

The volume of microscopic disease surrounding the index tumor in the patient groups varies considerably across SRM widths. Figure 2 illustrates these various observed volumes beyond different distances from the edge of the index tumor. For instance, the average volume of surrounding microscopic disease beyond 5 mm is about 180 mm³, but the range of volume variance spans 0 to 760 mm³. Beyond distance of 10 mm, the surrounding microscopic disease can still be 100 mm³ on average, and may reach 380 mm³ in one-in-twenty cases. The cell density of microscopic disease was estimated at 4.6E+05 #cells / mm³ on average. The pathology grades of the index tumor are

Chapter 3

comparable in the MARGINS and the EORTC dataset. Patients are, however, 5 years younger on average in the EORTC dataset (P-value = 0.02), so that a case-control design was necessary for compensating a potential effect of age difference (Table 1).

Table 1: Patient and tumor characteristics in the original EORTC dataset and the MARGINS dataset

		EORTC 50 Gy (n=627)		EORTC 66 Gy (n=654)		MARGINS (n=60)	
		Number	%	Number	%	Number	%
Age (year)	Mean	54.0		53.7		58.4	
	Range	29-75		27-76		36-80	
	Younger (≤ 50)	238	38.0	255	39.0	12	20
	Older (> 50)	389	62.0	399	61.0	48	80
Tumor grade	Grade 1	300	47.8	352	53.8	27	45
	Grade 2	173	27.6	148	22.7	22	36.7
	Grade 3	141	22.5	142	21.7	11	18.3
	Missing	13	2.1	12	1.8	0	0

We randomly selected 495 patients in the boost arm and 499 patients in the no-boost arm from the EORTC dataset to match against patient ages and pathology grades in the MARGINS dataset. The local recurrence rate for each negative SRM width was computed from this EORTC subset.

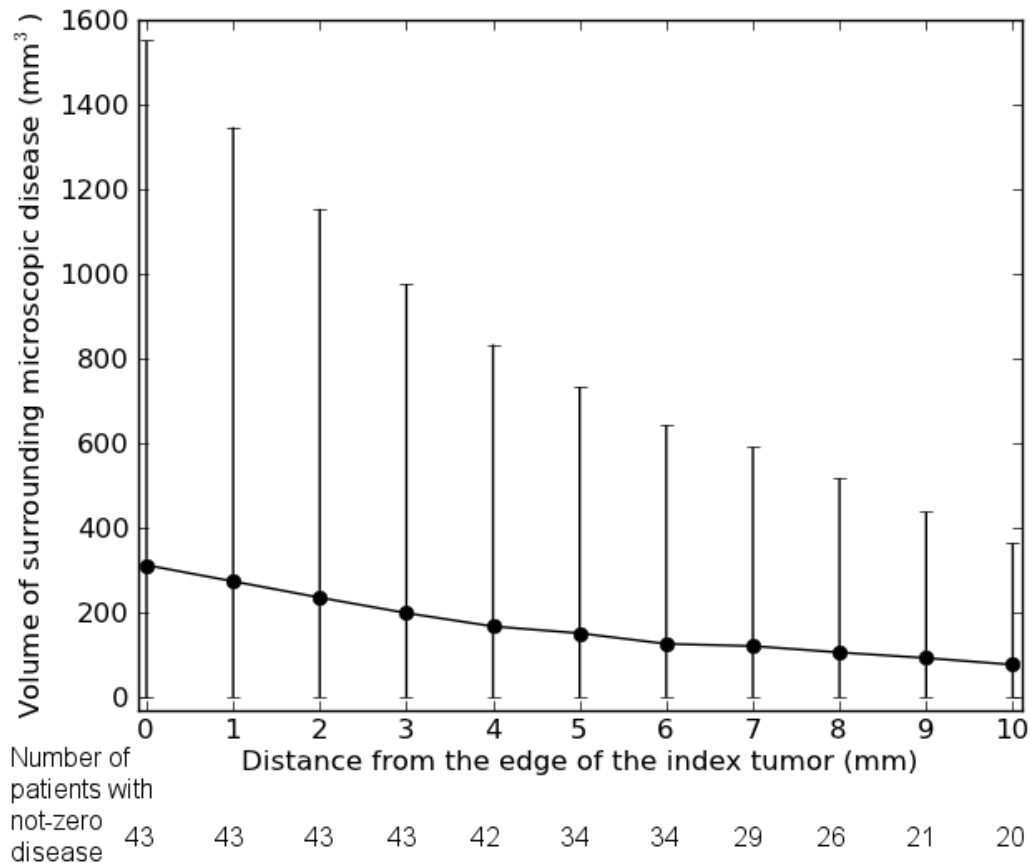
Monte Carlo simulation

The Bayesian Inference technique with the data of two radiation arms (66 Gy and 50 Gy) yielded a normally-distributed radiosensitivity parameter with mean 0.58 Gy^{-1} and standard deviation 0.18 Gy^{-1} . The resulting TCP curves of Webb's model for the two dose levels are shown in Figure 3. With increasing disease volume, the LR risk increases at different speeds by different radiation dose levels. The boost dose (66 Gy)

Impact of Negative Margin Width on Local Recurrence in Breast Conserving Therapy

was associated with increased local control for all microscopic disease volumes, but particularly for larger volumes.

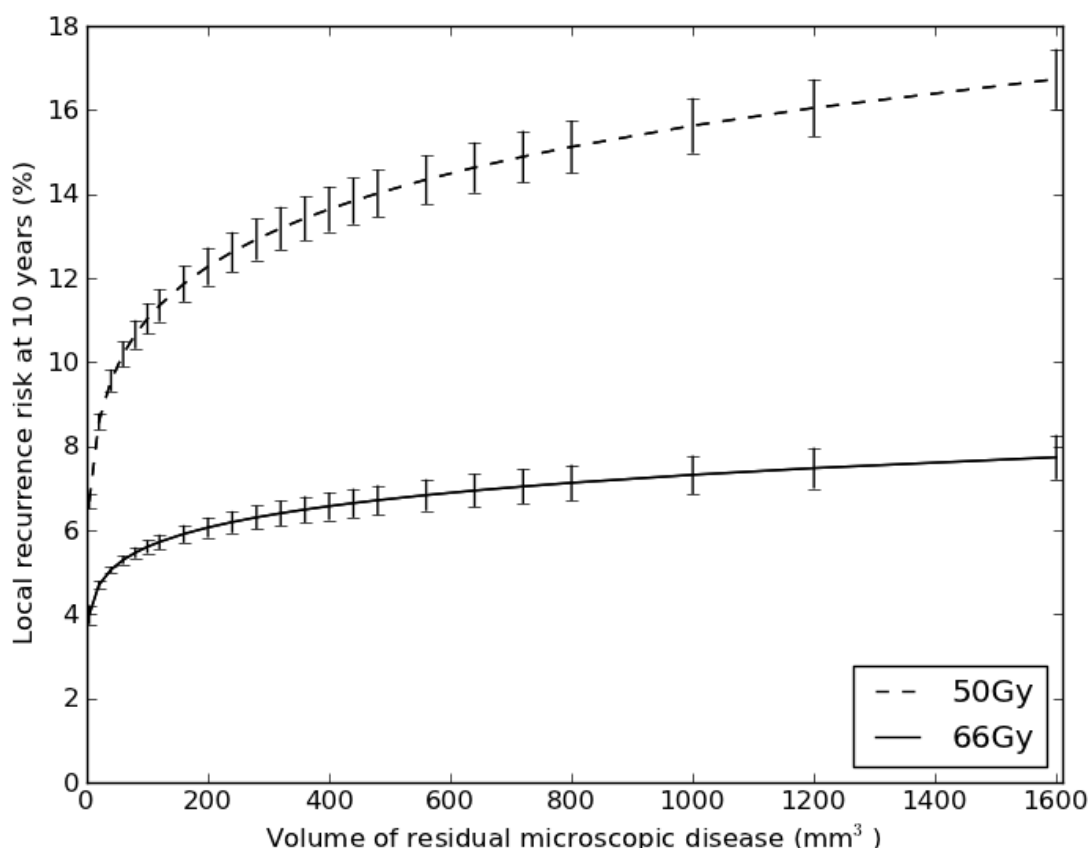
Figure 2: The various volumes of microscopic disease beyond different distance from the edge of the index tumor in the MARGINS database of 60 patients. (Mean \pm 2* Standard Deviation)



The Monte Carlo simulation reproduced the findings in the EORTC dataset at a Pearson's correlation of 0.652 (significant at the 0.05 level) for the no-boost patients and 0.862 (significant at the 0.01 level) for the boost patients (Figure 4). A weak association between the width of the negative margins and the local recurrence rate was observed (linear regression coefficient = -0.13 %/mm for the no-boost patients and -0.05 %/mm for the boost patients). The results suggest that the weak association between the risk of LR and the SRM width in the EORTC trial is caused by the residual

volume of microscopic disease and the variation in volume around the index tumor among the patients.

Figure 3: Webb's TCP model of two radiation-dose arms illustrating the relationship between volume of residual microscopic disease and the risk of LR at 10 years. The error bar illustrates the 95% confidence interval of the estimated LR values.

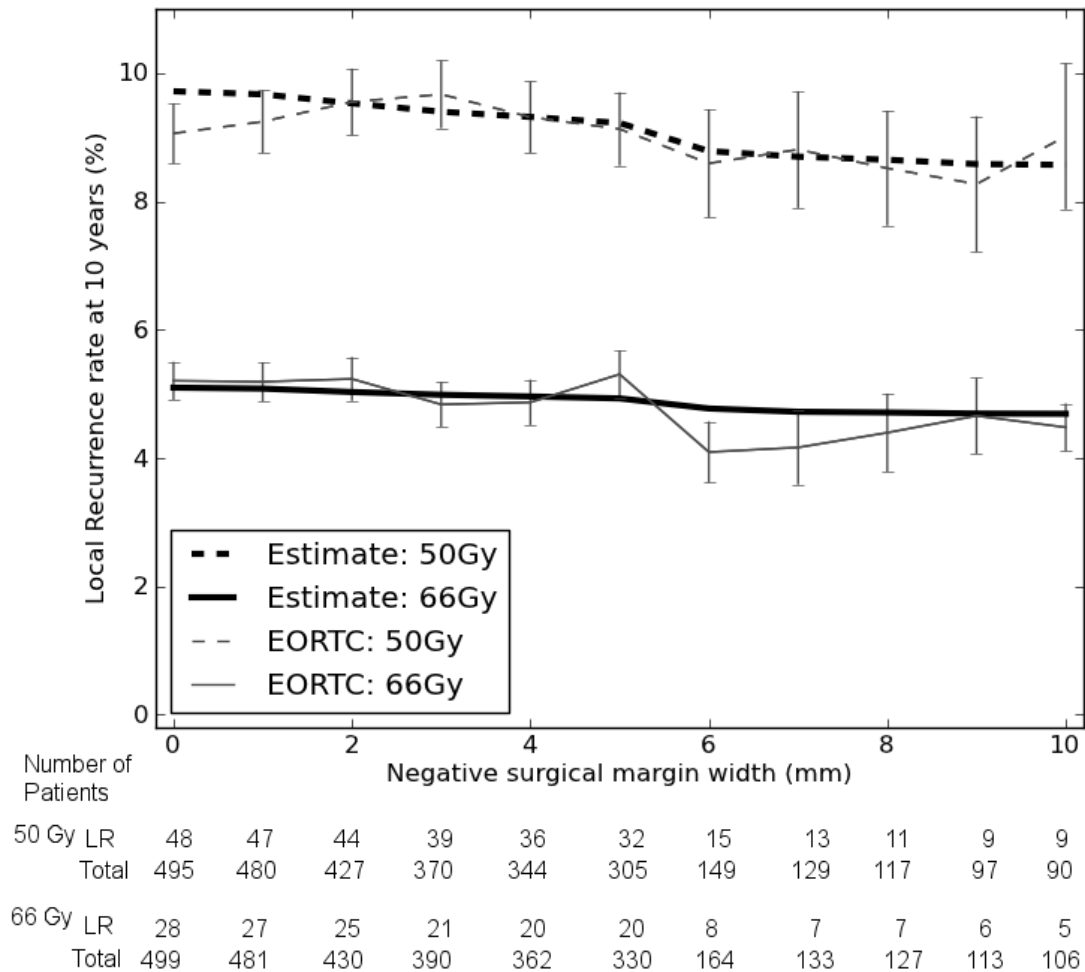


Discussion

A large SRM width is often considered as an indicator for small residual quantity of tumorous disease, which may result in a better treatment outcome. Using the pathology information in the current study, we found, however, that the negative SRM width is only weakly associated with the risk of local recurrence. Patients with negative or close SRM may have similar local recurrence risk because of varying quantities of microscopic disease in the remaining breast tissue.

Impact of Negative Margin Width on Local Recurrence in Breast Conserving Therapy

Figure 4: The association between the width of negative margins and the local recurrence rate in the EORTC dataset (thin lines) and in our simulations (thick lines). The error bar illustrates the 95% confidence interval of the estimates in the EORTC dataset.



Clinical consequences

Consensus exists that a positive margin after breast-conserving surgery is one of the strongest predictors of local recurrence for patients with invasive breast cancer [14]. However, negative or close surgical resection margins after BCS are defined, interpreted and handled differently by surgeons and radiation oncologists [15], and controversy exists about the impact of the width of negative margins on the risk of local recurrence [6-8]. A survey [14] has shown no direct relationship between the width of

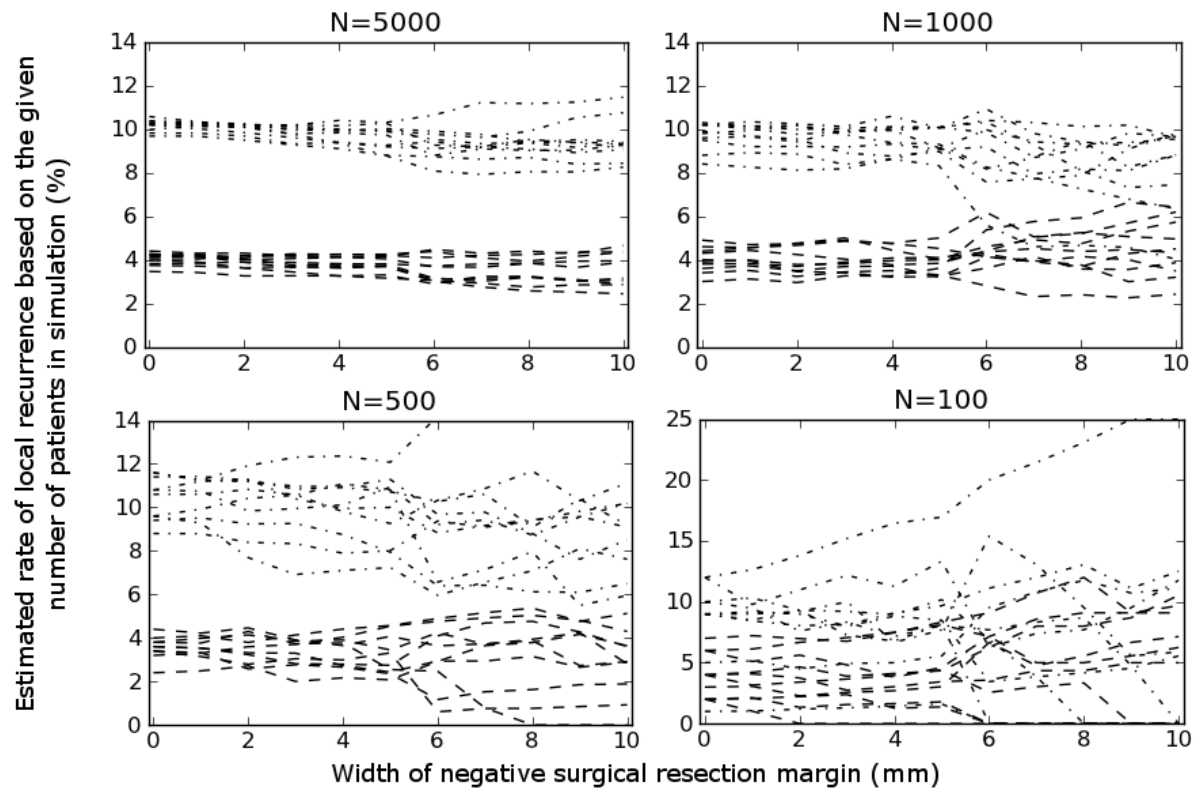
negative margins and the risk of LR in ten large trials. This observation was explained by some confounding effects of other factors that influence LR after BCT. Recently, Pleijhuis et al. [16] supplemented this result with another survey of trials, in which eight of ten studies showed that a close margin is not one of the risk factors for local recurrence. Nonetheless, it was recommended [15] that large surgical margin widths are necessary in order to assure low risk of LR, which seems a contradiction to the existing outcome of clinical trials [14,16]. Our study suggests that the lack of correlation between surgical margin width and LR can be explained by inaccuracy in the concept that the negative surgical margin width is a good indicator of residual microscopic disease quantity in the remaining breast tissue. Patients with the same SRM width may have widely varying quantity of residual disease, and this variation makes the effect of the SRM width on the LR risk surprisingly small. Another support for this hypothesis is that when we decreased the number of patients in our simulation, resulting in an apparent but arbitrary distribution of residual microscopic disease, the estimated LR rates conversely become random (Figure 5). It suggests that if the number of patients in a trial is small, we may observe a strong effect of surgical margin width on local recurrence rate, which is actually caused by the distinctness of data or a statistic approach without enough power.

To quantify residual tumor load without detailed microscopic analysis, two approaches may be possible: 1) to establish an estimate from pre-and-postoperative imaging modalities such as magnetic resonance imaging [17]; 2) to establish an estimate based on the examination of the surgical specimens using a specific sampling method and a computer model (an initial attempt was provided in [18]). In the first approach, characteristics of the index tumor at pretreatment imaging in combination with information from a core biopsy are analyzed to enrich subgroups of patients at low risk for surrounding microscopic disease. However, the current resolution of pretreatment images cannot visualize microscopic disease. In the second approach, multiple samples from the surgical specimen are checked for the presence of microscopic disease, and the findings can be extrapolated to predict remaining microscopic disease in the breast using an existing model of microscopic disease spread. One difficulty of this approach

Impact of Negative Margin Width on Local Recurrence in Breast Conserving Therapy

lies in the increased workload for pathologists. In current clinical setting, microscopic examination is typically restricted to locations in the index tumor and on the edge of specimen to indentify tumor grade and surgical margin status. Future studies on the clinical, biological, and imaging factors related to patient disease load are expected to fill in this gap.

Figure 5: The uncertainty of observed LR rates at difference surgical margins become larger with smaller number of patients in the simulation (ten simulations in each subfigure; the result of each simulation is reported by two curves. Dotted curve: 50 Gy, Dashed curve: 66Gy).



An additional boost to the primary tumor bed significantly increased local control in patients with negative or close margins at median follow-up of 10 years [3--5]. This observation suggests that the local recurrences are caused by the existence of residual tumor cells in the region near the primary tumor bed [10], and that the radiation boost improves cell kill in that region. Several authors have reported comparable clinical

results after conventional RT, IMRT, or brachytherapy [19--21]. Our study suggests that instead of further increasing the margin width at surgery, an adaptive therapeutic approach may be considered, in which the radiation dose and its distribution are tailored to patients in subgroups with different levels of microscopic disease load, provided that these subgroups can be identified. Few study results are currently available on this 'dose-painting'-like concept [22--23], but none specifically for breast cancer. Nevertheless, this concept shows potential to benefit patients with uneven-diffused disease load [24].

Study novelty

To the best of our knowledge, this is the first study to explain the effect of the width of negative surgical margins on local-recurrence risk (the EORTC boost-vs-no-boost trial) in BCT by taking pathology information (the MARGINS study) into account.

Study limitations

Our study also has some limitations. First, we obtained the distributions of microscopic disease around the invasive index tumor from only 60 patients in the MARGINS study, while we used 1616 patients with a pathology review in the EORTC database. Patients in the MARGINS study received preoperative MRI. Multicentric disease detected at MRI was excluded in the MARGINS data but presumably present in the EORTC data. However, so far, no correlation has been found between the risk of LR and multicentric disease at MRI [25]. Moreover, the characteristics of patients in the EORTC group were matched to those in the MARGINS group.

The second limitation is that only WLE specimens were analyzed in the MARGINS study. The average thickness of the specimen slices is 4mm, which may result in disease undersampling at pathology. However, we applied the same sampling strategy to estimate the remaining disease quantity for all patients, so undersampling (which may affect the estimated volume, but is compensated by the estimated values of radiosensitivity and its variance in the simulation) is not expected to change the conclusion of our findings. Another issue is that disease may have been present in

regions beyond the surgical specimens in the MARGINS data, so that the quantity of surrounding microscopic disease may be underestimated. Nevertheless, large variations exist in the ability of surgeons to center the tumor in the excision [16]. Hence, in the overall population of patients, tissue information is available at close as well as at larger distances from the edge of the invasive tumor. Moreover, we made the assumption that the negative SRM width in the EORTC study can be directly compared to the distance to the edge of the index tumor in the MARGINS study, which may lead to an biased volume of residual microscopic disease in the remaining part of the breast. However, this is so far the best we can do, because little knowledge is available on the quantity of residual microscopic disease outside any resection margins. We could not use mastectomy specimens for detailed microscopic analysis, because mastectomy patients typically have different tumor characteristics than BCT patients and may not be readily compared to radiotherapy studies after BCT.

The third limitation is that we assumed the mean radiosensitivity of residual microscopic disease to be comparable within different patient subgroups and only varies according to a Gaussian distribution. Further, we did not consider the intra-patient radiosensitivity difference. More detailed analysis of radiosensitivity should be preformed in the future. Compared to the findings from our Monte-Carlo simulation with in-vivo data (0.58 Gy^{-1}), Ruiz de Almodóvar reported radiosensitivity values ranging from 0.1 to 0.6 Gy^{-1} using in-vitro experiments [26]. Guerrero and Li did a synthesis study with the data from three trials and obtained 0.3 Gy^{-1} [27]. However, they assumed the same radiosensitivity parameter for all patients and did not consider any heterogeneity. Webb [11] obtained a paired value ($\alpha_{\text{mean}} = 0.325 \text{ Gy}^{-1}$, $\alpha_{\text{std}} = 0.13 \text{ Gy}^{-1}$, $\rho = 10^9 \text{ cells/cm}^3$) by using the volume V estimated from the gross tumor diameter. However, the gross tumor is removed after BCS and the residual microscopic disease extension should be considered as the main contributor of local recurrence.

Conclusion

The impact of the negative margin width on local recurrence is limited due to the large variation of microscopic disease that can reach large quantities beyond any given distance from the edge of the index tumor. Due to this variation, the negative margin width is being observed as an insignificant parameter for prognosis in large trials. Rather than further increasing the width of the surgical margins, future developments in radiotherapy after breast-conserving surgery should focus on techniques to tailor the radiation dose to the expected distribution of surrounding microscopic disease.

Reference

- [1] Veronesi U, Cascinelli N, Mariani L, et al. Twenty-year follow-up of a randomized study comparing breast-conserving surgery with radical mastectomy for early breast cancer. *N Engl J Med* 2002;347:1227-32.
- [2] Darby SC, McGale P, Taylor CW, et al. Long-term mortality from heart disease and lung cancer after radiotherapy for early breast cancer: Prospective study of about 300,000 women in US SEER cancer registries. *Lancet Oncol* 2005;6:557–565.
- [3] Bartelink H, Horiot JC, Poortmans PM, et al. Impact of a higher radiation dose on local control and survival in breast-conserving therapy of early breast cancer: 10-year results of the randomized boost versus no boost EORTC 22881-10882 trial. *J Clin Oncol* 2007;25:3259-65.
- [4] Antonini N, Jones H, Horiot JC, et al. Effect of age and radiation dose on local control after breast conserving treatment: EORTC trial 22881-10882. *Radiother Oncol* 2007;82:265-71.
- [5] Jones HA, Antonini N, Hart AA, et al. Impact of pathological characteristics on local relapse after breast-conserving therapy: a subgroup analysis of the EORTC boost versus no boost trial. *J Clin Oncol* 2009;27:4939-47.
- [6] Park CC, Mitsumori M, Nixon A, et al. Outcome at 8 years after breast-conserving surgery and radiation therapy for invasive breast cancer: influence of margin status and systemic therapy on local recurrence. *J Clin Oncol* 2000;18:1668-75.
- [7] Touboul E, Buffat L, Belkacémi Y, et al. Local recurrences and distant metastases after breast-conserving surgery and radiation therapy for early breast cancer. *Int J Radiat Oncol Biol Phys* 1999;43:25-38.
- [8] Smitt MC, Nowels KW, Zdeblick MJ, et al. The importance of the lumpectomy surgical margin status in long-term results of breast conservation. *Cancer* 1995;76:259-67.
- [9] Holland R, Connolly JL, Gelman R, et al. The presence of an extensive intraductal component following a limited excision correlates with prominent residual disease in the remainder of the breast. *J Clin Oncol* 1990;8:113-8.

Chapter 3

- [10] Schmitz AC, van den Bosch MA, Loo CE, et al. Precise correlation between MRI and histopathology - Exploring treatment margins for MRI-guided localized breast cancer therapy. *Radiother Oncol* 2010;97:225-32.
- [11] Webb S. Optimum parameters in a model for tumour control probability including interpatient heterogeneity. *Phys Med Biol* 1994;39:1895-914.
- [12] Aperio Technologies Inc. A digital pathology solution for immunohistochemistry - Digital IHC - User's Guide. Part Number / Revision: Man-0099, Revision B 2009.
- [13] Chen W, Stroom J, Schmitz AC, et al. Tumour control probability for residual microscopic disease in breast conservation therapy. *Radiother Oncol* 2010;96(Suppl. 1):509.
- [14] Singletary SE. Surgical margins in patients with early-stage breast cancer treated with breast conservation therapy. *Am J Surg* 2002;184:383-93.
- [15] Taghian A, Mohiuddin M, Jagsi R, et al. Current perceptions regarding surgical margin status after breast-conserving therapy: results of a survey. *Ann Surg* 2005;241:629-39.
- [16] Pleijhuis RG, Graafland M, de Vries J, et al. Obtaining adequate surgical margins in breast-conserving therapy for patients with early-stage breast cancer: current modalities and future directions. *Ann Surg Oncol* 2009;16:2717-30.
- [17] Schmitz AC, Pengel KE, Loo CE, et al. Pre-treatment Imaging and Pathology Characteristics of Invasive Breast Cancers of Limited Extent – Potential Relevance for MRI-guided Localized Therapy. *Radiother Oncol* 2012, In press.
- [18] Stroom JC, Siedschlag C, Gilhuijs K. A Monte-Carlo study to improve the assessment of residual tumor load for postoperative irradiation of the breast. In: *Proceedings of the XVth International Conference on the Use of Computers in Radiation Therapy* (J Bissonnette, ed). Novel Digital Publishing, Oakville, Ontario. 2007;1:28-31.
- [19] Cowen D, Houvenaeghel G, Bardou V, et al. Local and distant failures after limited surgery with positive margins and radiotherapy for node-negative breast cancer. *Int J Radiat Oncol Biol Phys* 2000;47:305-12.
- [20] Freedman G, Fowble B, Hanlon A, et al. Patients with early stage invasive cancer with close or positive margins treated with conservative surgery and radiation have an

Impact of Negative Margin Width on Local Recurrence in Breast Conserving Therapy

increased risk of breast recurrence that is delayed by adjuvant systemic therapy. *Int J Radiat Oncol Biol Phys* 1999;44:1005-15.

[21] Vicini F, Baglan K, Kestin L, et al. The emerging role of brachytherapy in the management of patients with breast cancer. *Semin Radiat Oncol* 2002;12:31-9.

[22] Duprez F, De Neve W, De Gersem W, et al. Adaptive Dose Painting by Numbers for Head-and-Neck Cancer. *Int J Radiat Oncol Biol Phys* 2011;80:1045-55.

[23] Girinsky T, Ghalibafian M, Bonniaud G, et al. Is FDG-PET scan in patients with early stage Hodgkin lymphoma of any value in the implementation of the involved-node radiotherapy concept and dose painting? *Radiother Oncol* 2007;85:178-86.

[24] Bentzen SM, Gregoire V. Molecular imaging-based dose painting: a novel paradigm for radiation therapy prescription. *Semin Radiat Oncol* 2011;21:101-10.

[25] Solin LJ, Orel SG, Hwang WT, et al. Relationship of breast magnetic resonance imaging to outcome after breast-conservation treatment with radiation for women with early-stage invasive breast carcinoma or ductal carcinoma in situ. *J Clin Oncol* 2008;26:386-91.

[26] Ruiz de Almodóvar JM, Núñez MI, McMillan TJ, et al. Initial radiation-induced DNA damage in human tumour cell lines: a correlation with intrinsic cellular radiosensitivity. *Br J Cancer* 1994;69:457-62.

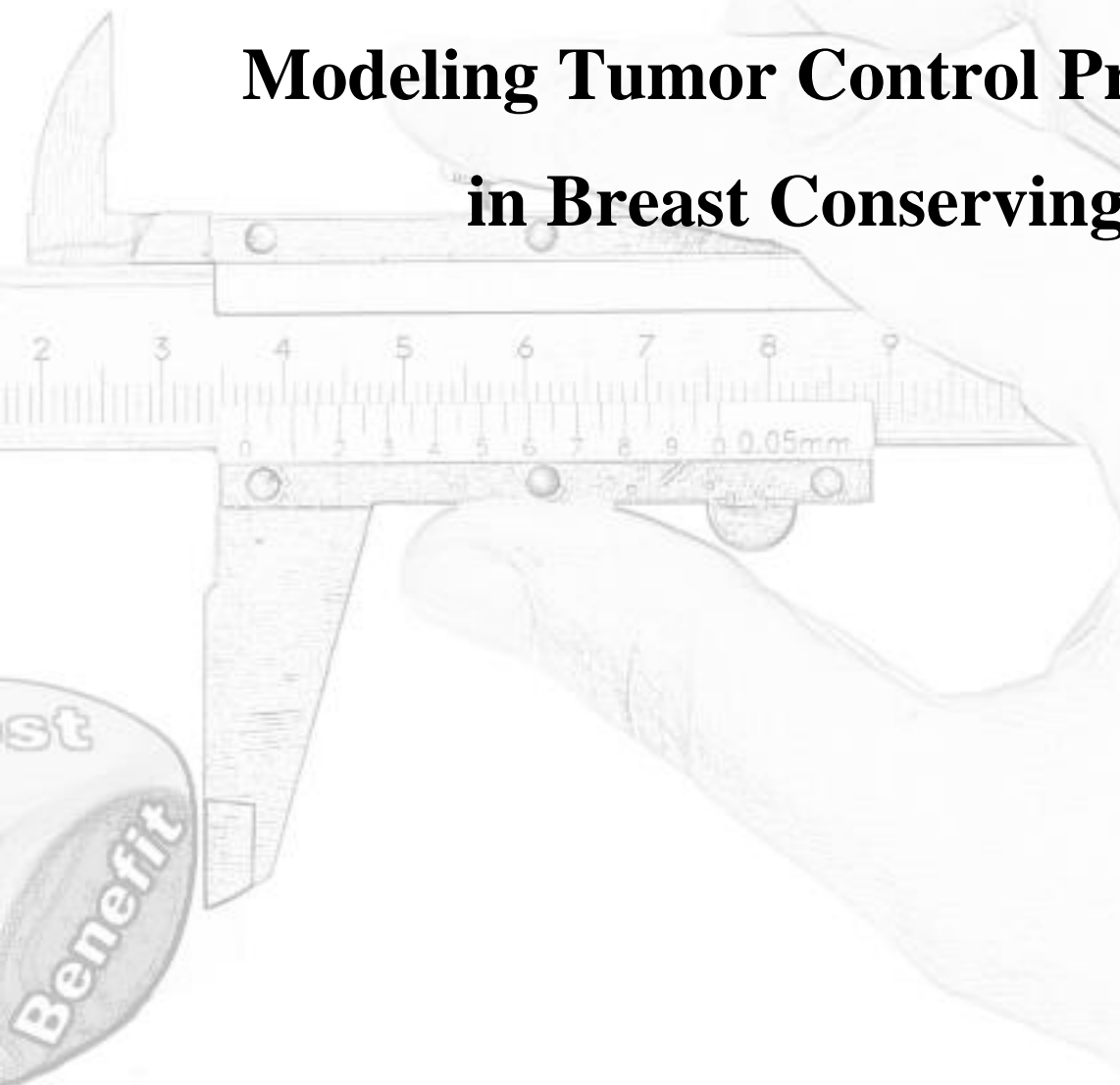
[27] Guerrero M, Li XA. Analysis of a large number of clinical studies for breast cancer radiotherapy: estimation of radiobiological parameters for treatment planning. *Phys Med Biol* 2003;48:3307-26.



Part II Risk Modeling Framework

Chapter 4

A Simulation Framework for Modeling Tumor Control Probability in Breast Conserving Therapy



Chen, Wei, Kenneth Gilhuijs, Joep Stroom, Harry Bartelink, and Jan-Jakob Sonke. "A simulation framework for modeling tumor control probability in breast conserving therapy." *Radiotherapy and Oncology* 111, no. 2 (2014): 289-295.

Abstract

Background and Purpose

Microscopic disease (MSD) left after tumorectomy is a major cause of local recurrence in breast conserving therapy (BCT). However, the effect of microscopic disease and RT dose on tumor control probability (TCP) was seldom studied quantitatively.

Materials and Methods

The simulation framework contains three components: disease load prediction, surgery simulation, and radiotherapy modeling. We first modeled total disease load and microscopic spread with a pathology dataset. Then we estimated the remaining disease load after tumorectomy through surgery simulation. The Webb-Nahum TCP model was extended by clonogenic cell fraction to model the risk of local recurrence. The model parameters were estimated by fitting the simulated results to the observations in two clinical trials.

Results

Higher histopathology grade has a strong correlation with larger MSD quantity. 12.5% of the MSD cells remained in the patient's breast after surgery on average. However, this fraction varies considerably among patients (0% to 100%); it indicates the high risk of omitting radiotherapy. A small fraction of cells is clonogenic (one in every 2700000 cells). The mean radiosensitivity was estimated at 0.067 Gy^{-1} with standard deviation 0.022 Gy^{-1} .

Conclusions

A relationship between radiation dose and TCP was established in a newly designed simulation framework with the detailed disease load, surgery and radiotherapy models.

Introduction

Breast cancer is the second leading cause of cancer death in women in Europe and the United States [1]. In the past decades it has been demonstrated that the treatment of early-stage breast cancer with breast conserving therapy (BCT) yields local tumor control and survival equivalent to mastectomy [2,3]. Typically, after conservative surgery in which the gross tumor is removed, the whole breast is treated with external beam radiotherapy (RT) of 40 to 50 Gy in 3 to 5 weeks, in order to reduce the risk of local recurrence (LR) due to microscopic disease (MSD). Since the results of the EORTC boost-vs-no-boost trial were published, showing significantly improved local control [4], a 16-Gy boost on the part of the tumor excision site especially in young breast cancer patients became a treatment of choice.

Application of a radiation boost field reduces local recurrence [5,6]. However, higher radiation dose may lead to inferior cosmetic outcome [7] and cardiac damage [8]. Further improvement of the balance between local control and normal tissue complication is thwarted by the long follow-up time and large patient numbers required to sufficiently power randomized controlled trials. If the relationship between patient characteristics, MSD, radiation dose and tumor control probability (TCP), is better understood, patients may be stratified more effectively by their risk following radiotherapy. As a result, trials can be powered more efficiently as comparing subgroups of patients at increased risk of local recurrence with those at reduced risk. Besides, applications of the more conformal radiation techniques become increasingly popular in BCT [9]. Managing the uncertainty on the MSD spread therefore becomes more important in treatment planning. There are, however, currently no models available that addressed these issues. Therefore, the aim of this study is to create statistical models that quantify the effectiveness of surgery and radiotherapy on MSD cell kills, and through a simulation framework to establish the relationship between MSD, radiation dose and TCP.

Material and Methods

Overview

We propose a Monte-Carlo simulation framework for analyzing the relationship between microscopic disease (MSD) and tumor control probability (TCP). We first present the pathology dataset of MSD load and spread distribution in the operated breasts, and then describe the outcome datasets of patient panel data that contain the TCP results with median 10 years follow-up. Finally, the simulation framework is explained in detail.

Pathology Dataset

One of the aims of the Multi-modality Analysis and Radiological Guidance IN breast-conserving therapy study (MARGINS) was to chart the presence of MSD around the primary invasive breast cancer [10]. Patients in this study underwent additional and more extensive assessment of the pathology specimen. More than 1800 microscopic slides of invasive breast cancers in sixty patients were examined by two experienced breast cancer pathologists [11]. The MSD around the primary invasive tumor was observed on the microscopic slides. The disease load and the distance from the bulk of the tumor were recorded after the geometric reconstruction of the pathology slides [10].

Outcome Datasets

In the European Organization for Research and Treatment of Cancer (EORTC) 22881-10882 (boost-versus-no-boost) trial [5], all patients underwent lumpectomy and auxiliary lymph node dissection followed by radiotherapy. After informed consent, patients after surgery were randomly assigned to receive whole breast irradiation (total dose of 50 Gy in 5 weeks with a dose per fraction of 2 Gy) with or without a boost of 16 Gy (2 Gy per fraction) on the tumor bed. The negative surgical margin width at pathology (minimal distance from specimen edge to tumor bulk) was measured for each patient in a subset of 1616 patients with central pathology review.

The Early Breast Cancer Trialists' Collaborative Group (EBCTCG) centrally reviewed the randomized trials for early-stage breast cancer worldwide every five years since

1985. The sixth cycle data in 2011 consisted of 10801 women from 17 trials [12]. The pooled results from 4138 patients in the breast-conserving surgery-only arm were selected to determine the TCP without radiotherapy after primary surgery.

Simulation Framework

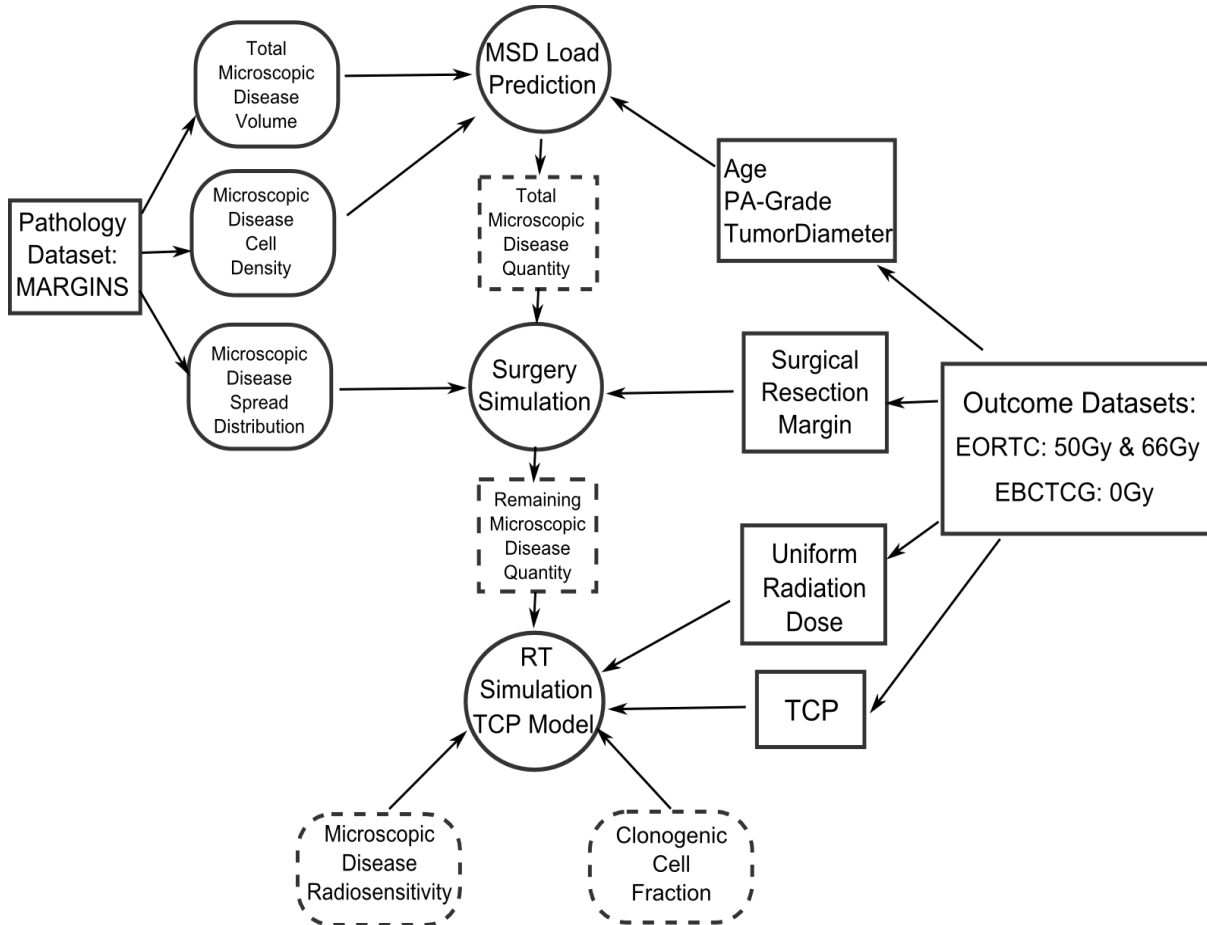
We designed a simulation framework to model the three following steps in breast conserving therapy: MSD load prediction, surgery and radiotherapy (Figure 1). In the MSD load prediction step (Stage 1), we built a quantitative model to estimate the total cell number of MSD and the spread distribution from the sixty patients in the MARGINS dataset. In the surgery step (Stage 2), we built a geometrical model for the operated breast and estimated the remaining quantity of MSD after the primary surgery. In the radiotherapy step (Stage 3), the irradiation of residual MSD was modeled following three RT protocols which were used in the past clinical trials (surgery only, uniform dose 50 Gy and uniform dose 50 Gy plus 16 Gy boost at the tumor bed). TCP was analyzed using an extended Webb-Nahum TCP model. We simulated ten thousand patients each time in our framework. In order to take into account uncertainties in outcome data, we repeated the simulations for fifty times. The resulting TCPs of the simulated patients were compared with the actual outcome data in the EORTC trial and the EBCTCG study. Consequently radiobiology parameters in the TCP model were optimized to minimize the difference between the simulation results and the clinical outcome results.

MSD Load Prediction (Stage 1)

The MSD load model (total cell number) was developed based on the pathology data and consisted of two components. The first component is a Zero-Inflated model for quantifying the MSD volume of patients [13]. We chose the Zero-Inflated model because a relatively large proportion of patients (17 out of 60) in the pathology study did not have microscopic disease around the invasive tumor. Hence, the fit by a simple linear regression model would be deteriorated by a large proportion of zeros. We considered three covariates in our model which include age at diagnosis, tumor histopathology grading (PA-Grade) and tumor diameter, because these covariates were previously recognized as the most influential factors that affect TCP in most randomized

trials [14]. We then applied the classical backwards selection method using the Akaike information criterion [15] to find the optimal combination of covariates. Note that MSD is occult at any breast imaging (ultrasonography, mammography and MRI). Hence, the estimated total MSD volume was only based on the pathology data.

Figure 1: The flow chart of our simulation framework. The round modules represent the simulation steps; the square modules represent the statistics obtained from the outcome datasets; the round-cornered square modules represent the mathematical model derived from the pathology dataset; and the modules with dashed borders represent the model parameters obtained through this simulation framework.



The second component of the total MSD load model was a Gaussian model of cell density. This cell density was estimated from a set of 36 digitized microscopy slides

selected from twelve patients (top seven oldest patients and top five youngest patients) using a special slide scanner and a cell-counting software (Aperio Technologies Inc., US [16]). The average and the standard deviation of the MSD cell density of these twelve patients were calculated and fitted in the Gaussian model. Finally, the total MSD load for each simulated patient was estimated as the product of her MSD volume and cell density [17].

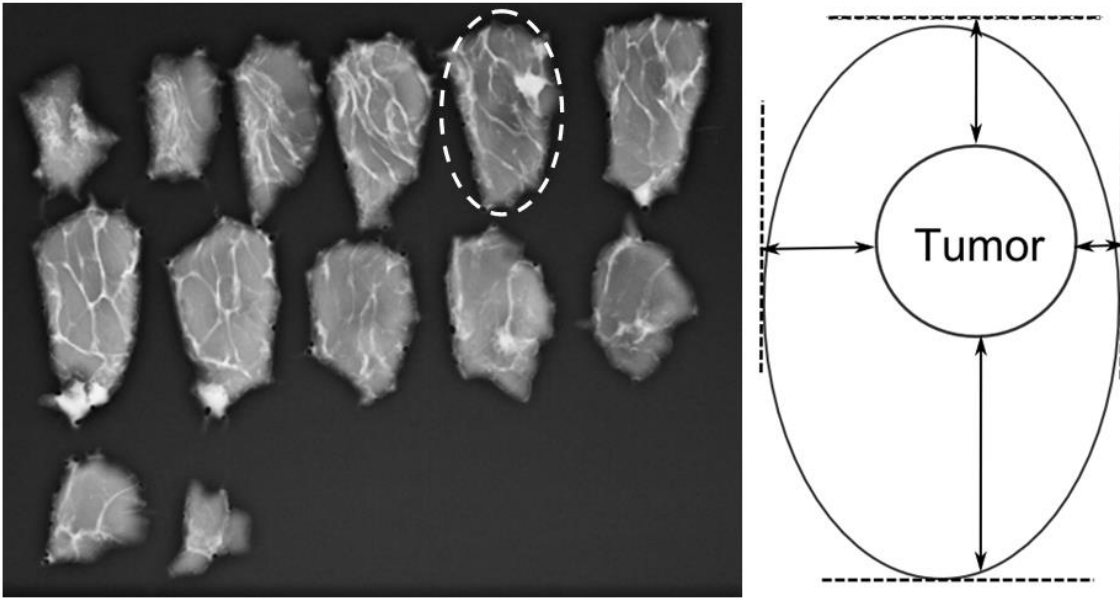
We also quantified the MSD spread distribution around the invasive tumor as a function of distance to the edge of invasive tumor using a normalized term of MSD. This normalized term represents the ratio of the MSD load at each distance over the total MSD load for each patient. For example, if we only found 5×10^7 cells, 2×10^7 cells and 3×10^7 cells at the distances of 1mm, 5mm and 10mm respectively from the nearest edge of the invasive tumor, the normalized ratios of this patient would be 0.5, 0.2 and 0.3 at distances of 1mm, 5mm and 10mm and zeros at the other distances. We fitted the normalized ratios of each patient with a discretized truncated Gaussian model (at the distance of 1 mm, 2mm, etc., until 30 mm) and found that the means and standard deviations of these fitted truncated Gaussian models can be described with a negative binomial distribution and a Poisson distribution, respectively. To obtain a new spread distribution for a simulated patient, we generated a random number from the negative binomial distribution for the mean of the truncated Gaussian model and a random number from the Poisson distribution for the standard deviation of the truncated Gaussian model. Finally, we obtained all the thirty values of the normalized ratios from the truncated Gaussian model of this patient. This MSD spread distribution was used in the simulation of surgery in the next section.

Surgery (Stage 2)

In our simulation, it is assumed that the invasive tumor was always removed with surrounding normal tissue by surgery. The remaining MSD quantity after surgery was approximated as the difference between the total MSD load estimated in the first stage and the expected MSD load in the removed normal tissue. By simplifying the shape of the surgical resection specimen to an ellipsoid (Figure 2), the removed volume was

calculated based on the six surgical margins in three orthogonal directions. The surgical margin in each direction was usually anisotropic [10]. We first evaluated statistical models to describe the distribution of margins and then generated some simulated values for each patient as described below.

Figure 2: Four surgical margins were measured from the slicing plane of macro-pathology specimen and the other two surgical margins perpendicular to the slicing plane were approximated by the number of slices without invasive tumor.



The minimal surgical resection margin (MinSRM) was subtracted from six surgical margins for twenty patients in the MARGINS dataset resulting in the ‘normalized’ margins. We then modeled the sum of two normalized margins in the opposite direction using the Poisson distribution. We chose the Poisson model based on experience of observation. The partition ratio of each normalized margin over the corresponding sum of two was fitted to a Beta-distribution model due to the characteristics of data.

To obtain the six margins in each virtual patient, we first simulated the MinSRM of the virtual patients by adopting the fitted probability density of the MinSRM from the EORTC outcome dataset and then applied two above models to obtain the margin sums of three

orthogonal directions and the partition ratios of two directions (one margin is set to be the MinSRM which indicated zero for one partition ratio). With these data, we could calculate the remaining five margins besides MinSRM for each virtual patient. Finally, the volume of normal tissue within the ellipsoid around gross tumor was considered to be removed such that the expected MSD load after surgery was decreased correspondingly.

Radiotherapy (Stage 3)

We extended the Webb-Nahum TCP model [18] for our purposes. Specifically, we considered remaining MSD cell quantity as a variable among patients and separated the MSD cells into two categories: indolent cells and clonogenic cells. We considered that only clonogenic cells contribute to the risk of local recurrence and proposed a factor named clonogenic cell fraction (CCF), being the ratio of the number of clonogenic MSD cells over the number of total MSD cells. CCF was introduced to model the TCP for surgery only patients receiving 0 Gy dose. We tested the importance of introducing CCF into our TCP model by examining the null hypothesis that every MSD cell is clonogenic. The TCP formula can be written as

$$TCP = \int_V \int_\rho \int_\alpha f_V f_\rho f_\alpha \exp[-c V \rho \cdot \exp(-D \cdot \alpha)] dV d\rho d\alpha,$$

where V , ρ , c , α , and D represent the remaining MSD volume after surgery, cell density, CCF, MSD radiosensitivity and prescribed dose, respectively. f_V , f_ρ and f_α were the probability distribution function of the corresponding parameter, which represent the variation across the patient population.

Model Parameters and Dose-TCP Relationship

MSD volume, cell density and TCP were obtained from the pathology dataset and the outcome datasets. The radiosensitivity and CCF parameters were unknown and estimated through the proposed TCP model. Note that only three treatment results were considered, which include two traditional treatments (50 Gy & 66 Gy) in the EORTC dataset and breast conserving surgery (where we assumed patients received 0 Gy) in

the EBCTCG dataset. The parameter estimation problem was casted into a Bayesian simulation framework where the uncertainties on the TCP results of three treatments were taken into account [19]. In other words, we maximized the Gaussian likelihood function of the estimated TCP from simulated patients using the mean and the standard deviation of TCPs from the three corresponding treatments in the outcome datasets. We obtained the unknown parameters in two steps. First by setting the radiation dose to zero in the equation, we ruled out the effect of the radiosensitivity on TCP and obtained the estimate of the CCF after running our simulation framework for fifty times. Second we considered the CCF as a known variable in the equation and obtained the mean and standard deviation of the radiosensitivity in a similar manner. To estimate the relationship between radiation dose and TCP, we utilized the TCP model by varying the dose parameter in calculation. To account for the uncertainty of estimates, we randomly generated a hundred sets of parameters in the framework based on their distributions and obtained a correlation between the radiation dose and TCP for each set. The average and the confidence interval of these correlations were reported.

Results

MSD Load Prediction

Only the baseline coefficients and the covariates of tumor grade remained significant in our zero-inflated model using the backwards selection method. The total microscopic disease (MSD) volume was positively associated with higher tumor grade (Table 1). For example, the patients with tumor grades I, II or III had average MSD volumes of 198 mm³, 288 mm³ or 447 mm³, respectively. Besides, the probability of patients having no MSD extension decreased with higher tumor grade. The average MSD cell density was 450000 cells/mm³ +/- 84000 cells/mm³ (1 SD). The fitted spread distribution model (Table 2) was compared with the observed data in Figure 3.

Surgery

We found that in the EORTC dataset a large proportion of these margins were scored at 5 mm intervals, which might be caused by rounding effect introduced at pathology

(Figure 4). Therefore, we blurred the sampling of the biased observation (every 5 mm) with a simple Gaussian model ($SD = 2$). We obtained the parameters in the surgery simulation and their corresponding 95% confidence intervals (Table 2). Based on this simulation method, we found that the average quantity of MSD per patient decreased from 104000000 cells before surgery to 13000000 cells after surgery such that 12.5% of the total MSD cells remained after surgery. This fraction varied between patients from 0 to 100% with a large standard deviation as large as 17.2%, which indicates a large range of outcomes for surgery performance and the high risk of omitting radiotherapy.

Table 1: Regression results in the MSD load prediction model.

Geometric model coefficients :			
	Estimate	Std. Error	P-value
(Intercept)	3.524	0.407	< 0.001
Histopathology Grade	0.406	0.197	0.0391
Zero-inflated part coefficients:			
	Estimate	Std. Error	P-value
(Intercept)	1.732	0.937	0.0645
Histopathology Grade	-1.886	0.696	0.0068

Table 2: The estimated parameters in our simulation framework. The negative binomial model and the first Poisson model are used in the MSD spread model in the first stage. The Beta model and the second Poisson model are used in the surgery simulation in the second stage. CCF and the mean and the standard deviation of radiosensitivity are used in the TCP model in the third stage.

	Estimate	95% Confidence Interval
Negative Binomial μ	5.64	4.38 ~ 6.90
Scale	2.72	1.06 ~ 4.38
Poisson (Spread)	2.59	2.11 ~ 3.07
Poisson (Margin)	17.37	16.31 ~ 18.42
Beta (symmetric)	1.477	1.010 ~ 1.944

CCF	$3.66 \cdot 10^{-7}$	$1.89 \cdot 10^{-7} \sim 5.43 \cdot 10^{-7}$
Radiosensitivity <i>mean</i>	0.067	0.060 ~ 0.074
Radiosensitivity <i>sd.</i>	0.022	0.013 ~ 0.030

Figure 3: The means and the standard deviations of the normalized MSD load ratios (the percentage of the MSD load at each distance over the total MSD load per patient) in the pathology dataset and the fitted model. The dot points represent the mean of ratios for sixty patients in the pathology dataset and the triangle points represent the mean of ratios estimated from the truncated Gaussian model. The error bars represent one standard deviation of data at each distance.

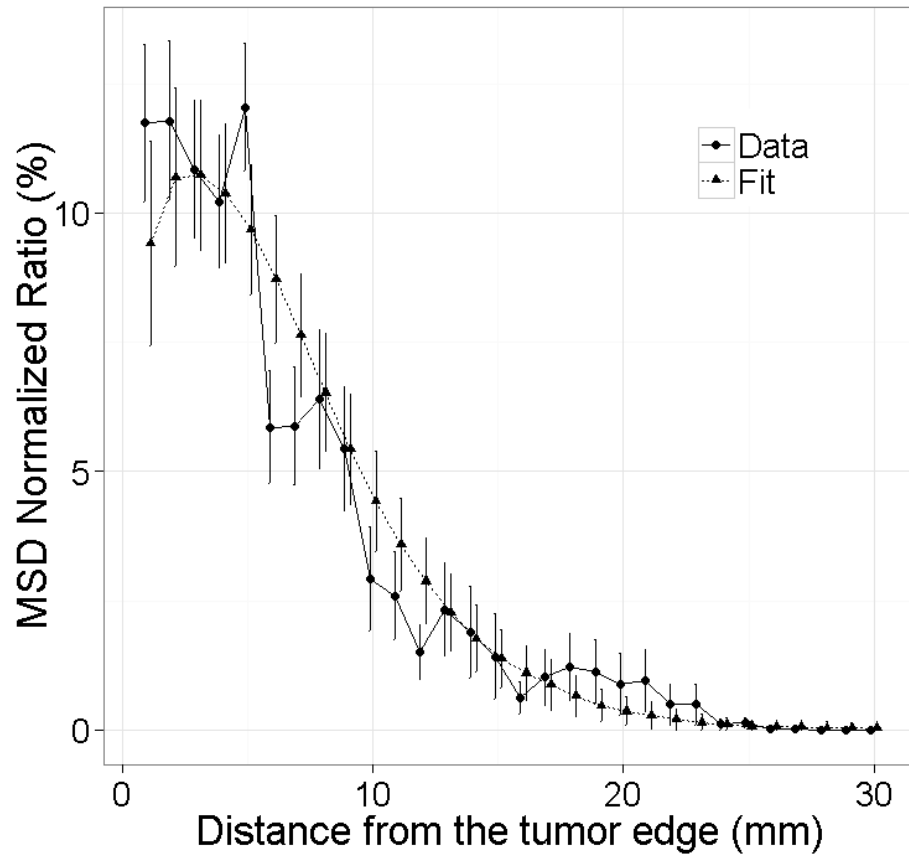
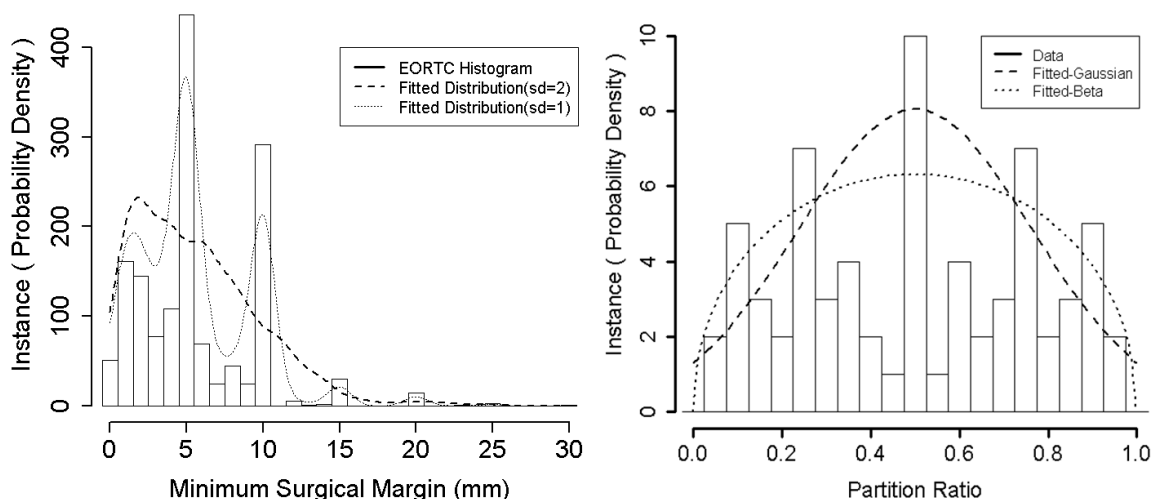


Figure 4: (Left) The probability density distribution of minimum surgical margin in the EORTC dataset. The biased observation on every five millimeter interval is compensated by a diffused sampling strategy with a standard Gaussian model. (Right) The probability density distribution of the partition ratios as the normalized surgical margin over the sum of two in the opposite direction. The original data is fitted to a Gaussian model and a Beta model. We chose to use the Beta model for further analysis in the following sections.



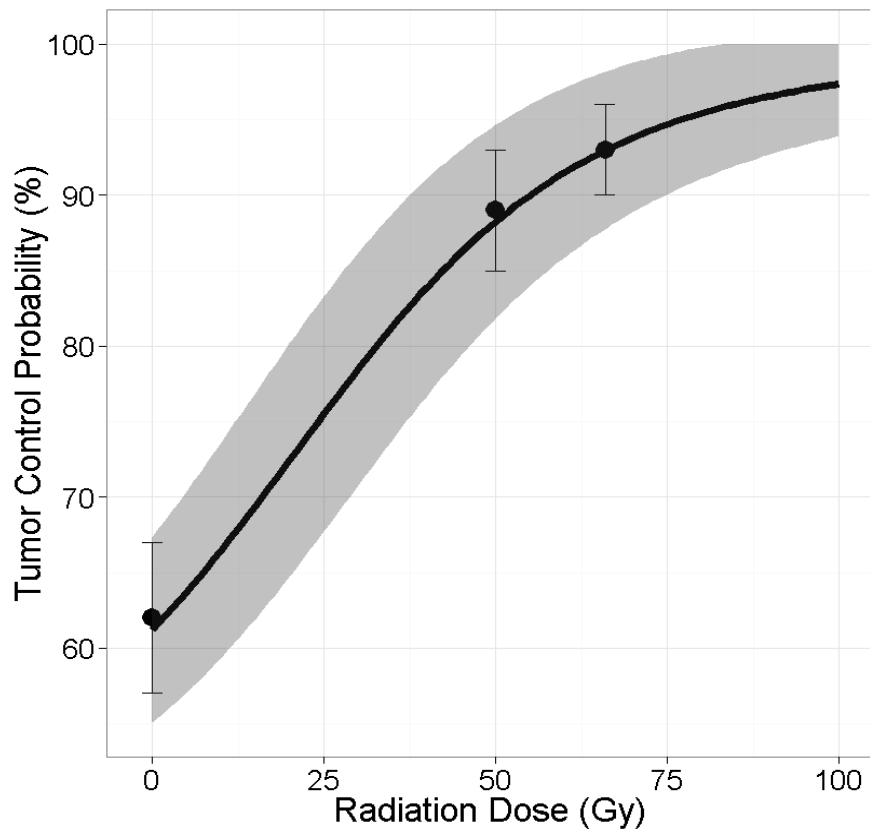
Radiotherapy

The estimated clonogenic cell fraction (CCF) and radiosensitivity parameters are shown in Table 2. The null hypothesis of ignoring CCF was rejected at 1% level of significance, which indicates the importance to know that only a small fraction of MSD cells are clonogenic. Using these estimated parameters, we obtained the quantitative relationship between radiation dose and the predicted TCP at 10 years (Figure 5). We observed that the TCP is increased with the increased prescription dose; however we cannot reach 100% TCP even with 100 Gy as the model predicted. We also observed that the uncertainty of the outcomes decreases with the increased prescription dose.

Figure 5: The obtained relationship between radiation dose and TCP which were estimated with a hundred groups of framework parameters. The black curve represents the mean of the estimates and the shade area represents the 95% confidence interval.

Chapter 4

The dot points represent the true clinical data with the 95% confidence interval on the top of them.



Discussion

Our proposed framework for simulating breast conserving therapy established the relationship between microscopic disease (MSD), surgical margin, radiation dose and tumor control probability through a quantitative model. To analyze MSD quantity in each treatment stage, we modeled the quantity and the spread distribution and simulated the effect of quantity change by surgery and radiotherapy. Clonogenic cell fraction and radiosensitivity parameters in our TCP model were estimated through comparing the simulation results with the true observations from the clinical trials. Finally, we obtained the quantitative relationship between radiation dose and tumor control probability.

Most previous studies on the risk of local recurrence after breast conserving therapy are based on the regression analysis of outcome data observed through clinical randomized

trials [20]. Various clinical and histopathologic factors, immunohistochemical markers and molecular subtypes have been applied as prognosticators. Some are referred to as therapy predictors, since they allow the oncologists the choice of a specific therapy [21]. However, heterogeneity in outcome exists even when patients have the same predictors [4]. Hence, a Monte-Carlo simulation framework may be more suitable for TCP modeling because the analysis is tailored to individual patient characteristics.

Our modeling framework considers the MSD quantity and change thereof before and after breast conserving surgery and radiotherapy. It explains the risk of local recurrence from MSD quantity and cell kills. Prediction of remaining microscopic disease volume after primary surgery for individual patient has been attempted before [22], however, it proved inaccurate in other datasets [23]. Hence, we applied a stochastic model in predicting the MSD quantity and carefully utilized it on a population-based simulation. The inaccuracy of individual prediction is improved by modeling group variance. In addition to the MSD quantity, the spread distribution of MSD also plays a significant role in the risk model [24]. The MSD spread was previously modeled with exponential distribution [25] or half Gaussian [24]. Similarly, we chose to use the truncated Gaussian model with normalized ratios so that MSD quantity is disassociated with MSD spread. Previously, patients were selected for accelerated partial breast irradiation based on the risk of local recurrence [26]. However, the treatment plans could not be optimized further due to the lack of knowledge about the MSD spread distribution. Our framework provides the feasibility to optimize TCP to a population-based MSD spread distribution with inhomogeneous dose. For instance, with different surgical margins, the MSD spread distribution of patients may differ considerably. The radiation dose may be optimized for the different distributions.

For predicting the total volume of microscopic disease in breast patients, we only chose to use the histopathology grade of tumor rather than patient age and the diameter of tumor, because the limited number of patients in our pathology data did not provide sufficient statistical power to consider all three factors simultaneously in our prediction model. We therefore applied the backward selection method to choose the best

candidates from these three factors. Also, some strong correlations between patient age, histopathology grade and tumor diameter were found previously [27].

Tumor control probability models for breast cancer have been studied extensively [28]. However, consensus on the values of radiosensitivity for cancerous cell has not yet been reached. Guerrero et al. analyzed three clinical studies and obtained a plausible set of radiobiological parameters with $\alpha = 0.3 \text{ Gy}^{-1}$, $\alpha/\beta = 10 \text{ Gy}$ [29]. A more recent study [30] showed that α/β ratio should be much lower based on the result of the retrospective analysis on different fractionation scheme of ten randomized trials. In their paper [30], they found α is a much smaller value (0.08 Gy^{-1}) and α/β is equal to 3.89 Gy. The reason for the smaller α can be that only a small proportion of MSD cells are clonogenic [31]. In our study, we also obtained a small α (0.067 Gy^{-1}) in the Webb-Nahum TCP model, however we should point out our α is the sum of α_{LQ} and $2 \times \beta_{\text{LQ}}$ in the standard linear-quadratic model. Assuming $\alpha/\beta = 3.89 \text{ Gy}$, we find an α_{LQ} is equal to 0.044 and comparable to the result in [30].

Breast conserving therapy is a combination treatment based on the collaborative effort from surgery, pathology, radiotherapy and medical oncology. However, the information transition is often limited between each department; therefore the treatment outcome could not be optimized further within the structure of the individual department. For instance, the width of negative surgical margins were not used in the planning step of radiotherapy and the whole breast was irradiated to compromise the outcome uncertainty as the consequence [17]. Our study indicates that even if a very large dose such as 100 Gy is given to the whole breast of patients, the tumor control probability at 10 years will not reach 100% within the current clinical treatment setting. It indicates that the optimization should be performed at the hospital level instead of the department level as the current situation. Our framework therefore can be applied as the foundation of the simulation for the changes in the treatment settings.

A Simulation Framework for Modeling Tumor Control Probability in Breast Conserving Therapy

Several limitations of our study should be mentioned. First, despite complete embedding of the resection specimens, it was likely that the MSD was still under-sampled at pathology. The resection specimens were first sliced macroscopically with 4 mm interval and then further trimmed and examined on microscopic slices with 4 μ m thickness. To account for this issue, we performed a robustness test in which we varied the MSD quantity by a scaling factor applied to the original sixty patient data in the MARGIN dataset. We found that the relationship between radiation dose and TCP was not affected by this scaling factor. Conversely, CCF was linearly dependent on this change. This can be explained by the fact that the baseline TCP (0 Gy) is only affected with CCF when the RT dose is set to zero in Equation (2). This result illustrates that the undersampling issue at pathology did not deteriorate the accuracy of the estimated dose-response relationship in our framework.

Second, the adjuvant therapy was more frequently used to treat patients and our framework does not include the effect of chemotherapy or hormone therapy. However, to the best of our knowledge, this work is the first one that attempts to model the local procedures in the breast conserving therapy in a quantitative manner. To correct for the impact of systemic treatment on local control after BCT, one may approximate the answer by multiplying the local recurrence risk with a correction factor of 0.5, if adjuvant therapy was used. As it is well demonstrated both Tamoxifen and chemotherapy reduces the local recurrence risk after BCT by half, as seen for example in the complete data of the boost-versus-no-boost trial of 5318 patients [14].

Third, we assumed that the disease spread observed in the MARGINS dataset was comparable to that in the EORTC dataset and the EBCTCG dataset. Fourth, we assumed the EBCTCG dataset has similar minimal surgical margins as the EORTC dataset. Fifth, the microscopic cell density was estimated from only 12 patients. Finally, we assumed that all MSD cells received the prescribed dose, ignoring dose heterogeneity and setup errors.

Conclusion

The effectiveness of surgery and radiotherapy on microscopic disease cell kills was quantified with our statistical models. The relationship between microscopic disease, radiation dose and tumor control probability was established through the simulation framework.

Reference

- [1] Ma J, Jemal A. Breast Cancer Statistics. In: Ahmad A, editor. Breast Cancer Metastasis Drug Resist., Springer New York; 2013, p. 1–18.
- [2] Fisher B, Anderson S. Twenty-year follow-up of a randomized trial comparing total mastectomy, lumpectomy, and lumpectomy plus irradiation for the treatment of invasive breast cancer. *N Engl J Med* 2002;347:1233–41.
- [3] Litière S, Werutsky G, Fentiman IS, Rutgers E, Christiaens M-R, Van Limbergen E, et al. Breast conserving therapy versus mastectomy for stage I-II breast cancer: 20 year follow-up of the EORTC 10801 phase 3 randomised trial. *Lancet Oncol* 2012;13:412–9.
- [4] Bartelink H, Horiot J-C, Poortmans P, Struikmans H, van den Bogaert W, Barillot I, et al. Recurrence rates after treatment of breast cancer with standard radiotherapy with or without additional radiation. *N Engl J Med* 2001;345:1378–87.
- [5] Bartelink H, Horiot J-C, Poortmans PM, Struikmans H, Van den Bogaert W, Fourquet A, et al. Impact of a higher radiation dose on local control and survival in breast-conserving therapy of early breast cancer: 10-year results of the randomized boost versus no boost EORTC 22881-10882 trial. *J Clin Oncol* 2007;25:3259–65.
- [6] Antonini N, Jones H, Horiot JC, Poortmans P, Struikmans H, Van den Bogaert W, et al. Effect of age and radiation dose on local control after breast conserving treatment: EORTC trial 22881-10882. *Radiother Oncol* 2007;82:265–71.
- [7] Curran D, Dongen J Van. Quality of life of early-stage breast cancer patients treated with radical mastectomy or breast-conserving procedures: results of EORTC Trial 10801. *The European. Eur J Cancer* 1998;34:307–14.
- [8] Darby SC, Ewertz M, McGale P, Bennet AM, Blom-Goldman U, Brønnum D, et al. Risk of ischemic heart disease in women after radiotherapy for breast cancer. *N Engl J Med* 2013;368:987–98.
- [9] Sheets NC, Goldin GH, Meyer A-M, Wu Y, Chang Y, Stürmer T, et al. Intensity-modulated radiation therapy, proton therapy, or conformal radiation therapy and morbidity and disease control in localized prostate cancer. *JAMA* 2012;307:1611–20.

Chapter 4

- [10] Stroom J, Schlief A, Alderliesten T, Peterse H, Bartelink H, Gilhuijs K. Using histopathology breast cancer data to reduce clinical target volume margins at radiotherapy. *Int J Radiat Oncol Biol Phys* 2009;74:898–905.
- [11] Schmitz AC, Pengel KE, Loo CE, van den Bosch MAA, Wesseling J, Gertenbach M, et al. Pre-treatment imaging and pathology characteristics of invasive breast cancers of limited extent: Potential relevance for MRI-guided localized therapy. *Radiother Oncol* 2012;104:11–8.
- [12] Darby S, McGale P, Correa C, Taylor C, Arriagada R, Clarke M, et al. Effect of radiotherapy after breast-conserving surgery on 10-year recurrence and 15-year breast cancer death: meta-analysis of individual patient data for 10,801 women in 17 randomised trials. *Lancet* 2011;378:1707–16.
- [13] Cheung YB. Zero-inflated models for regression analysis of count data: a study of growth and development. *Stat Med* 2002;21:1461–9.
- [14] Werkhoven E Van, Hart G, Tinteren H Van, Elkhuisen P, Collette L, Poortmans P, et al. Nomogram to predict ipsilateral breast relapse based on pathology review from the EORTC 22881-10882 boost versus no boost trial. *Radiother Oncol* 2011;100:101–7.
- [15] Echeverria AE, McCurdy M, Castillo R, Bernard V, Ramos NV, Buckley W, et al. Proton therapy radiation pneumonitis local dose-response in esophagus cancer patients. *Radiother Oncol* 2013;106:124–9.
- [16] Cardiff RD, Hubbard NE, Engelberg JA, Munn RJ, Miller CH, Walls JE, et al. Quantitation of fixative-induced morphologic and antigenic variation in mouse and human breast cancers. *Lab Invest* 2013;93:480–97.
- [17] Chen W, Stroom J, Sonke J-J, Bartelink H, Schmitz AC, Gilhuijs KG. Impact of negative margin width on local recurrence in breast conserving therapy. *Radiother Oncol* 2012;104:148–54.
- [18] Webb S, Nahum AE. A model for calculating tumour control probability in radiotherapy including the effects of inhomogeneous distributions of dose and clonogenic cell density. *Phys Med Biol* 1993;38:653.
- [19] Alía A, Mar J, Pastor-Barriuso R. Reliability of portal control procedure in irradiation of breast cancer: a Bayesian analysis. *Radiother Oncol* 2005;75:28–33.

- [20] Van der Leij F, Elkhuizen PHM, Bartelink H, van de Vijver MJ. Predictive factors for local recurrence in breast cancer. *Semin Radiat Oncol* 2012;22:100–7.
- [21] Goldhirsch A, Glick JH, Gelber RD, Coates AS. Meeting Highlights : International Consensus Panel on the Treatment of Primary Breast Cancer. *J Clin Oncol* 2001;19:3817–27.
- [22] Margenthaler J a, Gao F, Klimberg VS. Margin index: a new method for prediction of residual disease after breast-conserving surgery. *Ann Surg Oncol* 2010;17:2696–701.
- [23] Fisher CS, Klimberg VS, Khan S, Gao F, Margenthaler JA. Margin index is not a reliable tool for predicting residual disease after breast-conserving surgery for DCIS. *Ann Surg Oncol* 2011;18:3155–9.
- [24] Stroom J, Gilhuijs K, Vieira S, Chen W, Salguero J, Moser E, et al. Combined Recipe for Clinical Target Volume and Planning Target Volume Margins. *Int J Radiat Oncol Biol Phys* 2013.
- [25] Chao KSC, Blanco AI, Dempsey JF. A conceptual model integrating spatial information to assess target volume coverage for IMRT treatment planning. *Int J Radiat Oncol* 2003;56:1438–49.
- [26] Polgár C, Van Limbergen E, Pötter R, Kovács G, Polo A, Lyczek J, et al. Patient selection for accelerated partial-breast irradiation (APBI) after breast-conserving surgery: recommendations of the Groupe Européen de Curiethérapie-European Society for Therapeutic Radiology and Oncology (GEC-ESTRO) breast cancer working group ba. *Radiother Oncol* 2010;94:264–73.
- [27] Vrieling C, Collette L, Fourquet a, Hoogenraad W., Horiot J-C, Jager J., et al. Can patient-, treatment- and pathology-related characteristics explain the high local recurrence rate following breast-conserving therapy in young patients? *Eur J Cancer* 2003;39:932–44.
- [28] Keall PJ, Webb S. Optimum parameters in a model for tumour control probability, including interpatient heterogeneity: evaluation of the log-normal distribution. *Phys Med Biol* 2007;52:291–302.
- [29] Guerrero M, Li XA. Analysis of a large number of clinical studies for breast cancer radiotherapy: estimation of radiobiological parameters for treatment planning. *Phys Med Biol* 2003;48:3307–26.

Chapter 4

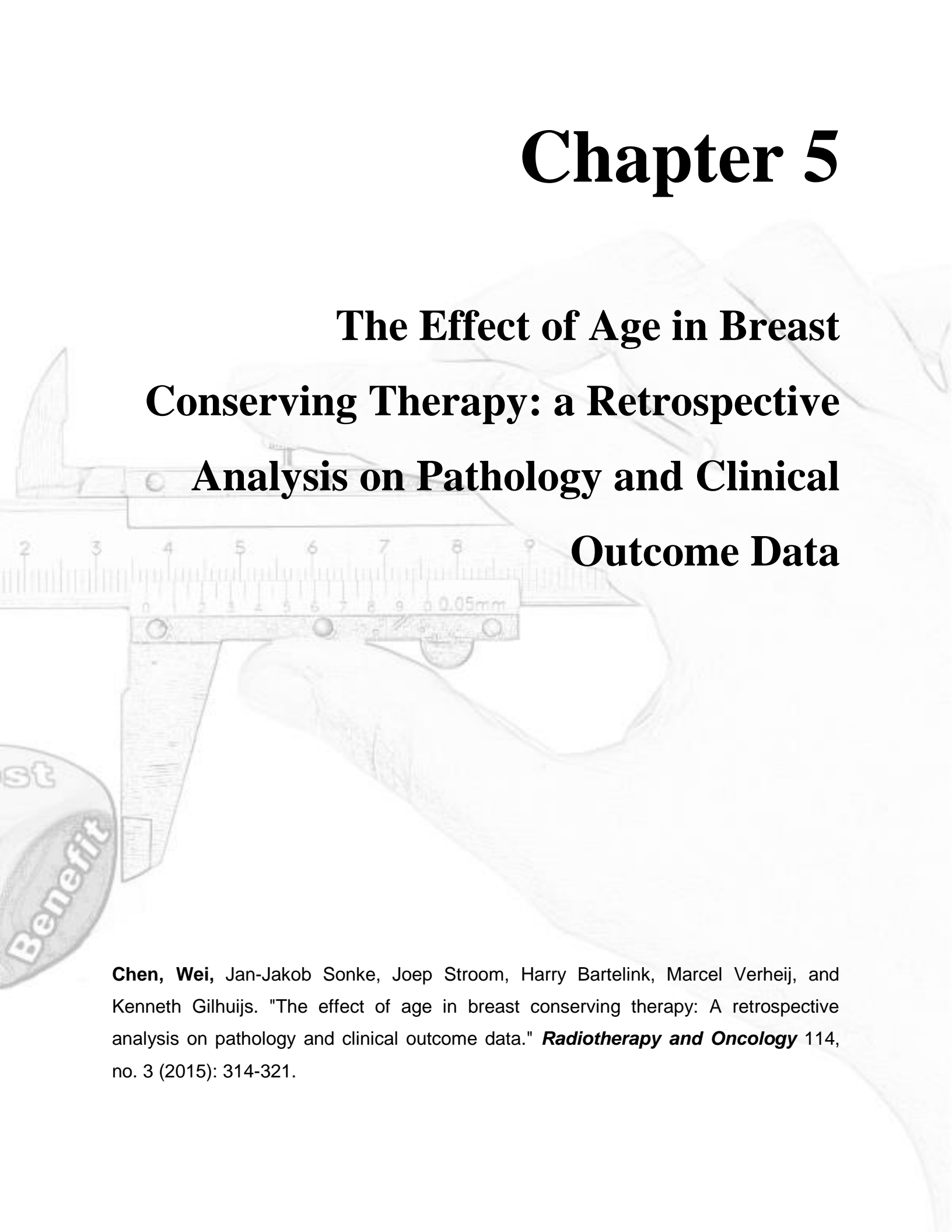
[30] Qi XS, White J, Li XA. Is α/β for breast cancer really low? Radiother Oncol 2011;100:282–8.

[31] Driessens G, Beck B, Caauwe A, Simons BD, Blanpain C. Defining the mode of tumour growth by clonal analysis. Nature 2012;488:527–30.



Chapter 5

The Effect of Age in Breast Conserving Therapy: a Retrospective Analysis on Pathology and Clinical Outcome Data



Chen, Wei, Jan-Jakob Sonke, Joep Stroom, Harry Bartelink, Marcel Verheij, and Kenneth Gilhuijs. "The effect of age in breast conserving therapy: A retrospective analysis on pathology and clinical outcome data." *Radiotherapy and Oncology* 114, no. 3 (2015): 314-321.

Abstract

Background and Propose

Age is an important prognostic marker of patient outcome after breast conserving therapy; however, it is not clear how age affects the outcome. This study aimed to explore the relationship between age with the cell quantity and the radiosensitivity of microscopic disease (MSD) in relation to treatment outcome.

Materials and Methods

We employed a treatment simulation framework which contains mathematic models for describing the load and spread of MSD based on a retrospective cohort of breast pathology specimens, a surgery simulation model for estimating the remaining MSD quantity and a tumor control probability model for predicting the risk of local recurrence following radiotherapy.

Results

The average MSD cell quantities around the primary tumor in younger (age \leq 50 years) and older patients were estimated at 1.9×10^8 cells and 8.4×10^7 cells, respectively ($P < 0.01$). Following surgical simulation, these numbers decreased to 2.0×10^7 cells and 1.3×10^7 cells ($P < 0.01$). Younger patients had smaller average surgical resection volume (118.9 cm^3) than older patients (162.9 cm^3 , $P < 0.01$) but larger estimated radiosensitivity of MSD cells (0.111 Gy^{-1} versus 0.071 Gy^{-1} , $P < 0.01$).

Conclusion

The higher local recurrence rate in younger patients could be explained by larger clonogenic microscopic disease cell quantity, even though the microscopic disease cells were found to be more radiosensitive.

Introduction

For many women with early-stage breast cancer, breast conserving therapy (BCT) has become a favorable option due to the comparable survival rates as those after mastectomy and better cosmetic outcome [1]. Despite the good results of BCT, younger patients (age \leq 50) are still at increased risk of breast cancer recurrence compared with older patients [2,3]. Underlying this observation may be differences in tumor biology [4], adjuvant systemic therapy [5], and margin status [6]. Indeed, young patient age is associated with increased risk of positive resection margins [7]. One possible explanation may be larger disease load in younger patients [6], although this hypothesis has not been investigated in detailed pathology studies.

The correlation between tumor control and age were studied previously. In 1994, Nixon reported a higher frequency of adverse pathological factors (necrosis, pathology grade, etc.) seen in patients under 35 years of age [8]. Zhou studied 130 patients under age 40, supported the previous result and argued that the majority of the breast excisions should be performed with careful evaluation of microscopic margin status [9]. However, very few studies to date have examined the combined effect of surgical margins and age on local control rates.

In this study, we focused on the potential role of pathology and radiobiology differences to explain differences in treatment local control between younger and older patients. For this purpose we employed a previously developed treatment simulation framework [10] to model the treatment outcome. We aimed specifically at answering three questions:

- (1) Does age affect the quantity of microscopic tumor cells?
- (2) Does age affect the radiosensitivity of these tumor cells?
- (3) Which factor, if any, plays a more important role, quantity or radiosensitivity?

Material and Methods

Overview

In order to study the effect of patient age on the outcome of breast conserving therapy (BCT), we deployed a retrospective analysis of patients in two different age groups: patients at age 50 years or below, and patients older than 50 years [3]. The effect on the treatment local control was analyzed by tracking the change in microscopic disease (MSD) quantity around the primary tumor after each treatment component through an earlier developed simulation framework [10]. In short, this framework contains three sequential stages: disease load prediction, surgery simulation and radiotherapy (RT) modeling. MSD quantity and spread distribution was first estimated using a patient model derived from a retrospective cohort of pathology data. The simulated surgery was performed and the remaining MSD quantity was quantified using typical surgical resection margins. The tumor control probability (TCP) was estimated using an extended Webb-Nahum model and compared with local control in separate datasets. In the following subsections, we first describe the pathology dataset and the outcome datasets, and then explain how the simulation framework was employed to model the effect of age on TCP.

Pathology Dataset

We used the pathology data from the MARGINS (Multi-modality Analysis and Radiological Guidance IN breast-conServing therapy) study to model the MSD quantity and spread distribution in the breasts of patients with early breast cancer eligible for breast conserving therapy [11]. More than 1800 microscopic slides of invasive breast cancers in 60 patients (48 patients with age >50 and 12 with age ≤ 50) were examined by two experienced breast cancer pathologists [12,13]. MSD was observed on the microscopic slides. The disease quantity and distance from the primary tumor were recorded after slice three-dimension reconstruction. The MSD cell densities were estimated using a nuclei counting software on digitalized microscopic slides [14].

The Effect of Age in Breast Conserving Therapy: a Retrospective Analysis on Pathology and Clinical Outcome Data

Outcome Datasets

In the EORTC (European Organization for Research and Treatment of Cancer) 22881-10882 (boost-versus-no-boost) trial [15], a subset of 1616 patients with central pathology review showed that an increased risk of local recurrence was associated with age younger than 50 years and omission of a boost dose of 16 Gy to the tumor bed [16]. We accordingly separated our data into four groups to calculate the local control rates. These four groups were younger patients (≤ 50 years) with and without a boost, and older patients (> 50 years) with and without a boost.

In addition to the EORTC trial data, we used data from the EBCTCG (Early Breast Cancer Trialists' Collaborative Group), who centrally reviewed the randomized trials performed world-wide in early breast cancer every five years since 1985. The sixth cycle data in 2011 consists of 10801 women from 17 trials [17]. The reported result of 4138 pooled patients who only received breast conserving surgery (BCS) (i.e., no RT) was selected to determine the baseline values in the two age groups at 0 Gy dose.

Disease Load Prediction

To model disease quantity as a function of age, a Zero-Inflated Model was employed [10]. To estimate disease cell density, we selected 36 pathology slides from the five youngest patients and the seven oldest patients and analyzed the difference between these two groups. The cell density data in the two age groups were fitted separately to a Gaussian model.

The MSD spread model was described as disease quantity within each 1 mm distance from the edge of the macroscopic tumor relative to the total quantity recorded for each patient. The MSD spread distribution (thirty relative ratios) of each patient was modeled with a truncated Gaussian distribution independently. The mean and the standard deviation of these truncated Gaussian models were described with a negative binomial distribution and a Poisson distribution, respectively. The mean of the Gaussian model describes the center of disease load and the standard deviation parameter of the

Gaussian model indicates how wide the distribution of tumor cells was. The parameters of the spread model were compared using Student-t tests between two groups.

Surgery Simulation

The remaining MSD in the operated breast was estimated as the difference between the total MSD quantity and that within the volume of the tissue removed together with the macroscopic tumor. It was previously reported that younger patients have a larger probability of smaller excision volumes [18]. We compared the distribution of the negative surgical margins in the two age groups in the EORTC dataset using the Kolmogorov-Smirnov test and incorporated this difference in excision volumes between the two age groups within our surgery simulation module. As reported previously [10], the removed tissue around the primary tumor in the MARGINS dataset was estimated using the surgical margins in six directions. The sum of surgical margins minus minimal surgical resection margin was modeled with a Poisson distribution. The asymmetry in each direction was modeled with a Beta distribution. We compared the parameters of the Poisson model and the Beta model using Student-t tests. The similarity of the remaining MSD quantities between the two age groups was evaluated using the Mann-Whitney U test because the estimated values did not follow a Gaussian distribution.

Radiotherapy Modeling

The estimated remaining MSD quantity after simulated surgery was taken as the input into the extended Webb-Nahum TCP model [19] to model the local control of radiotherapy. The unknown parameters in the TCP model (i.e., MSD radiosensitivity, clonogenic cell fraction¹) were estimated by fitting the simulation results to the clinical outcome for three different treatments: uniform irradiation with 50 Gy, 50Gy plus 16 Gy boost and no radiation (i.e., 0 Gy). We defined the local control rate at median 10 year follow-up as the TCP of the patients. We then compared the clonogenic cell fraction (CCF) between the two groups of patients using Mann-Whitney U test as the estimated

¹ Clonogenic cell is a cell that has the potential to proliferate and give rise to a colony of cells. We assume only a proportion of microscopic disease cells are clonogenic [19].

The Effect of Age in Breast Conserving Therapy: a Retrospective Analysis on Pathology and Clinical Outcome Data

values of CCF across patients do not follow a Gaussian distribution. We used Student-t tests for comparing the mean and standard deviation of radiosensitivity.

Statistical Tests

We ran all statistical tests on the open-source software R². A Bayesian Inference framework was implemented with the software package 'mcmc' (Markov Chain Monte Carlo simulation). In order to quantify the statistical accuracy, we designed a framework to implement our simulations one-hundred times and ran the statistical tests one-hundred times accordingly. We reported the combined p-value as the average of all p-values times two with 1.0 as maximum [20]. The rejection of the null hypothesis for equivalence was reported at the 0.05 level of significance.

Factors potentially associated with TCP

To further study which patient/tumor/clinical factors underlie the inferior outcome of younger patients, we explored two scenarios in which we tested the impact of four factors on the dose-TCP relationship: total disease quantity before surgery, surgical effect (removed tissue volume and disease spread), clonogenic cell fraction, and radiosensitivity of tumor cells. In the first scenario, we estimated the dose-TCP relationship using the average parameter values over older and younger patients in three of the four factors while the remaining factor was set to the average of the two age groups separately. Consequently, the heterogeneity between patients was ignored and the effect of age on each of four specific factors was observed.

In the second scenario, patient heterogeneity was taken into account. To that end, the heterogeneity with the combined population of older and younger patients was modeled for three out of four parameters while modeling the remaining parameter separately for the two age groups. Similarly, we compared the variation of dose-TCP relationship by age difference on each of four factors.

² www.r-project.org

For both scenarios and all four factors we estimated the dose-TCP relationships separately. The effect of age on TCP was analyzed by comparing the difference in TCP results between the younger and older groups with the varying radiation dose.

Results

Disease Load Prediction

The total microscopic disease (MSD) volume was negatively associated with age ($P=0.03$) (Table 1). The probability of a patient having zero MSD increased with age but a significant difference between the two age groups was not observed. Therefore, we discarded the age term in the zero-inflated part of the model. As a result, younger patients had an estimated average (one standard deviation (SD)) MSD volume of 431 (632) mm^3 compared to MSD in older patients: 180 (241) mm^3 .

Table 1: Regression parameters in Zero-inflated Geometric Model. The quantity was modeled with the Geometric distribution and a larger-proportion of zeroes was corrected with the Zero-inflation part of the model.

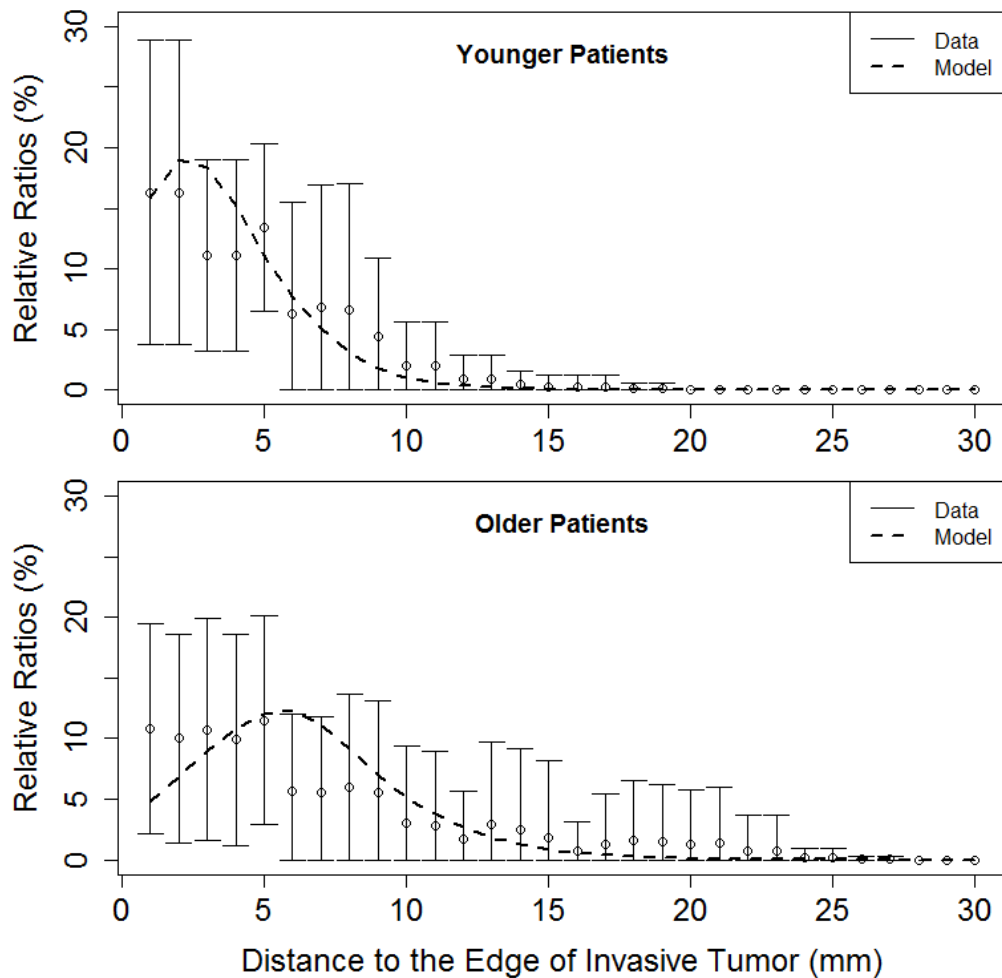
Geometric model coefficients:			
	Estimate	Std. Error	P-value
Intercept	4.09	0.18	<0.001
Age≤50	0.77	0.35	0.028
Zero-inflation model coefficients:			
Intercept	-0.98	0.30	<0.001

The average cell density of MSD in younger patients was measured at 4.8×10^5 cells/ mm^3 (SD 5.9×10^4 cells/ mm^3) (N=5). In older patients, the average MSD cell density was 4.3×10^5 cells/ mm^3 (SD 9.5×10^4 cells/ mm^3) (N=7). No significant difference between cell densities was found between these two age groups. Therefore in the following sections we modeled the cell density using one single model. We took the average as 4.5×10^5 cells/ mm^3 and the standard deviation as 8.4×10^4 cells/ mm^3 from the twelve patients.

The Effect of Age in Breast Conserving Therapy: a Retrospective Analysis on Pathology and Clinical Outcome Data

Regarding the distribution of disease spread, the mean and the standard deviation of the relative quantity ratios per shell are shown in Figure 1. We observed a larger tail in the distribution for older patients while the disease is more focused around the macroscopic tumor for younger patients. The results from the Student-t test showed that the parameters in the Negative Binomial distribution and the Poisson distribution of the spread model are significantly different between the two age groups (Table 2).

Figure 1: Relative ratios of disease quantity (disease quantity in a shell over total disease quantity) as a function of distance to the edge of macroscopic tumor for both patient groups derived from pathology data. The circles represent the average and the error bars represents one standard deviation for each shell.



Surgery Simulation

Significant difference in the negative surgical margin width was not found in the two age groups in the EORTC dataset ($P=0.27$). However, we found significant differences between margin widths of the specimen in the pathology dataset (Table 2). The average width of the surgical margin was 23.6 mm in the older age group, and 17.6 mm in the younger age group. We found that the removed volume of tissue was significantly smaller in younger patients than in older patients ($P<0.01$), while the average tumor diameter was slightly larger in younger patients (17.7 mm vs. 16.6 mm). Younger patients had $1.2 \times 10^2 \text{ cm}^3$ tissue removed on average (standard deviation: $1.1 \times 10^2 \text{ cm}^3$), ranging from 1.3 cm^3 to $1.1 \times 10^3 \text{ cm}^3$ (a normal breast size is roughly between $1.7 \times 10^2 \text{ cm}^3$ and $2.7 \times 10^3 \text{ cm}^3$ [21]). The average removed tissue volume in older patients was $1.6 \times 10^2 \text{ cm}^3$ (standard deviation: $1.5 \times 10^2 \text{ cm}^3$), ranging from 1.1 cm^3 to $1.5 \times 10^3 \text{ cm}^3$.

Table 2: The estimated parameters from our simulation framework. The Negative Binomial model and the first Poisson model (Spread) are used in the MSD spread model in Disease Load Prediction. The Beta model and the second Poisson model (Margin) are used in Surgery Simulation. CCF and the mean and the standard deviation of radiosensitivity are used in the TCP model in Radiotherapy Modeling. (CI=Confidence Interval)

	Patients ≤ 50 years		Patients > 50 years		Combined P-value
	Estimate	95% CI	Estimate	95% CI	
Negative Binomial	3.92	[2.5 - 5.3]	6.87	[5.7 - 9.0]	<0.001
<i>Mu</i>					
Scale	15.25	[1.5 - 95.2]	3.91	[3.0 - 4.9]	0.576
Poisson (Spread)	2.67	[2.1 - 3.4]	3.32	[2.8 - 4.0]	0.013
Poisson (Margin)	12.23	[11.3 - 13.9]	17.85	[16.9 - 18.9]	<0.001
Beta (symmetric)	1.97	[1.3 - 2.6]	1.34	[1.1 - 1.7]	<0.001
Clonogenic Cell	1.86×10^{-5}	$[4.3 \times 10^{-7} -$	2.57×10^{-7}	$[0.5 \times 10^{-7} -$	<0.001

The Effect of Age in Breast Conserving Therapy: a Retrospective Analysis on Pathology and Clinical Outcome Data

Fraction		$8.5 \cdot 10^{-5}$]		$4.8 \cdot 10^{-7}$]	
Radiosensitivity <i>mean</i> (Gy^{-1})	.111	[.091 -	.071	[.050 - .091]	<0.001
		.132]			
Radiosensitivity <i>s.d.</i> (Gy^{-1})	.037	[.030 -	.018	[.012 - .023]	<0.001
		.044]			

After simulated surgery, younger patients had significantly larger quantity of MSD remaining in the breast ($P < 0.01$). The average MSD quantity in younger patients was decreased from $1.9 \cdot 10^8$ cells to $2.0 \cdot 10^7$ cells. The percentage of the remaining MSD quantity over the original MSD quantity for younger patients ranged from 0 to 100% with a mean (1SD) of 10.4 (18.1)%. The average MSD quantity in older patients was decreased from $8.4 \cdot 10^7$ cells to $1.3 \cdot 10^7$ cells by surgery. The mean (1SD) percentage of reduction was 16.4 (25.1) %, range 0%-100%.

Radiotherapy Modeling

The tumor control probabilities in the two age groups in the EORTC boost-versus-no-boost trial and the EBCTCG collective study are listed in Table 3. Note that the average TCP in the EORTC study is larger than the average TCP in the EBCTCG study, but falls into the 95% confidence interval of the EBCTCG study [17]. We took the TCP outcome at 10 years in the breast conserving surgery (BCS) arm only in the EBCTCG dataset and the 50 Gy and 66 Gy radiotherapy arm in the EORTC dataset. We estimated the clonogenic cell fractions for younger and older patients to be one in $5.2 \cdot 10^4$ cells and one in $3.7 \cdot 10^6$ cells respectively ($P < 0.001$; Table 2). The mean radiosensitivity in the younger age group was estimated at 0.111 Gy^{-1} , and in the older age group at 0.071 Gy^{-1} ($P < 0.001$). The standard deviations were 0.037 Gy^{-1} in the younger age group and 0.018 Gy^{-1} in the older age group ($P < 0.001$).

Table 3: The TCP outcome of patients with an median 10 year follow-up in the EBCTCG dataset [17] and the EORTC dataset [15]. (BCS=Breast Conserving Therapy, RT=Radiation Therapy, CI=Confidence Interval)

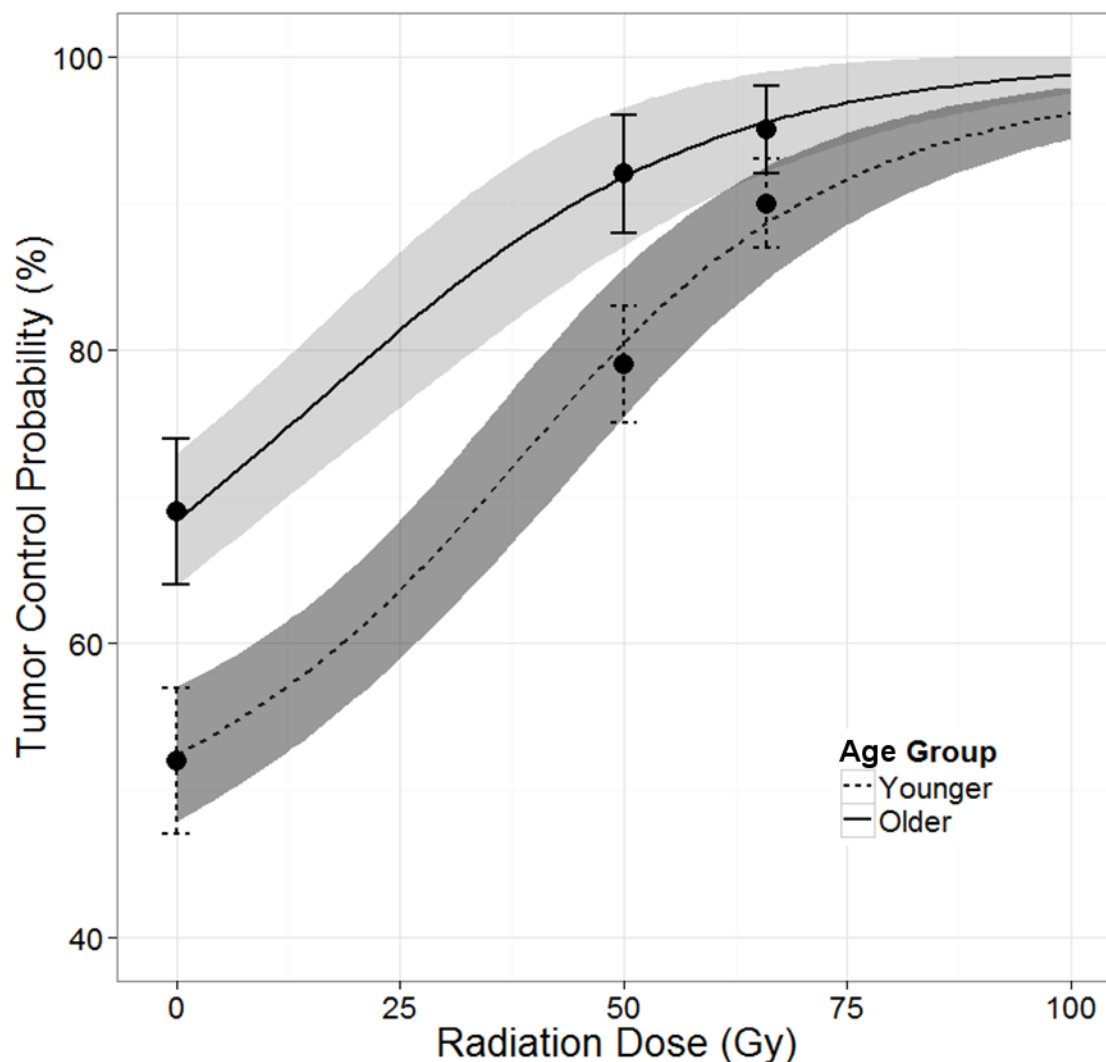
Outcome TCP	BCS only ³	BCS + RT 50Gy	BCS + RT 66Gy
Age ≤ 50 years	52%	78.9%	89.9%
95% CI	[47% - 56%]	[73.9% - 83.5%]	[86.2% - 93.1%]
# Patients	932	273	296
Age > 50 years	69%	92.5%	95.6%
95% CI	[67% - 72%]	[90.1% - 94.6%]	[93.6% - 97.2%]
# Patients	3206	528	519

With the above estimated model parameters, we obtained the relationship between radiation dose and TCP (Figure 2). These two dose-TCP curves for the two age groups had different slopes. In the younger patient group, a higher absolute increase of TCP with the same increase of radiation dose was observed, but the starting point (TCP after breast conserving surgery only) was significantly lower.

Figure 2: The relationship between radiation dose and TCP in the different age groups. The shaded areas indicate the 95% confidence interval of the estimates. The error bars represent the reported clinical outcome from the EORTC and the EBCTCG studies.

³ In EBCTCG study, patients were separated into five categories by age. We took the first two categories as the younger patients and the other as the older patients.

The Effect of Age in Breast Conserving Therapy: a Retrospective Analysis on Pathology and Clinical Outcome Data



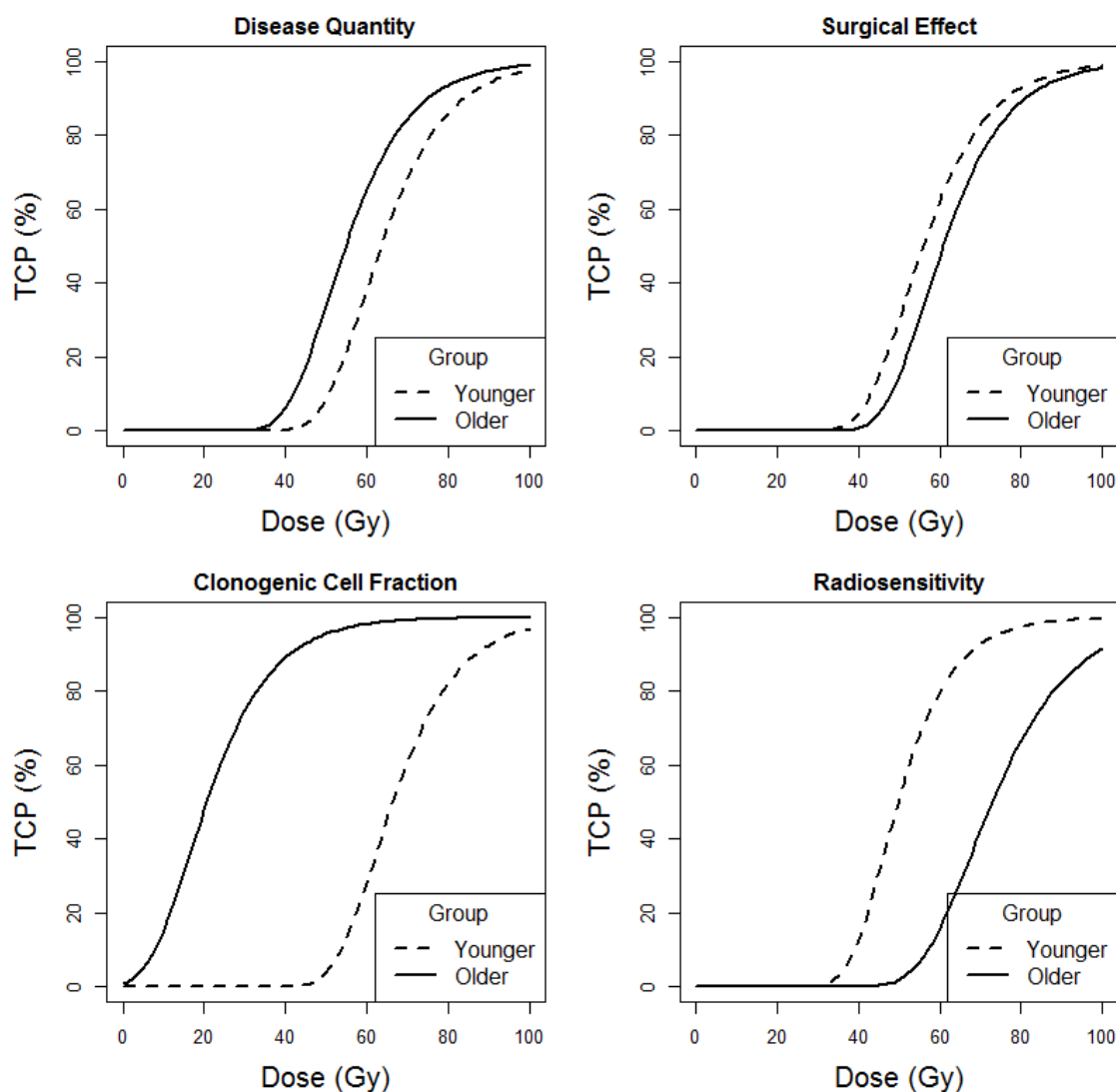
Factors potentially associated with TCP

Comparison of the impact of four factors on TCP for the first scenario is illustrated in Figure 3. It was observed that total disease quantity and clonogenic cell fraction play an important role in explaining the inferior outcome of younger patients while surgery and the radiotherapy have more positive impact on younger patients. Note that by modeling that every patient had the same amount of non-zero residual clonogenic cells, the dose-response curve starts at zero TCP at zero dose.

In the second scenario, including realistic patient heterogeneity, we obtained a similar result as for the first scenario but with smaller differences between two groups (Figure

4). The TCP difference by age for these four factors is shown in Figure 5. We found the difference in TCP was increasing with increasing dose for radiosensitivity to reach a maximum at 59 Gy. Differences in surgery had little impact on the TCP and were mostly compensated by large radiation dose. Total MSD quantity of younger patients had a negative impact on TCP and this impact was gradually reduced by increasing dose after 23 Gy. The clonogenic cell fraction was the most important factor we may use to explain the difference in TCP between younger and older patients.

Figure 3: The dose-TCP relationship curves for younger and older patients stratified for different factors that affect TCP in the first scenario. The dash curve represents the result for younger patients; the solid curve represents the result for older patients.



The Effect of Age in Breast Conserving Therapy: a Retrospective Analysis on Pathology and Clinical Outcome Data

Figure 4: The dose-TCP relationship curves for younger and older patients stratified for different factors that affect TCP in the second scenario. The dash curve represents the result of younger patients; the solid curve represents the result of older patients.

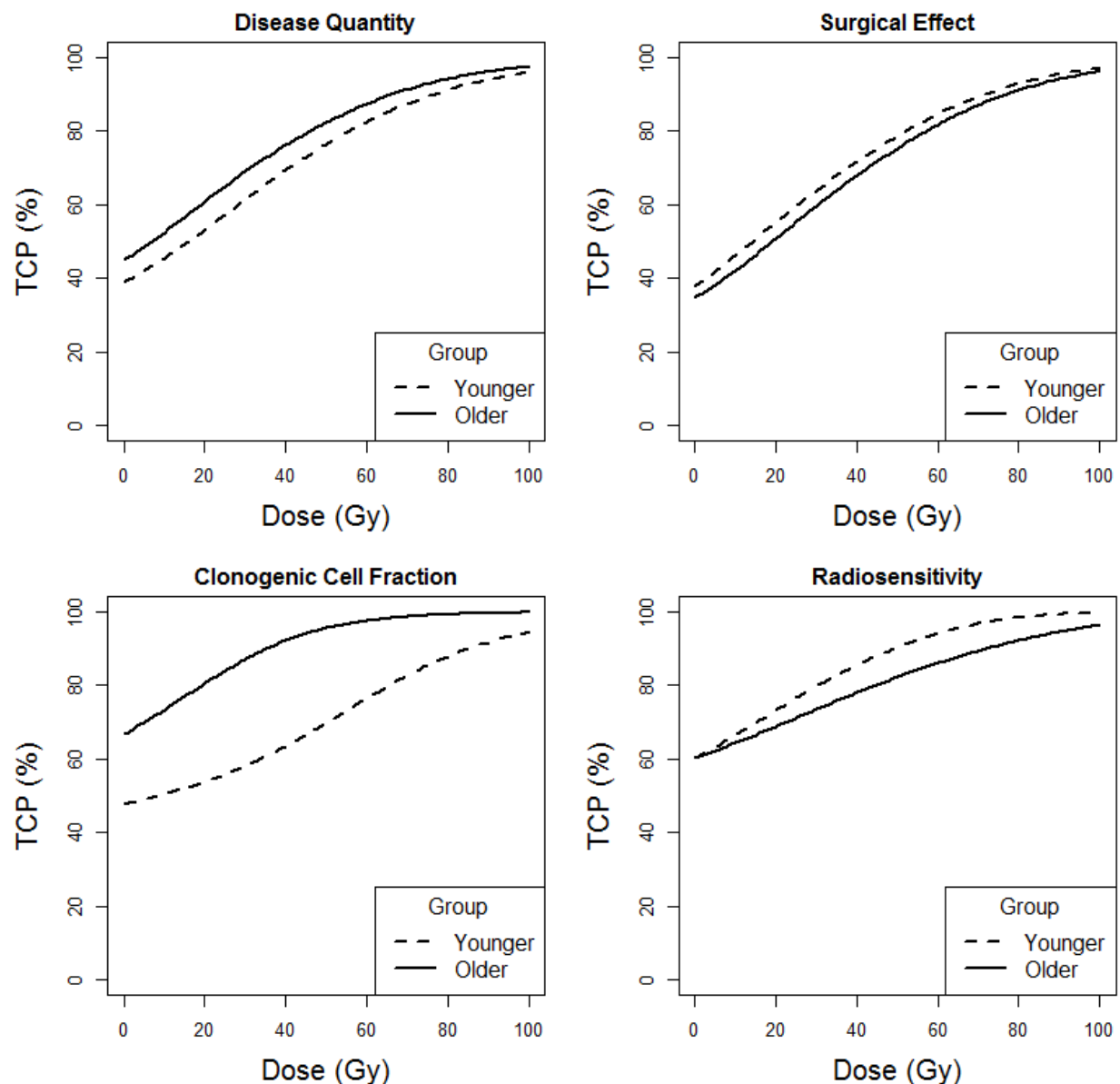
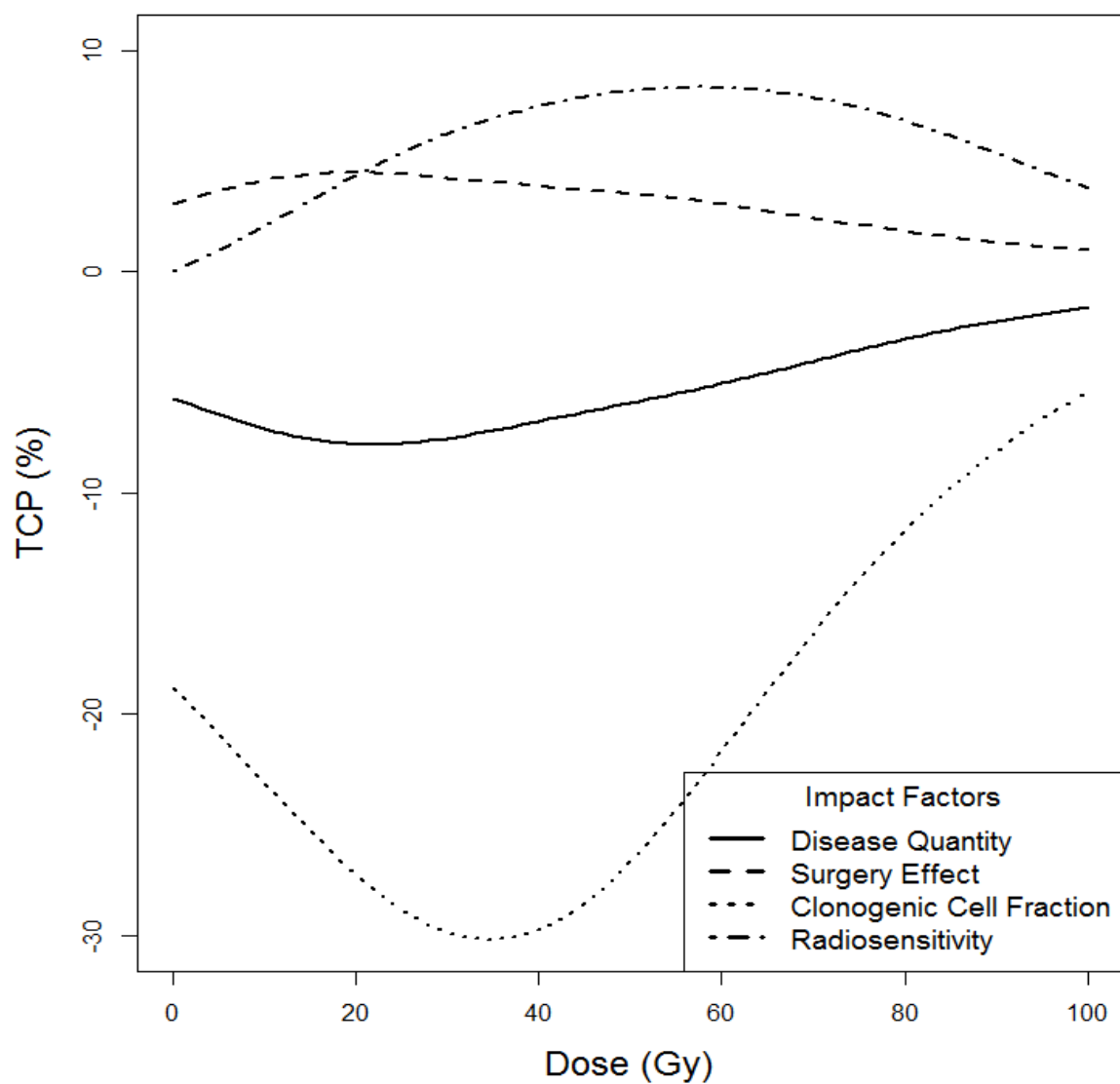


Figure 5: The TCP difference curves as a function of radiation doses for the four factors impacting treatment outcome between the two age groups. Total MSD quantity (solid), surgery effect (dash), clonogenic cell fraction (dot) and radiosensitivity (dash-dot).



Discussion

This study aimed to explain the effect of age on the tumor control probability (TCP) in patients undergoing breast conserving therapy (BCT) for early-stage breast cancer. To pursue this goal, we used a simulation framework which contains mathematic models for describing the load and spread of microscopic disease (MSD) based on a retrospective cohort of breast pathology specimens, a surgery simulation model for estimating the remaining disease quantity and a TCP model for predicting the risk of local recurrence. The results indicated that the inferior outcome in younger patients may be explained by larger total MSD quantity and larger clonogenic cell fraction (CCF), even though MSD cells in the younger patients are more radiosensitive.

An overview of clinical trial data has shown that breast conserving surgery (BCS) should be followed by radiotherapy to achieve results comparable with mastectomy in terms of recurrence and survival [3]. However, the value of radiotherapy (RT) after BCS in older breast cancer patients is still subject of debate [3,22]. In the current clinical setting, over 60% of breast cancer patients are diagnosed at the age above 50 years. The treatments of these older patients vary and the outcome differ [23]. For some older women, breast conserving surgery without radiation may be used to minimize potential treatment-related complications [24]. Gruenberger et al. suggested that radiation may be safely omitted for low-risk tumors in women over age 60 years [22]. Unfortunately, different results were reported by the Harvard 2006 pilot study [25] and the Italian randomized trial [26]. Consequently, these lead to the conclusion that the omission of RT should be considered carefully in subgroups of patients. However, this goal was not straightforward due to the lack of knowledge on the correlation between radiation dose and TCP. This study pursued to fill in this research blank and provided a quantified relationship between radiation dose, MSD and TCP for the older patients.

On the same note, several studies reported that younger breast cancer patients had inferior outcome than older patients [2,27,28]. The EORTC boost-versus-no-boost trial showed that local recurrence was strongly correlated with age. Although there was a

statistically significant benefit to the boost in all age groups, the absolute benefit was higher for younger women. A randomized phase III trial [29] was initiated in 2005 to investigate the potential benefit of an additional 10 Gy dose to the tumor bed in younger patients in addition to a uniform 50 Gy dose and a standard boost 16 Gy. The 10 year local recurrence results have not been reported yet. Using our simulation framework for younger patients, we predict that the TCP at 10 years will increase from 81.8% to 89.8% by a standard boost of 16 Gy and further to 91.9% (95% CI: 89.2%~94.6%) using a standard boost plus the additional 10 Gy with the same eligibility criteria for adjuvant chemotherapy / hormone therapy as the EORTC boost-verse-no-boost trial. Note that the local recurrence rate of the total cohort in the young boost trial [29] shall be better than our prediction on this patient-matched case, because more patients in the young boost trial received the adjuvant systemic therapy and benefited from many improvements in the treatment technology. These issues are discussed in the following sections.

In previous work [10], the total MSD quantity was considered as a function of age at diagnosis, tumor grade and tumor diameter, and the function parameters were estimated using the pathology dataset. In the current study, the effect of age on treatment outcome was the major focus; therefore, we only chose age to establish a link with the patient's disease quantity. The younger patients had significantly larger quantity of disease than older patients both before and after surgery. This finding supports the necessity of an additional radiation dose in younger patients.

Different from the previous research paper [33], we treated the age parameter as a discrete variable instead of a continuous variable. The advantage of separating patients into two groups is that we can deploy a structural modeling approach for analyzing the correlation between the histopathology characteristics of tumors and the outcome of the trials. Clearly, our study approach has the predictive ability on the local recurrence rate in a new trial with varying radiation doses. A similar prediction is impossible to obtain in a regression-form analysis. So far, to the best of our knowledge, no similar study exists that provides a predictive modeling platform.

The Effect of Age in Breast Conserving Therapy: a Retrospective Analysis on Pathology and Clinical Outcome Data

The radiosensitivity in younger patients was estimated to be larger on average than that in the older patients, which may explain the larger absolute TCP benefit of the boost dose in the younger age group [15]. Moreover, the analyses of factors that may affect TCP suggest that clonogenic MSD cell quantity plays a more important role on the TCP than radiosensitivity. A large research focus exists world-wide on genomic profiling and experimental study to understand the radiobiology of breast cancer [4,30,31], but very few studies address the prediction of tumor cell quantity [32]. We recommend that additional effort should be spent on predicting tumor cell quantity (e.g., building mathematic models to predict microscopic disease extension using multiple imaging modalities [13]) in order to design effective treatment plans for high-risk subgroup patients.

Due to the nature of a retrospective study, our analysis is only based on the simulations using the cohorts, which consist of the treatments of surgery and radiotherapy. Adjuvant therapy is frequently used to treat patients while our framework does not include the effect of chemotherapy or hormone therapy. As has been well demonstrated, both Tamoxifen and chemotherapy reduce the risk of local recurrence by half, seen for example in the complete data of the boost-versus-no-boost trial of 5318 patients [33]. To incorporate systemic treatment in our framework, one may thus approximate the local recurrence risk with a correction factor of 0.5 when adjuvant therapy is given, however, should be also always cautious on the interaction between different types of treatments.

Several limitations of our study should be mentioned. First, we split our cohort data by age into only two groups due to the limitation of a small number of younger patients (N=12) in our completely embedding pathology dataset. Menopausal status or other age related factors (e.g. ER receptor) may also play an important role on the local recurrence rate which unfortunately could not be investigated using the current datasets of this study. However, the analysis can be easily empowered with a larger pathology dataset for the desired factors. Second, the higher recurrence risk of breast cancer

Chapter 5

patients was observed in our study than those in other recent studies. Possible explanations for the lower rate in new trials are better preoperative staging imaging procedures, use of image-guided surgery with pathological assessment of the margins, optimized radiotherapy with 3D treatment planning, and more widespread use of effective adjuvant systemic treatment [34]. Third, under-sampling may have occurred in the estimated microscopic disease quantity data. The resection specimens were first sliced macroscopically in 4 mm slabs, and then further trimmed and examined on microscopic slices of 4 μ m thickness. To increase the robustness of the estimation, we proposed to use statistical models and a simulation framework to account for the uncertainties in data. Fourth, we generalized the disease spread from the pathology data in our own institute (N=60) to the patients enrolled in the multi-institutional clinical trials based on the assumption that the patient groups have comparable characteristics. We believed this was a valid assumption because all patients in the pathology study received BCT. Fifth, the microscopic cell density was estimated from only 12 patients. No further data was analyzed because the likelihood to find a significant difference between younger and older patients is small due to the close average values and the large variation. Sixth, we assumed that all MSD cells received the prescribed dose, ignoring dose heterogeneity and setup errors.

Conclusion

The microscopic disease quantity, impact of surgery, radiosensitivity and clonogenic cell fraction of breast cancer patients were studied and compared between two age groups. Inferior outcome of treatment in younger patients could be explained by the larger microscopic disease quantity and larger clonogenic cell fraction, even though the microscopic disease cells in younger patients were estimated to be more radiosensitive.

Reference

- [1] Early Breast Cancer Trialists' Collaborative Group. Effects of Radiotherapy and Surgery in Early Breast Cancer — An Overview of the Randomized Trials. *N Engl J Med* 1995;333:1444–56.
- [2] Antonini N, Jones H, Horiot JC, Poortmans P, Struikmans H, Van den Bogaert W, et al. Effect of age and radiation dose on local control after breast conserving treatment: EORTC trial 22881-10882. *Radiother Oncol* 2007;82:265–71.
- [3] Beadle BM, Woodward W a, Buchholz T a. The impact of age on outcome in early-stage breast cancer. *Semin Radiat Oncol* 2011;21:26–34.
- [4] Nuyten DS, Kreike B, Hart A a M, Chi J-TA, Sneddon JB, Wessels LF a, et al. Predicting a local recurrence after breast-conserving therapy by gene expression profiling. *Breast Cancer Res* 2006;8:R62.
- [5] Elkhuizen PH, van Slooten HJ, Clahsen PC, Hermans J, van de Velde CJ, van den Broek LC, et al. High local recurrence risk after breast-conserving therapy in node-negative premenopausal breast cancer patients is greatly reduced by one course of perioperative chemotherapy. *J Clin Oncol* 2000;18:1075–83.
- [6] Dillon MF, Hill ADK, Quinn CM, McDermott EW, O'Higgins N. A pathologic assessment of adequate margin status in breast-conserving therapy. *Ann Surg Oncol* 2006;13:333–9.
- [7] Tartter P, Kaplan J, Bleiweiss I. Lumpectomy margins, reexcision, and local recurrence of breast cancer. *Am J Surg* 2000;179:81–5.
- [8] Nixon a J, Neuberg D, Hayes DF, Gelman R, Connolly JL, Schnitt S, et al. Relationship of patient age to pathologic features of the tumor and prognosis for patients with stage I or II breast cancer. *J Clin Oncol* 1994;12:888–94.
- [9] Zhou P, Gautam S, Recht A. Factors affecting outcome for young women with early stage invasive breast cancer treated with breast-conserving therapy. *Breast Cancer Res Treat* 2007;101:51–7.
- [10] Chen W, Gilhuijs K, Stroom J, Bartelink H, Sonke J. A simulation framework for modeling tumor control probability in breast conserving therapy. *Radiother Oncol* 2014;doi: 10.1016/j.radonc.2014.03.004.

The Effect of Age in Breast Conserving Therapy: a Retrospective Analysis on Pathology and Clinical Outcome Data

[11] Stroom J, Schlief A, Alderliesten T, Peterse H, Bartelink H, Gilhuijs K. Using histopathology breast cancer data to reduce clinical target volume margins at radiotherapy. *Int J Radiat Oncol Biol Phys* 2009;74:898–905.

[12] Schmitz AC, van den Bosch M a a J, Loo CE, Mali WPTM, Bartelink H, Gertenbach M, et al. Precise correlation between MRI and histopathology - exploring treatment margins for MRI-guided localized breast cancer therapy. *Radiother Oncol* 2010;97:225–32.

[13] Schmitz AC, Pengel KE, Loo CE, van den Bosch MAA, Wesseling J, Gertenbach M, et al. Pre-treatment imaging and pathology characteristics of invasive breast cancers of limited extent: Potential relevance for MRI-guided localized therapy. *Radiother Oncol* 2012;104:11–8.

[14] Chen W, Stroom J, Sonke J-J, Bartelink H, Schmitz AC, Gilhuijs KG. Impact of negative margin width on local recurrence in breast conserving therapy. *Radiother Oncol* 2012;104:148–54.

[15] Bartelink H, Horiot J-C, Poortmans PM, Struikmans H, Van den Bogaert W, Fourquet A, et al. Impact of a higher radiation dose on local control and survival in breast-conserving therapy of early breast cancer: 10-year results of the randomized boost versus no boost EORTC 22881-10882 trial. *J Clin Oncol* 2007;25:3259–65.

[16] Jones HA, Antonini N, Hart AAM, Peterse JL, Horiot J-C, Collin F, et al. Impact of pathological characteristics on local relapse after breast-conserving therapy: a subgroup analysis of the EORTC boost versus no boost trial. *J Clin Oncol* 2009;27:4939–47.

[17] Darby S, McGale P, Correa C, Taylor C, Arriagada R, Clarke M, et al. Effect of radiotherapy after breast-conserving surgery on 10-year recurrence and 15-year breast cancer death: meta-analysis of individual patient data for 10,801 women in 17 randomised trials. *Lancet* 2011;378:1707–16.

[18] Vrieling C, Collette L, Fourquet a, Hoogenraad W., Horiot J-C, Jager J., et al. Can patient-, treatment- and pathology-related characteristics explain the high local recurrence rate following breast-conserving therapy in young patients? *Eur J Cancer* 2003;39:932–44.

Chapter 5

- [19] Webb S, Nahum A. A model for calculating tumour control probability in radiotherapy including the effects of inhomogeneous distributions of dose and clonogenic cell density. *Phys Med Biol* 1999;38:653–66.
- [20] Rüschemdorf L. Random variables with maximum sums. *JSTOR Adv Appl Probab* 1982;14:623–32.
- [21] Hoe AL, Mullee MA, Royle GT, Guyer PB, Taylor I. Breast size and prognosis in early breast cancer. *Ann R Coll Surg Engl* 1993;75:18–22.
- [22] Gruenberger T, Gorlitzer M, Soliman T, Rudas M, Mittlboeck M, Gnant M, et al. It is possible to omit postoperative irradiation in a highly selected group of elderly breast cancer patients. *Breast Cancer Res Treat* 1998;50:37–46.
- [23] Mandelblatt JS. Predictors of Long-Term Outcomes in Older Breast Cancer Survivors: Perceptions Versus Patterns of Care. *J Clin Oncol* 2003;21:855–63.
- [24] Cirrincione C, McCormick B, Shank B, Ph D, Wheeler J, Champion LA, et al. Lumpectomy plus Tamoxifen with or without Irradiation in Women 70 Years of Age or Older with Early Breast Cancer 2013:971–7.
- [25] Lim M, Bellon JR, Gelman R, Silver B, Recht A, Schnitt SJ, et al. A prospective study of conservative surgery without radiation therapy in select patients with Stage I breast cancer. *Int J Radiat Oncol Biol Phys* 2006;65:1149–54.
- [26] Tinterri C, Gatzemeier W, Costa A, Gentilini MA, Zanini V, Regolo L, et al. Breast-conservative surgery with and without radiotherapy in patients aged 55-75 years with early-stage breast cancer: a prospective, randomized, multicenter trial analysis after 108 months of median follow-up. *Ann Surg Oncol* 2014;21:408–15.
- [27] Van der Leij F, Elkhuizen PHM, Bartelink H, van de Vijver MJ. Predictive factors for local recurrence in breast cancer. *Semin Radiat Oncol* 2012;22:100–7.
- [28] Miles RC, Gullerud RE, Lohse CM, Jakub JW, Degnim AC, Boughey JC. Local recurrence after breast-conserving surgery: multivariable analysis of risk factors and the impact of young age. *Ann Surg Oncol* 2012;19:1153–9.
- [29] The Netherlands Cancer Institute. Radiation Dose Intensity Study in Breast Cancer in Young Women. In: *ClinicalTrials.gov* [Internet]. Bethesda (MD): National Library of

The Effect of Age in Breast Conserving Therapy: a Retrospective Analysis on Pathology and Clinical Outcome Data

Medicine (US). 2000- [April 18, 2014]. Available from: <http://clinicaltrials.gov/show/NCT00212121> NLM Identifier: NCT00212121.

[30] Veer L van't, Dai H, Vijver M Van De. Gene expression profiling predicts clinical outcome of breast cancer. *Nature* 2002;415:530–6.

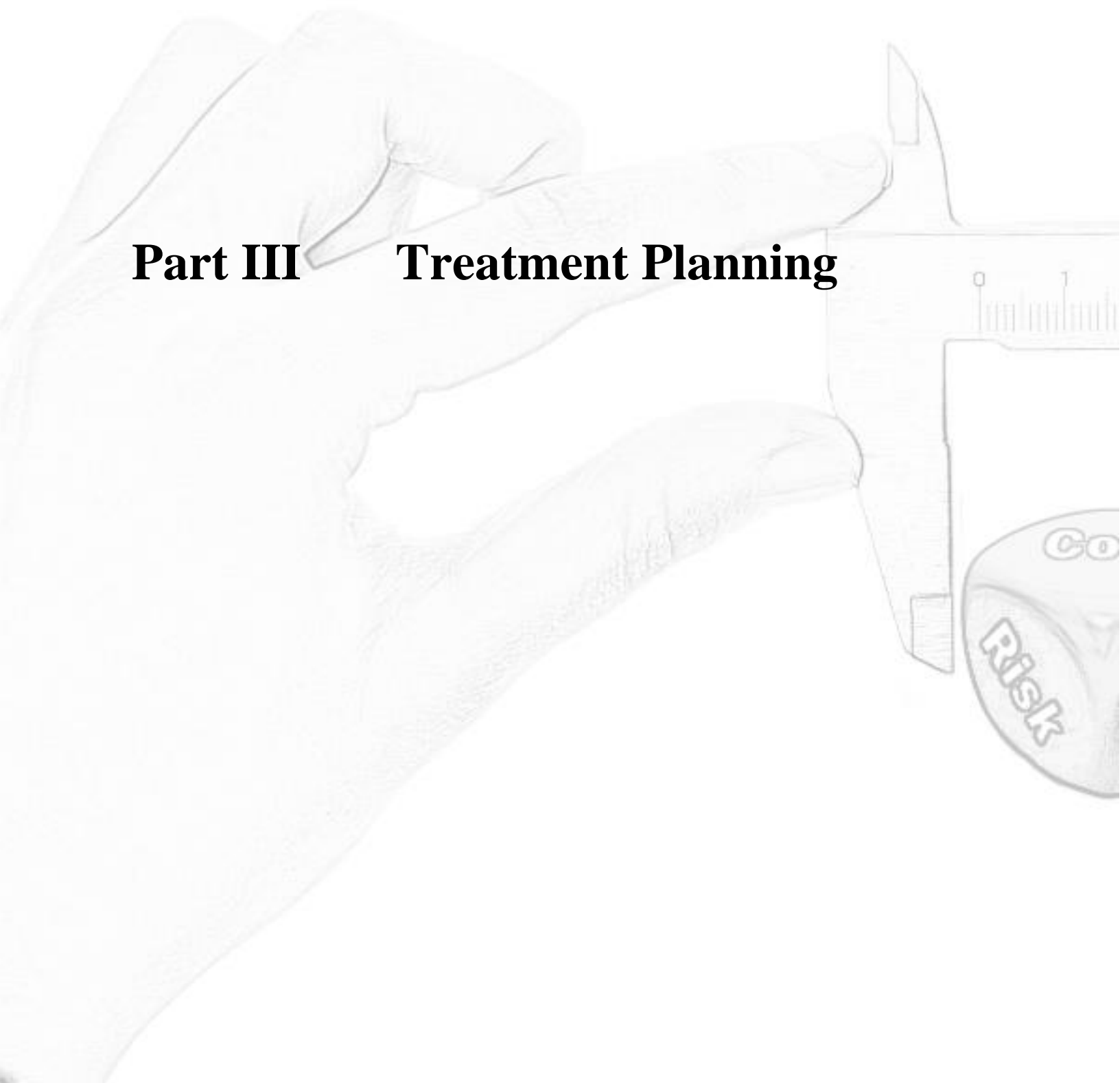
[31] Van de Vijver MJ, He YD, van't Veer LJ, Dai H, Hart AAM, Voskuil DW, et al. A gene-expression signature as a predictor of survival in breast cancer. *N Engl J Med* 2002;347:1999–2009.

[32] Margenthaler J, Gao F, Klimberg VS. Margin index: a new method for prediction of residual disease after breast-conserving surgery. *Ann Surg Oncol* 2010;17:2696–701.

[33] Werkhoven E van, Hart G, Tinteren H Van, Elkhuizen P, Collette L, Poortmans P, et al. Nomogram to predict ipsilateral breast relapse based on pathology review from the EORTC 22881-10882 boost versus no boost trial. *Radiother Oncol* 2011;100:101–7.

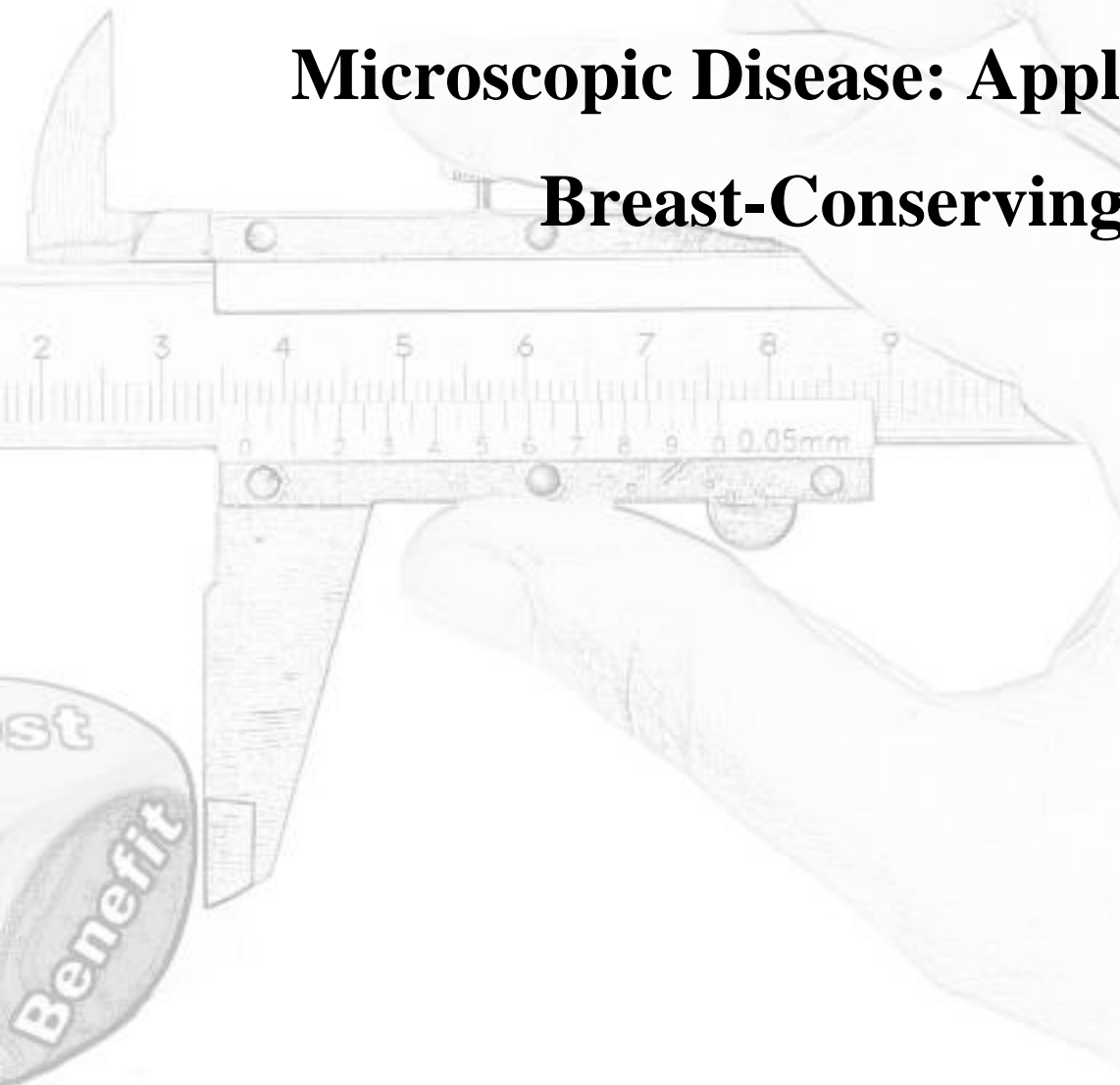
[34] Bartelink, H, Maingon P, Poortmans P, Weltens C, Fourquet A, Jager J, et al. Whole-breast irradiation with or without a boost for patients treated with breast-conserving surgery for early breast cancer: 20-year follow-up of a randomised phase 3 trial. *Lancet Oncol*, 2014;16: 47–56.

Part III Treatment Planning



Chapter 6

Towards Dose-painting for Microscopic Disease: Application to Breast-Conserving Therapy



Chen, Wei, Joep Stroom, Kenneth Gilhuijs, Harry Bartelink, Marcel Verheij, and Jan-Jakob Sonke. "Towards dose-painting for microscopic disease: application to breast-conserving therapy." submitted to ***Radiotherapy and Oncology***.

Abstract

Background

Residual microscopic disease is a major risk of local recurrence in breast-conserving therapy. Little knowledge, however, is available on the optimal radiation dose distribution in relation to this microscopic disease. Therefore we investigated the effect of inhomogeneous dose distribution on tumor control probability (TCP) taking into account inhomogeneously distributed tumor cells and setup errors.

Method

We used a simulation framework to analyze the outcome of breast-conserving therapy. First, we simulated the effect of surgery on the spatial distribution of microscopic disease. Second, we designed and simulated two dose planning scenarios with/without maximum-dose constraints, and calculated the effect on TCP. In each scenario, we tested three magnitudes of systematic and random geometric errors, and compared the TCP results under homogeneous dose plans (HDP) with the same mean dose.

Result

Surgery reduced the quantity of microscopic disease by about 87% but flattened the spatial distribution. The overall TCP was significantly improved by adopting dose-painting plans compared to HDP. By aiming at 80% TCP on average 13.3% increase of TCP in the no-constraint scenario and 10.9% increase in the maximum-dose-constraint scenario were observed by inhomogeneous dose distributions. However, the improvement deteriorates with increasing target TCP and decreasing setup error.

Conclusion

Inhomogeneous dose distributions improve TCP but the improvement depends on target TCP and setup error.

Introduction

Gross tumor volume (GTV)⁴, clinical target volume (CTV) and planning target volume (PTV) are well defined in the literature [1–3] and in radiotherapy guidelines [4]. The GTV comprises the region containing the macroscopic tumor, i.e., what can be seen, palpated or imaged; CTV represents the gross tumor volume plus a margin for sub-clinical microscopic disease spread which therefore cannot be directly imaged; PTV adds a safety margin to the CTV to account for uncertainties in planning and treatment delivery, and is a geometric concept designed to ensure that the dose is actually delivered to the CTV. Not all of these volumes, however, are present in clinical practice. In early stage breast cancer, for example, the gross tumor is removed in breast-conserving surgery (BCS). The GTV thus typically has zero volume, but the remaining breast might still contain residual microscopic disease (MSD) [5].

Treating MSD is important but also complex [6]. Due to the risk of the extended spread of MSD, the whole breast has been irradiated for the past three decades [7,8]. The side effects include additional risk of fibrosis [9] and ischemic heart disease [10]. More recently, partial breast irradiation (PBI) has become a new option for treatment [11,12] with promising tumor control rates and low incidences of adverse effects [13]. These findings provide a rationale to further optimize the dose distribution in order to reduce the side effects to the organs at risk (e.g., the whole breast). Nonetheless, how to formulate the CTV in PBI and how to add PTV margins for geometric errors are still subject of debate.

The spatial patterns of MSD from pathology studies were previously used to support the decision on defining the CTV [14]. However, it is unclear whether the CTV is defined in such a way that the MSD is optimally treated since a homogeneous dose is prescribed to the CTV. After all, MSD is sparsely and inhomogeneously distributed in the breast [15]. An additive CTV-PTV margin to obtain an adequate coverage in the presence of geometric uncertainties may not be a good choice because a quadratically combined

⁴ Abbreviation list: gross tumor volume (GTV), clinical target volume (CTV), planning target volume (PTV), microscopic disease (MSD), tumor control probability (TCP), partial breast irradiation (PBI), breast-conserving surgery (BCS), breast-conserving therapy (BCT), the Center of Mass (CoM).

CTV-PTV margin recipe can reduce radiation dose without compromising tumor control probability [16]. As an alternative approach, Witte *et al.* previously introduced a dose-painting concept for dealing with the geometric uncertainties of MSD cells, in which the MSD cells were assumed to be homogeneously distributed [17]. The power of their study is that they developed a planning tool based on probabilistic optimization with inhomogeneous target dose while monitoring the confidence level on proper target coverage. In this study we aim to combine the above-mentioned different concepts to optimize dose-painting solution for the inhomogeneously distributed MSD while simultaneously accounting for setup errors (Figure 1).

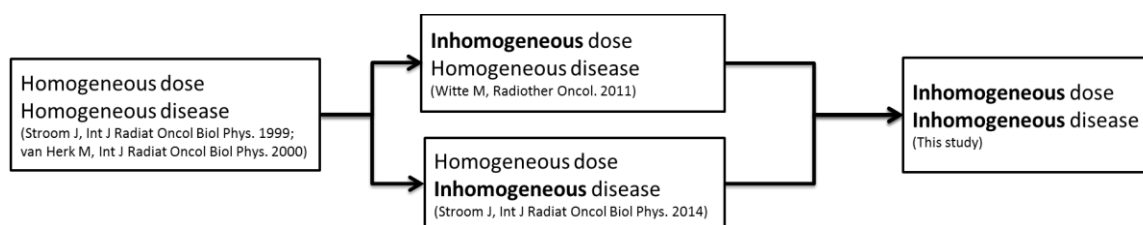


Figure 1: A schematic overview of the development of dose planning strategies. It also illustrates the correlation between this study and the previous studies.

Materials & Methods

Study Overview

We employed a previously developed framework [18] and adapted it to our specific goal in this study, which is to explore the optimal radiation dose distribution for the inhomogeneously distributed microscopic disease in the presence of geometric uncertainties. To that end, we simulated breast-conserving therapy with data obtained from multiple trials. This study consists of three steps: 1) we simulated the post-surgical microscopic disease distribution (MSD) of a large group of patients using data from a pathology study; 2) we designed an optimization algorithm based on tumor control probability (TCP) to obtain the ‘ideal’ inhomogeneous dose to eradicate inhomogeneously distributed disease, and introduced dose constraints to the planning problem; 3) we compared the TCP of the dose-painting plans with the TCP of the homogeneous dose plans. The details of this study are explained below.

Disease Spread Analysis

The pathology dataset in the MARGINS (Multi-modality Analysis and Radiological Guidance IN breast-conServing therapy) study [19] was employed to model the microscopic disease quantity and spread distribution. The MARGINS study included patients with early breast cancer who were eligible for breast conserving therapy. Population statistics of microscopic disease were derived from 1818 histopathology slides of 60 breast-cancer patients. The disease quantity and distance from the primary tumor edge were recorded after three-dimensional reconstruction [20]. The absolute quantity was previously fitted to a zero-inflated model and the spread distribution was modeled with a half-Gaussian distribution [18]. Due to the size of the excision specimens, the disease spread was available up to a distance of 30 mm, which is considered to be sufficient to cover the spread of microscopic disease [15,16].

To investigate the impact of breast-conserving surgery on the disease distribution, we compared the distribution of two surgical scenarios: 1) only the gross tumor is removed; and 2) the tumor is removed with a margin of surrounding normal tissue (a typical BCS [21]). To derive the disease distribution post-surgically, we simplified the complex

situation by assuming a unifocal spherical tumor [22] with different diameters (diameters extracted from a clinical trial [23]). The tumor was also surgically removed from the center of a half spherical breast of 14 cm diameter. Subsequently, the cavity caused by surgery was filled with the surrounding tissue, i.e., no seroma appeared after surgery. We will explain the impact of seroma in the discussion section.

We first determined the distribution of MSD following the removal of the gross tumor only (i.e., the first scenario). We used the distance to the center of mass (CoM) of the gross tumor as the metrics to describe the distribution of MSD in breast. As stated above, we used a large sample of tumor diameters in a clinical trial from a comparable patient population [21] to infer the size of the tumors. We assumed the tissue with MSD to collapse isotropically towards the CoM and simulated the disease quantity and spread beyond the gross tumor with the disease spread model [18]. After we completed the simulation of the isotropic tissue-collapse process, we calculated the residual disease quantity and distribution relative to the CoM.

To simulate the disease relocation in the second scenario (i.e., a typical BCS), we first obtained the surgical margins in our pathology data and combined with the obtained tumor sizes above to simulate the sizes of the surgically removed volume [18]. We simulated the disease distribution beyond the surgically removed volume and again calculated the disease quantity from the center after tissue collapses isotropically to the CoM.

Optimized Dose Distribution

We focused on the typical BCS scenario in the following sections. Given the disease spread distribution above, the optimal dose distribution was estimated iteratively in a simulation framework with a previously derived TCP model⁵ [18]. The overall TCP of the patient group was estimated as the average of the TCP of all patients. The TCP for each patient was estimated as the product of TCP in each cubic millimeter volume in

⁵ We considered the radiosensitivity of tumor cells is following a normal distribution with mean 0.067 and one standard deviation 0.022 [18].

breast. Note that due to the symmetric property⁶, we simplified the three-dimensional TCP model to a one-dimensional model for computational convenience as follows:

$$TCP_{overall} = \sum_p (\prod_d TCP_d^p) / N,$$

where d ($=1,2,\dots$) represents the distance to the CoM of the gross tumor, p is the ranked number of a patient in the patient population, and N denotes the total number of patients.

Two optimization scenarios were evaluated:

1. Start from zero dose and add dose iteratively by 1 Gy at the radial distance (corresponds to the distance d) where it shows the maximal increment of TCP over the increment of the mean dose of organ at risk (i.e., a sphere with a radius of 50 mm to the CoM of the tumor).
2. Same as above, however, with a constraint on the maximum prescribed dose (i.e., 66 Gy [23]).

Setup errors play an important role in optimizing the dose in the treatment. To illustrate the effect of setup errors, we followed the methodology proposed in [16]. To account for the systematic error (Σ), we first sampled the disease spread for each simulated patient from the disease spread model [18]. Then we simulated a systematic error for each patient by randomly sample a distance and a direction in the polar coordinate system, and applied the sampled systematic error on the disease distribution of that patient assuming that the disease cells are uniformly distributed within the spherical shell of each distance to the CoM. Finally we summed the disease quantity following the transformed distribution for each distance to the CoM resulting in a 1D disease distribution that can be used in the TCP formula described above.

Additionally, the effect of random errors (σ) and beam penumbra was accounted for by blurring the dose distribution with another Gaussian kernel in the Cartesian coordinate system and then transformed into the polar coordinate system in the dose optimization

⁶ $TCP^p = \prod_{i,j,k} TCP_{i,j,k}^p = \prod_d TCP_{(i,j,k) \text{ in } d}^p = \prod_d TCP_d^p$ where i, j, k are the indices of voxel in the Cartesian coordination and d is the radial distance of the half spherical volume.

process. The penumbra was modeled with a SD=3.2 mm as documented in [24]. We designed 12 cases with different TCP goals, systematic and random errors for both optimization scenarios (Table 1).

Table 1: Treatment plan scenarios and setup errors*

		$\Sigma=\sigma=0mm$ (1SD)	$\Sigma=\sigma=3mm$ (1SD)	$\Sigma=\sigma=5mm$ (1SD)
No constraint	Targeting at 80% overall TCP	N80-S0R0	N80-S3R3	N80-S5R5
	Targeting at 90% overall TCP	N90-S0R0	N90-S3R3	N90-S5R5
	Targeting at 80% overall TCP	M80-S0R0	M80-S3R3	M80-S5R5
	Targeting at 90% overall TCP	M90-S0R0	M90-S3R3	M90-S5R5
	Targeting at 80% overall TCP	H80-S0R0	H80-S3R3	H80-S5R5
	Targeting at 90% overall TCP	H90-S0R0	H90-S3R3	H90-S5R5

* $\Sigma(S)$: systematic error; $\sigma(R)$: random error; N: Non-constraint scenario; M: Maximum-dose-constraint scenario; H: Homogeneous dose scenario.

In the optimization process, the disease spread distributions of 10000 virtual patients were randomly sampled from the disease spread distribution model per simulation, and resampled if the systematic error exists. The inhomogeneous dose distribution was optimized to reach a specified target TCP. We repeated the above simulation process 49 times simultaneously and calculated the best outcome of the ratio of TCP increase over mean dose increase and the corresponding location for adding dose in each simulation. We took the location with the median of the 49 ratios as the step-wise dose increment in the optimization process. The optimization ceased if the target TCP was reached.

Homogeneous dose versus Dose-painting

We compared homogeneous dose plans and dose-painting plans in terms of mean dose to the organ at risk and TCP outcomes. In order to compare with the existing literature [3,16,22], we defined the CTV as a spherical volume containing the 100% MSD from 90% of the patients. The planning target volume was obtained by adding a CTV-to-PTV margin of $2.5 \cdot \Sigma + 0.7 \cdot \sigma$ to this CTV. In order to calculate the prescribed dose, we iteratively increased the dose homogeneously on each distance and finally satisfied the criterions that the target TCP is achieved and at least 95% of the PTV is covered (Table 1).

Finally, we estimated the TCP benefit of applying the dose-painting plan over the homogeneous dose plan. We calculated the difference of the TCP results in the simulations of two types of plans under the constraint of the same mean dose to the organ at risk (i.e., breast). Other organs at risk such as lung and heart were ignored in this study for simplicity. However, avoiding side effects on lung and heart is important [25].

Results

Disease Spread Analysis

The disease distributions in the ideal and realistic surgery scenarios were compared and shown in Figure 2. Note that the larger the tumor diameter, the further the spread of MSD in the coordinate system. The distance to the center of mass (CoM) can become larger than 30 mm. We observed that the spread of the disease quantity (the cumulative probability distribution of disease quantity) is more flattened in the realistic scenario than that in the ideal scenario. The quantity of microscopic disease after surgery (1.36×10^7 cells). is reduced to 13% in a typical breast-conserving surgery case compared to the original disease quantity (1.04×10^8 cells). Conversely, the average cell density with the respect to the center of mass has a different distribution compared to that of cell quantity. Larger cell density is observed within a small distance.

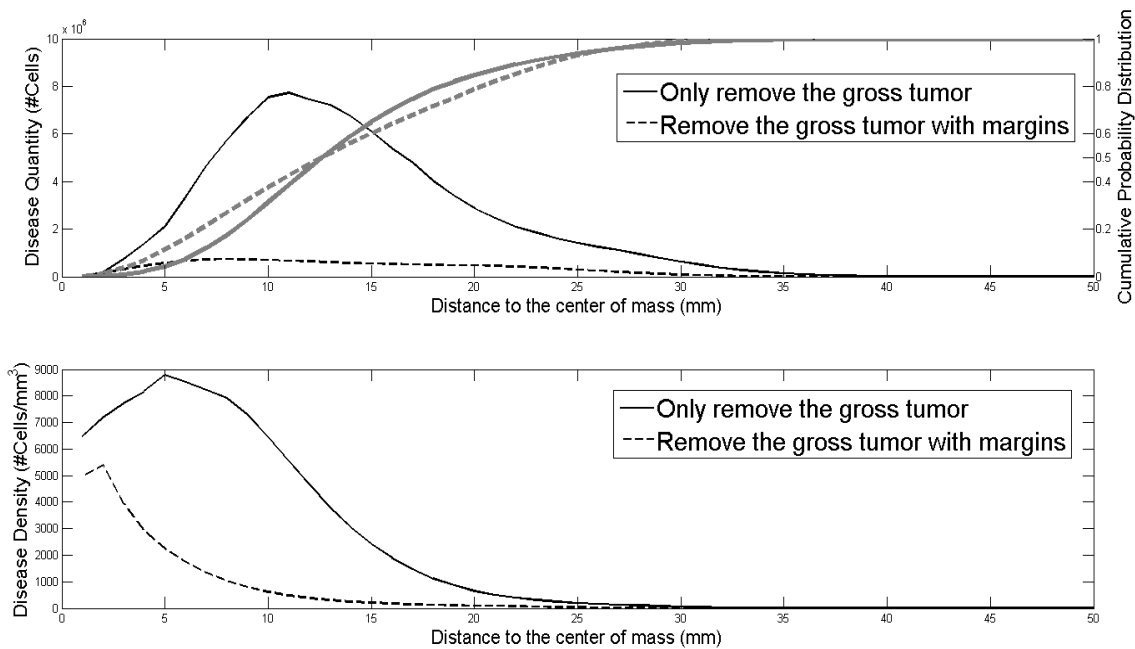


Figure 2: The simulated spatial disease distribution after the surgery in the two scenarios. (Upper) The solid curve (black) represents the disease quantity distribution in the case only the gross tumor is removed. The dashed curve (black) represents the disease quantity distribution in a typical BCS case where a surgical margin around the GTV is also removed. The grey curves denote the corresponding cumulative probability distributions. (Lower) The curves show the disease density distributions.

Optimized Dose Distribution

We compared the impact of the systematic error (Σ) on the post-surgical disease distribution of the patient population (Figure 3). We observed the distribution is shifting eccentrically and the maximum of average disease quantity decreases with increasing systematic error. Note that the volume of a spherical layer with a larger distance to CoM is larger than the volume of a layer with smaller distance to CoM. Consequently, the probability of MSD being relocating towards an outer spherical layer is higher than inward when the tissue with MSD is moving isotropically.

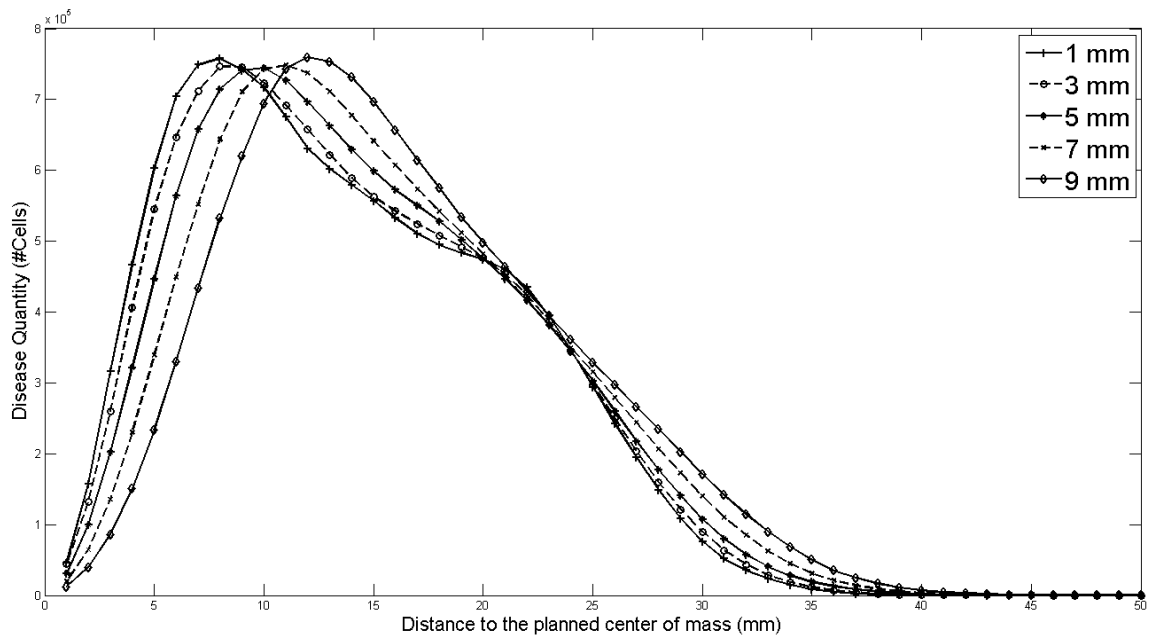


Figure 3: The disease distribution in the patient group shifts eccentrically with the increasing systematic error.

Considering no constraint ('N' cases) on the maximum dose (the first scenario), the optimal planned dose distributions are shown in Figure 4 for different TCP targets (i.e., 80% and 90%). Assuming no systematic error or random error, the maximum doses of achieving 80% TCP and 90% TCP are 64 Gy and 98 Gy, respectively. The dose distribution is shifting eccentrically with increasing setup errors. We observed that a larger mean dose is needed to achieve a higher TCP objective (Table 2).

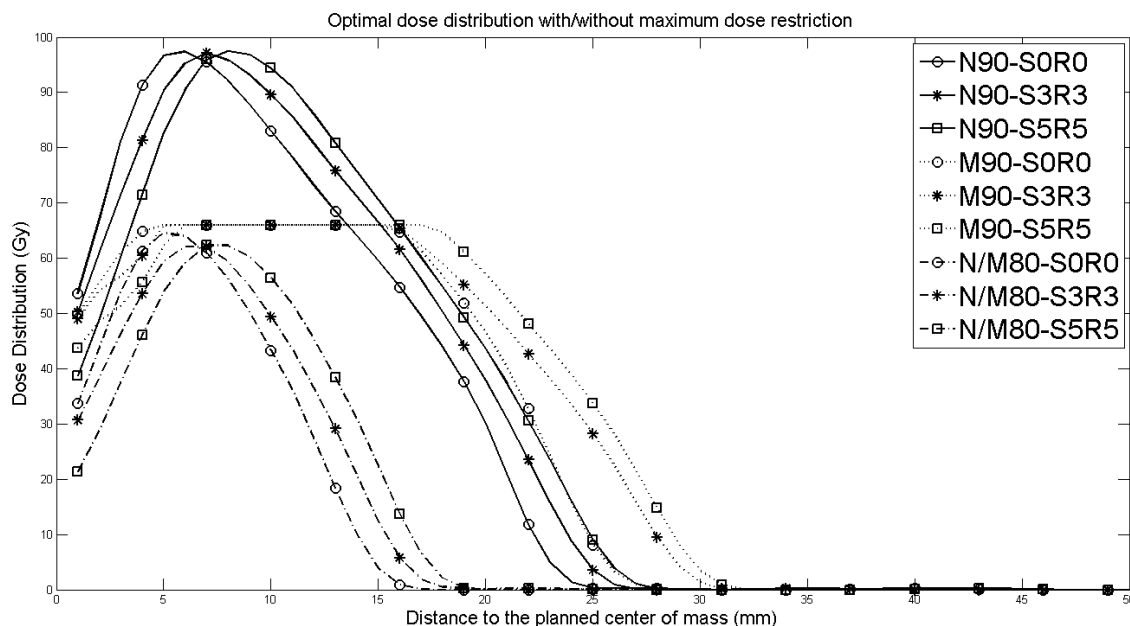


Figure 4: The optimal planned dose distributions with('M')/without('N') maximum dose constraint. The circle, star and square represent the cases with different setup errors. The solid lines represent the dose distributions for 90% TCP without maximum dose constraint (MDC); the dotted lines represent the dose distributions for 90% TCP with MDC; the dashed lines represent the planned dose for targeting TCP 80% with and without MDC, as the constraint is not reached.

In the second scenario (with constraint), only the cases in which we targeted at 90% overall TCP were affected by the maximum dose constraint (Figure 4). For all these three cases (i.e., M90-S0R0, M90-S3R3, M90-S5R5), the dose is distributed more eccentrically than those in the non-constraint scenario.

Homogeneous dose versus Dose-painting

While targeting the 80% overall TCP with a prescribed homogeneous dose to the PTV, the optimization results ended up with different dose distribution (36 Gy, 33 Gy and 32 Gy) for the three cases with different setup errors (Figure 5). The lower dose for larger setup errors indicates that the linear addition of CTV and PTV margins overestimates the impact of geometric uncertainties and can be partially compensated by a modest dose reduction. Similarly, different planned doses (65 Gy, 57 Gy and 56 Gy) were

Towards Dose-painting for Microscopic Disease: Application to Breast-conserving Therapy

required to target 90% TCP for 0 mm, 3 mm and 5mm systematic/random geometric uncertainties respectively.

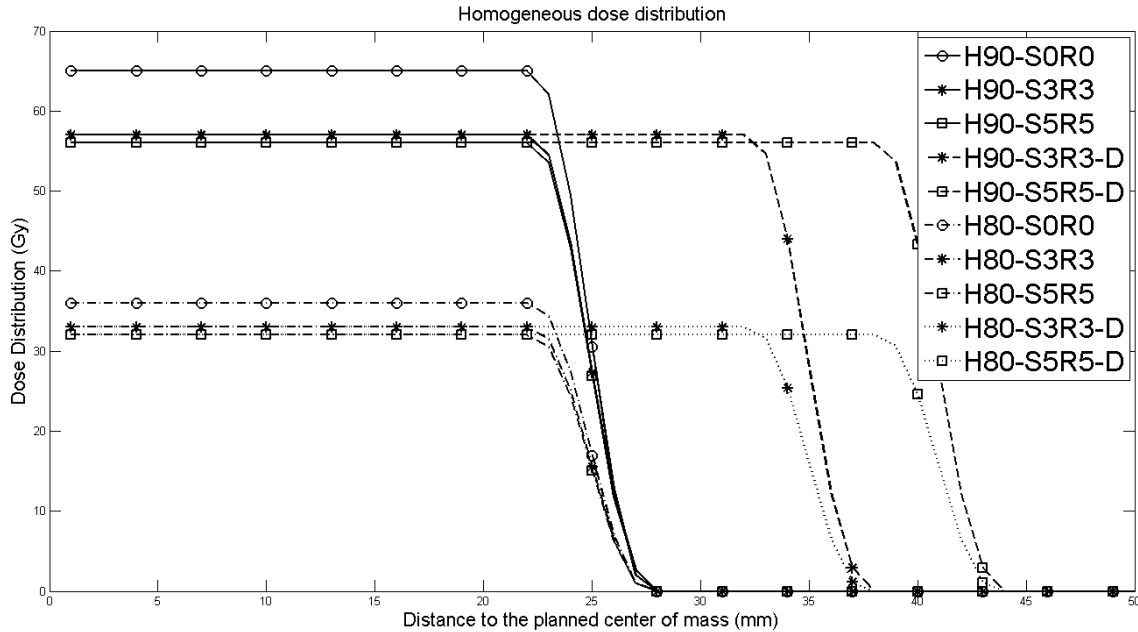


Figure 5: The homogeneous dose distribution with different setup errors. The circle, star and square represent three setup errors. The solid curves represent the delivered dose for targeting the overall TCP 90% and the dashed curves represent the delivered dose for targeting the overall TCP 80%.

The mean doses in the different dose distribution plans ('No Constraint', 'Maximum Dose Constraint', 'Homogeneous') are listed in Table 2. We observed that the required mean dose is significantly higher to achieve greater overall TCP and to compensate for larger setup errors. Also, the mean doses of the 'No Constraint' plans are significantly lower than those of the homogeneous dose plans. We observed that the mean dose by applying the 'Homogeneous' plan is increased by about a factor of five of that from a no-constraint inhomogeneous dose plan while targeting overall 80% TCP considering no setup errors. Similarly, the factor is about two for targeting overall 90% TCP. However, if both systematic and random errors increase to 5 mm, the above ratios increase to 12.6 and 4.8, respectively. In addition, higher mean doses (on average: 44%) are needed to

achieve 90% TCP target in the maximum dose constraint scenario compared to the non-constraint scenario.

Table 2: Relative mean dose to the breast for each scenario evaluated.

	Non Constraint		Maximum Dose Constraint		Homogeneous Dose	
Target TCP:	80%	90%	80%	90%	80%	90%
Setup Error						
S0R0	100%	510.0%	100%	740.3%	555.2%	979.8%
S3R3	140.5%	665.2%	140.5%	985.3%	1462.4%	2478.6%
S5R5	181.1%	793.3%	181.1%	1112.4%	2291.9%	3859.2%

In addition, we calculated the benefit of switching to the dose-painting plan from the homogeneous dose plan. We observed that if we restricted the same mean dose in three treatment plans, the TCP of the dose-painting plans are larger than those of the homogeneous dose plans (Figure 6). These results suggest that utilizing the disease distributions of a patient population, we can significantly improve overall TCP by adopting the dose-painting plan. By aiming at 80% TCP on average 13.3% increase of TCP in the no-constraint scenario and 10.9% increase in the maximum-dose-constraint scenario were observed. However, we also had two interesting observations: 1) the TCP benefit is reduced with increasing target TCP; 2) the TCP benefit is increased with increasing setup error. It indicates that the adoption of the dose-painting plan in breast conserving therapy should depend on target TCP and setup error. In addition, we also observed that to a certain high TCP target, the dose-painting plan becomes equivalent to the homogeneous dose plan because in both plans some tumor cells of particular patients may be not irradiated adequately (e.g., the maximum disease load in some spherical volume). The effect is more obvious in the 'Maximum Dose Constraint' scenarios as the benefit drops to zero where the target TCP is 96%.

Towards Dose-painting for Microscopic Disease: Application to Breast-conserving Therapy

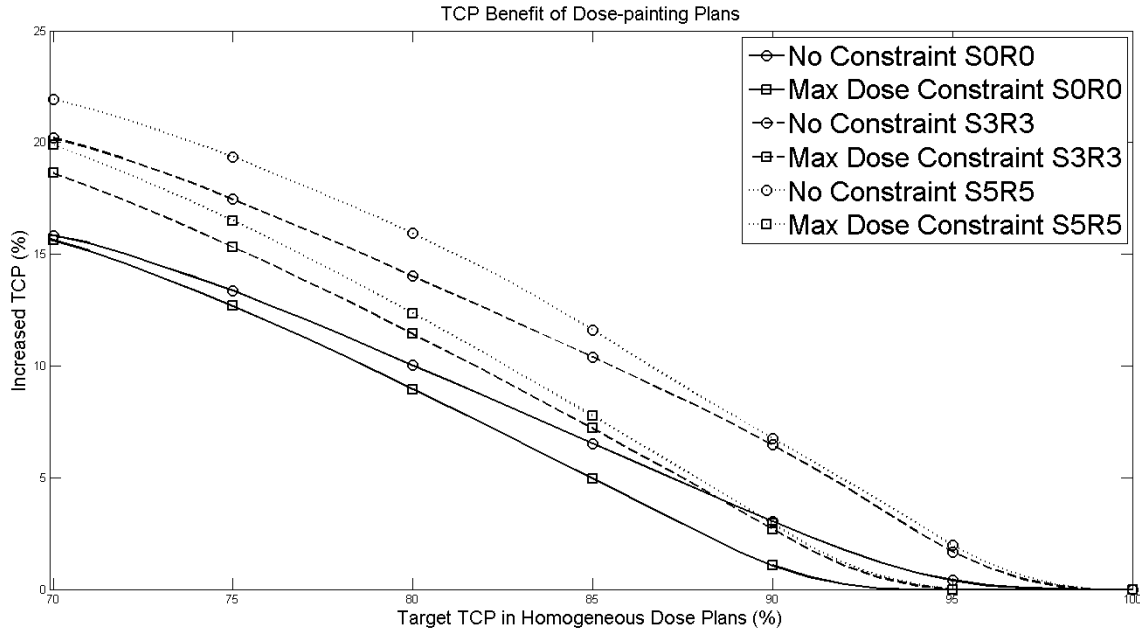


Figure 6: TCP benefit of adopting dose-painting plans with the same mean dose as the homogeneous dose plans. The circle markers represent the no-constraint dose-painting plans and the square markers represent the dose-painting plans with maximum dose constraint.

Discussion

A simulation study was conducted to investigate the optimal dose distribution for irradiating the residual microscopic disease after breast-conserving surgery. We found that the quantity of the microscopic disease is significantly reduced by 87% post-surgery. Moreover, the original half-Gaussian distribution of tumor cells, which is the basic assumption in many existing studies, is transformed to a log-normal-like distribution. It was observed that inhomogeneous dose distributions results in a significant increase in overall tumor control probability (TCP) for a given mean dose to the organ at risk in both the constraint and non-constraint scenarios. However, the benefit of dose-painting plan is decreasing by choosing a higher TCP target or smaller setup errors.

Many methods to define breast CTV and PTV have been investigated [6,12,14], and the results were reported with excellent performance on local or regional control. A complete overview of the interaction between target volume definition, TCP and planning dose optimization, however, is lacking in the current literature. Many previous efforts with partial targets have been added to this research field. Buffa *et al.* analyzed the relationship between radiosensitivity and volume effects in the TCP modeling [26]; Carlone *et al.* explored the correlation between the parameters in a population TCP model and the heterogeneity of clonogenic cell distribution [27]; Strigari *et al.* developed a more patient specific three dimensional dosimetry method using functional MRI imaging [28]; Perrin *et al.* analyzed the radiobiological factors and optimized the treatment plan using PET images [29]; South *et al.* investigated the dose prescription complexity in biologically guided radiotherapy and pursued an ‘ideal’ dose prescription [30]; Jin *et al.* designed a treatment planning scheme which incorporates setup uncertainty and tumor cell density variation [22]; Witte *et al.* developed a probabilistic planning method with biological cost functions that does not require the definition of margins [31]. Most recently, Stroom *et al.* proposed a new method to combine the margins of CTV and PTV while accounting the disease spread from pathology [16]. Our study extends on Stroom’s basic concept and further includes the optimization part of treatment planning into the analysis.

Towards Dose-painting for Microscopic Disease: Application to Breast-conserving Therapy

Adopting inhomogeneous dose distribution becomes more and more popular owing to the technical improvement of multi-modality imaging and genetic profiling, and increased knowledge gained from the analysis of treatment outcome. The inhomogeneous dose distribution is well captured by the 'dose painting' concept [32] and quickly adopted in experimental practice [33,34]. Methodologies and tools have been developed for lung cancer and prostate cancer. For example, additional functional image modality such as PET is used to assist the delineation of the denser / radioresistant tumor cell regions. Conversely, for a breast cancer case the gross tumor is removed during breast conserving surgery. The residual microscopic disease is the major risk of local recurrence but *impossible* to image with current imaging technologies. Our study results indicate a significant increase in overall TCP with the same mean dose to the breast by adopting the inhomogeneous dose concept. However, the TCP benefit is reduced with increasing target TCP and with decreasing setup error which indicates that the adoption of a dose-painting plan should depend on target TCP and setup error in practice.

Following most wide local excision procedures, tissue fluid enters the resulting cavity forming a seroma [6]. The distribution of microscopic disease will be impacted by the fluid volume. Moreover, the seroma volume decreases as time from surgery increases. In our current study, only the case without seroma was analyzed because of the lack of data with seroma to perform additional analysis. We expect, however, that the disease distribution will shift eccentrically in the presence of seroma compared to the non-seroma case. Consequently, the dose distribution would shift eccentrically as well.

Several limitations exist in our study. First, we generalized the disease distribution of 60 patients in our pathology study to the overall breast cancer patients. Second, the maximum extent of the microscopic disease could only be measured up to 30 mm approximately; however the microscopic disease outside this range should not be neglected. Third, we only modeled setup errors. In practice, there are other sources of geometric uncertainties, such as delineation uncertainty, breathing motion, intra-fraction motion, etc. Most of these uncertainties will have similar effects as the setup errors

modeled in this study. Fourth, we used mean dose as a surrogate of normal tissue complication probability (NTCP). More refined NTCP models including also dose to other organs at risk such as lung and heart should be used in future studies. Fifth, the optimized dose distributions can currently not be delivered in the clinic. This likely includes the lower dose towards the center of mass. Sixth, we modeled surgery as the removal of a sphere. In practice, other surgical techniques than lumpectomy are used as well, removing for instance a cylinder of tissue. Seventh, adjuvant therapy like chemotherapy and hormone therapy are commonly seen in clinical trials, which may lead to the increase of radiosensitivity of tumor cells or other biological effects. We assumed a classical setup of breast conserving therapy (surgery plus radiotherapy) in our analysis framework. Last but not least, we did not model fractionation effects. Further experimental research should be carried out before the findings of this theoretical study can be applied in the clinic.

Conclusion

The quantity and the distribution of microscopic disease are affected by surgery. The overall tumor control probability of a patient population is significantly improved under the dose-painting plan compared to the homogeneous dose plan with the same mean dose. However, the adoption of dose-painting plan should depend on target TCP and setup error in practice.

Reference

- [1] Burnet NG, Thomas SJ, Burton KE, Jefferies SJ. Defining the tumour and target volumes for radiotherapy. *Cancer Imaging* 2004;4:153–61.
- [2] Purdy JA. Current ICRU definitions of volumes: limitations and future directions. *Semin Radiat Oncol* 2004;14:27–40.
- [3] van Herk M, Remeijer P, Lebesque J V. Inclusion of geometric uncertainties in treatment plan evaluation. *Int J Radiat Oncol* 2002;52:1407–22.
- [4] Stroom JC, Heijmen BJM. Geometrical uncertainties, radiotherapy planning margins, and the ICRU-62 report. *Radiother Oncol* 2002;64:75–83.
- [5] Vinh-Hung V, Verschraegen C. Breast-Conserving Surgery With or Without Radiotherapy: Pooled-Analysis for Risks of Ipsilateral Breast Tumor Recurrence and Mortality. *JNCI J Natl Cancer Inst* 2004;96:115–21.
- [6] Kirby AM, Coles CE, Yarnold JR. Target volume definition for external beam partial breast radiotherapy: clinical, pathological and technical studies informing current approaches. *Radiother Oncol* 2010;94:255–63.
- [7] Fisher B, Anderson S. Twenty-year follow-up of a randomized trial comparing total mastectomy, lumpectomy, and lumpectomy plus irradiation for the treatment of invasive breast cancer. *N Engl J Med* 2002;347:1233–41.
- [8] Darby S, McGale P, Correa C, Taylor C, Arriagada R, Clarke M, et al. Effect of radiotherapy after breast-conserving surgery on 10-year recurrence and 15-year breast cancer death: meta-analysis of individual patient data for 10,801 women in 17 randomised trials. *Lancet* 2011;378:1707–16.
- [9] Collette S, Collette L, Budiharto T, Horiot J-C, Poortmans PM, Struikmans H, et al. Predictors of the risk of fibrosis at 10 years after breast conserving therapy for early breast cancer: a study based on the EORTC Trial 22881-10882 “boost versus no boost”. *Eur J Cancer* 2008;44:2587–99.
- [10] Darby SC, Ewertz M, McGale P, Bennet AM, Blom-Goldman U, Brønnum D, et al. Risk of ischemic heart disease in women after radiotherapy for breast cancer. *N Engl J Med* 2013;368:987–98.
- [11] Mannino M, Yarnold J. Accelerated partial breast irradiation trials: diversity in rationale and design. *Radiother Oncol* 2009;91:16–22.
- [12] Nguyen BT, Deb S, Fox S, Hill P, Collins M, Chua BH. A prospective pathologic study to define the clinical target volume for partial breast radiation therapy in women with early breast cancer. *Int J Radiat Oncol Biol Phys* 2012;84:1116–22.
- [13] Jothy Basu KS, Bahl A, Subramani V, Sharma DN, Rath GK, Julka PK. Normal tissue complication probability of fibrosis in radiotherapy of breast cancer: accelerated partial breast irradiation vs conventional external-beam radiotherapy. *J Cancer Res Ther* 2008;4:126–30.
- [14] Vicini FA, Kestin LL, Goldstein NS. Defining the clinical target volume for patients with early-stage breast cancer treated with lumpectomy and accelerated partial breast irradiation: a pathologic analysis. *Int J Radiat Oncol Biol Phys* 2004;60:722–30.
- [15] Holland R, Connolly J, Gelman R, Mravunac M, Hendriks J, Verbeek A, et al. The presence of an extensive intraductal component following a limited excision correlates with prominent residual disease in the remainder of the breast. *J Clin Oncol* 1990;8:113–

- 8.
- [16] Stroom J, Gilhuijs K, Vieira S, Chen W, Salguero J, Moser E, et al. Combined recipe for clinical target volume and planning target volume margins. *Int J Radiat Oncol Biol Phys* 2014;88:708–14.
- [17] Witte M, Shakirin G, Houweling A, Peulen H, van Herk M. Dealing with geometric uncertainties in dose painting by numbers: introducing the ΔVH . *Radiother Oncol* 2011;100:402–6.
- [18] Chen W, Gilhuijs K, Stroom J, Bartelink H, Sonke J. A simulation framework for modeling tumor control probability in breast conserving therapy. *Radiother Oncol* 2014;111:289–95.
- [19] Chen W, Stroom J, Sonke J-J, Bartelink H, Schmitz AC, Gilhuijs KG. Impact of negative margin width on local recurrence in breast conserving therapy. *Radiother Oncol* 2012;104:148–54.
- [20] Schmitz AC, van den Bosch M a a J, Loo CE, Mali WPTM, Bartelink H, Gertenbach M, et al. Precise correlation between MRI and histopathology - exploring treatment margins for MRI-guided localized breast cancer therapy. *Radiother Oncol* 2010;97:225–32.
- [21] Bartelink H, Horiot J-C, Poortmans PM, Struikmans H, Van den Bogaert W, Fourquet A, et al. Impact of a higher radiation dose on local control and survival in breast-conserving therapy of early breast cancer: 10-year results of the randomized boost versus no boost EORTC 22881-10882 trial. *J Clin Oncol* 2007;25:3259–65.
- [22] Jin J-Y, Kong F-M, Liu D, Ren L, Li H, Zhong H, et al. A TCP model incorporating setup uncertainty and tumor cell density variation in microscopic extension to guide treatment planning. *Med Phys* 2011;38:439.
- [23] Bartelink H, Horiot J-C, Poortmans P, Struikmans H, van den Bogaert W, Barillot I, et al. Recurrence rates after treatment of breast cancer with standard radiotherapy with or without additional radiation. *N Engl J Med* 2001;345:1378–87.
- [24] van Herk M. Errors and margins in radiotherapy. *Semin Radiat Oncol* 2004;14:52–64.
- [25] Darby SC, McGale P, Taylor CW, Peto R. Long-term mortality from heart disease and lung cancer after radiotherapy for early breast cancer: prospective cohort study of about 300,000 women in US SEER cancer registries. *Lancet Oncol* 2005;6:557–65.
- [26] Buffa FM, Fenwick JD, Nahum AE. An analysis of the relationship between radiosensitivity and volume effects in tumor control probability modeling. *Med Phys* 2000;27:1258–65.
- [27] Carlone MC, Warkentin B, Stavrev P, Fallone BG. Fundamental form of a population TCP model in the limit of large heterogeneity. *Med Phys* 2006;33:1634.
- [28] Strigari L, D'Andrea M, Maini CL, Sciuto R, Benassi M, D'Andrea M. Biological optimization of heterogeneous dose distributions in systemic radiotherapy. *Med Phys* 2006;33:1857.
- [29] Perrin R, Evans PM, Webb S, Partridge M. The use of PET images for radiotherapy treatment planning: An error analysis using radiobiological endpoints. *Med Phys* 2010;37:516.
- [30] South CP, Evans PM, Partridge M. Dose prescription complexity versus tumor control probability in biologically conformal radiotherapy. *Med Phys* 2009;36:4379.
- [31] Witte MG, van der Geer J, Schneider C, Lebesque J V, Alber M, van Herk M. IMRT optimization including random and systematic geometric errors based on the expectation

Towards Dose-painting for Microscopic Disease: Application to Breast-conserving Therapy

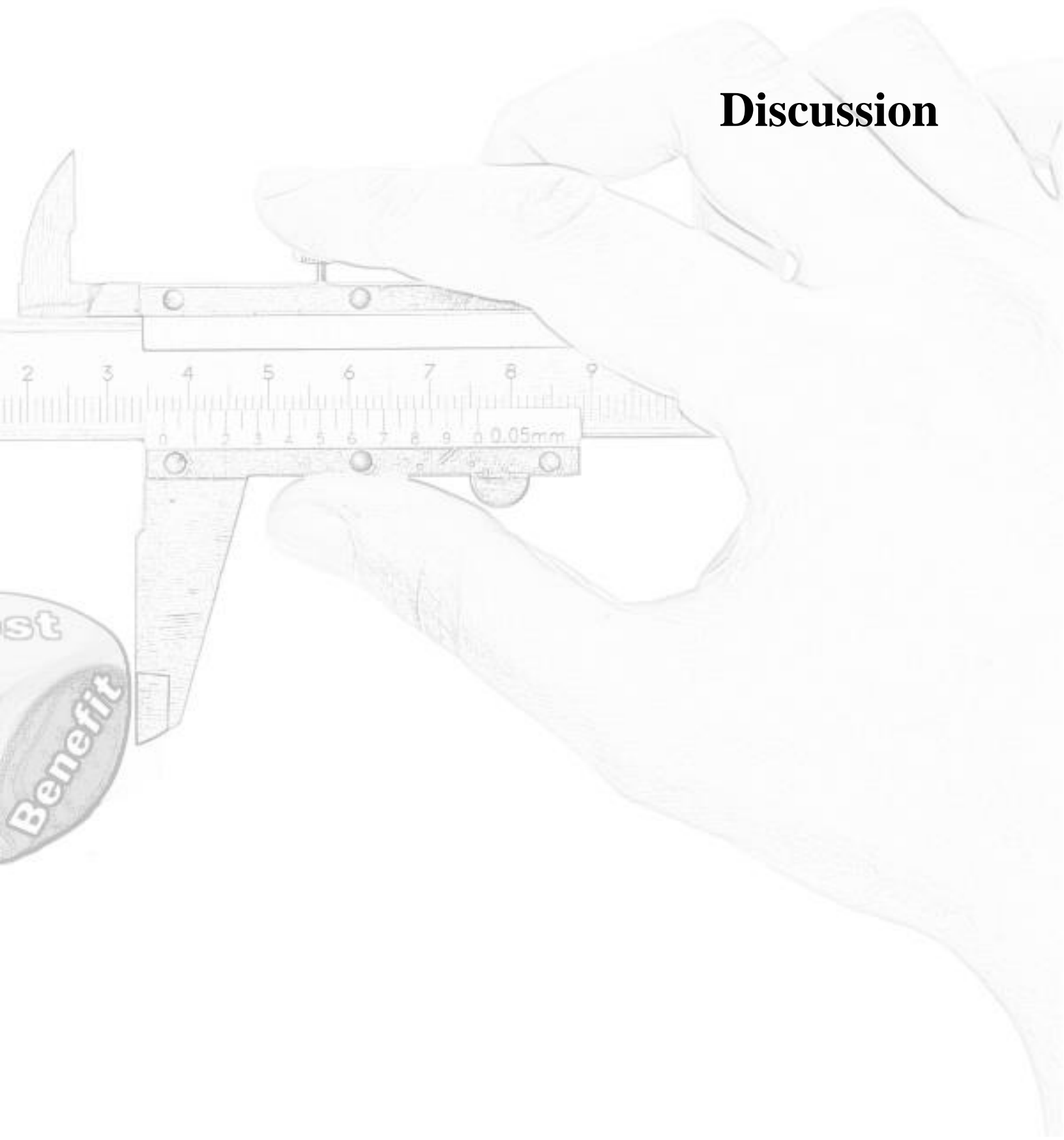
of TCP and NTCP. Med Phys 2007;34:3544–55.

- [32] Jaffray D a. Image-guided radiotherapy: from current concept to future perspectives. Nat Rev Clin Oncol 2012;9:688–99.
- [33] Fontanarosa D, Witte M, Meijer G, Shakirin G, Steenhuijsen J, Schuring D, et al. Probabilistic evaluation of target dose deterioration in dose painting by numbers for stage II/III lung cancer. Pract Radiat Oncol 2015.
- [34] Crook J, Ots A, Gaztañaga M, Schmid M, Araujo C, Hilts M, et al. Ultrasound-planned high-dose-rate prostate brachytherapy: dose painting to the dominant intraprostatic lesion. Brachytherapy 13:433–41.



Chapter 7

Discussion



Breast cancer is the most common cancer in women [1]. As a result of increased screening, the majority of patients now present with early-stage breast cancer [2]. Several large trials with at least 10 years follow-up have demonstrated local failure rates of 0.5–1% per year [3,4]. This leaves an open question on how to design a treatment for individual patient that can keep the same level of tumor control and reduce side effects. Previous efforts on boost strategies [5] and accelerated partial breast irradiation [6] demonstrate the potential benefits of modifying radiation dose distribution on patients. These provide the rationale to further investigate the way of optimizing treatment. However, little research has addressed this optimization issue [7,8], and most of the existing research focused on radiotherapy only instead of modeling the whole treatment process which consists of surgery, radiotherapy and systemic therapy. Therefore, in this thesis, we developed a risk modeling framework to model the outcome of breast conserving therapy. Consequently, using the developed framework, we could compare the current uniform dose strategy and a ‘dose-painting’ strategy.

Risk Modeling

Researchers and clinicians are increasingly interested in mathematical models designed to predict the outcome of cancer treatment [9]. As the number and sophistication of risk prediction models have grown, so has need in ensuring that they are correctly developed, and rigorously evaluated [10,11]. The National Cancer Institute (NCI) has identified ‘risk prediction’ as an area of extraordinary opportunity in “The Nation’s Investment in Cancer Research” [12].

Many of new models combine clinical and epidemiologic risk factors with new biologic, pathologic and genetic data to more accurately assess cancer risk in cohort studies [13–16]. These allow researchers to obtain baseline hazard of incidence, hazard of mortality from competing risks, and relative risk. However, cohort studies often focus on specific populations, lack covariate data, require long follow-up times, and collect only imprecise data on competing causes of death [17–20]. Sampling from a cohort (e.g., Chapter 3) to estimate relative risks and cumulative hazards with case–control designs can compensate for some of these limitations [21].

Discussion

Another strategy is to combine the trial outcome data with national registry data [22] (Chapter 4) for developing risk prediction models. This strategy can provide detailed information on risk predictors efficiently. Several of these studies can be combined to obtain a relative risk model. Disadvantages of this approach are the difficulties of matching the characteristics of cohorts and the lack of national registry data for many detailed treatment information.

The absolute risks of local recurrence in the breast cancer trials [23] or the absolute benefits and hazards of radiotherapy in these trials cannot be generalized easily because of changes in practice since the trials began [24–26]. Nevertheless, the quantitative relationship in these trials between local disease control and 15-year breast cancer mortality should still be relevant to current and future treatment decisions [4]. Where it is possible to estimate the absolute risk of a particular type of local recurrence after a particular type of surgery, it is also possible to estimate the absolute reduction in this risk that effective radiotherapy would achieve (as radiotherapy halves the rate at which the disease recurs and reduces the breast cancer death rate by about a sixth [4]) or that would have been avoided by more extensive surgery (as surgery eliminates the possibility of recurrence in the excised tissue [25]).

In fact, there is no theoretical boundary to the accuracy of identifying and modeling risk [27]. The more predictable the risk is, the greater the rationale is for focusing prevention strategies on high-risk individuals. On the other hand, we can also design population-based strategies which are more appropriate for less predictable risks. As new risk factors are identified, investigators are unlikely to be able to rely on single, large data sources to devise improved risk prediction models. Information will need to be assembled from different sources. Validation will be important for these models. Careful thoughts, appropriate conditions and model limitations should be aware by clinicians and researchers when they want to apply risk models in practice.

We developed a risk modeling framework for simulating breast conserving therapy in this thesis and established the relationship between microscopic disease, surgical

margin, radiation dose and tumor control probability through a quantitative model (Chapter 4). Sequentially we applied this framework to analyze the effect of age and provided insights of the inferior outcome in younger patients which is explained by larger total microscopic disease quantity and larger clonogenic cell fraction; even though microscopic disease cells in the younger patients seem more radiosensitive (Chapter 5). Compared to the case-control model in Chapter 3, the structural modeling framework provides more prediction power and feasibility in understanding the tumor control outcome of treatments.

Treatment Planning

Radiation therapy is often a double-edged sword. Radiation is usually given to destroy any cancer cells that may have been left behind after a breast tumor is surgically removed. But if there is evidence the disease has spread regionally — to the chest wall and nearby lymph nodes — the chest and multiple nodes must be targeted while minimizing the dose to the lungs and heart. Too much radiation to the lungs for the purpose of the dose coverage for breast can cause an inflammatory condition known as pneumonitis, while in the heart it can cause thickening and stiffness of muscle tissue and connecting arteries, increasing the risk of heart disease [28].

It is well known that radiation boost leads to improved local control in all age groups [3]. However, an increased risk of fibrosis due to radiation boost was also observed in large trials [29]. Tools were developed for clinician to assist decision making whether to deliver a radiation boost or not to an individual patient [26,29]. Typically boost dose is delivered to the tumor bed where tumorous cells locate densely. The clinical observations that most of the local recurrences occur at the original tumor site provide a good rationale to further optimize radiation dose profile by taking into account the inhomogeneous distribution of tumor cells.

Accelerated partial-breast irradiation (APBI) is a new treatment strategy that ultimately demonstrates long-term effectiveness and safety comparable to that of whole-breast irradiation for selected patients with early breast cancer [6]. However, no further

Discussion

agreement exists on the critical metrics in medical practice for preferred technique or classifying patients. Clinicians and oncologists could apply brachytherapy, external beam RT, intraoperative RT or the combination of those [30]. This introduces a pressing need on modeling the recurrence risk of different treatments and optimizing dose distributions for improving outcome of tumor control and/or reducing side-effects.

In this thesis, we utilized the risk modeling framework and analyzed the ‘dose-painting’ benefit and identified the effect of target TCP and setup error on switching to the ‘dose-painting’ method from the ‘homogeneous dose’ method (Chapter 6). We explained the benefit of switching to ‘dose-painting’ strategy when the large systematic or random errors exist. As high risk patients have lower tumor control probability compared to low risk patients, we identified that adopting the ‘dose-painting’ strategy has more potential to improve the treatment outcome for high risk patients. The results can serve as a simple recipe for APBI in future research as we designed a method of applying non-homogeneous dose for treating breast cancer.

Clinical Decision Support

Beyond the research content of breast cancer, this thesis provides a good example of applying data and knowledge for supporting clinical decisions (i.e., modeling the outcome of treatment and comparing different treatment strategies). Clinical decisions that are routinely taken by healthcare providers are often based on clinical guidance and evidence-based rules derived from medical science. However, the lack of efficiency in care pushes healthcare organization turning to clinical decision support (CDS) systems [31]. CDS through the interpretive analysis of large-scale patient data with intelligent and knowledge-based methods, “allow doctors and nurses to quickly gather information and process it in various ways in order to assist with making diagnosis and treatment decision” [32]. CDS can be applied in healthcare in diverse areas such as the examination of data from diverse monitoring devices, analyses of patient and family history, reviews of common characteristics and trends in medical record databases, and treatment outcomes as the analysis framework we built in the thesis.

One concept that can help address current limitations in clinical practice is called personalized healthcare where the CDS researchers put much effort in. It is known that standard treatments for many diseases are not effective in all patients. Some patients receive no benefit from, and are possibly harmed by, routine interventions. With personalized healthcare, we learn enough about a patient, and relevant healthcare information, to help make choices that are more likely to benefit that patient. For example, if we can predict which cancer patient needs a different therapy then we may improve outcomes and save money by not employing an ineffective or potentially dangerous treatment. A concomitant of personalized healthcare is the need to make evidence-supported decisions. We can only transform healthcare if we can effectively use all the information available to us to make better decisions. Although personalized healthcare is often discussed in the context of genomics, the idea is more than 40 years old and much broader than just genomics [33]. Using existing information, whether it is captured in a medical record, a research journal, or a gene sequence is the way of applying personalized healthcare. Compounding the fast development of information technology, operational data is accumulated in organizations and the size of data becomes enormous. Using analytics techniques such as text analytics [34], machine learning [35], data mining [36], statistics [37], and natural language processing [38], researchers can analyze previously untapped data sources independent or together with their existing data to gain new insights resulting in significantly better and faster decisions.

Limitation & Future work

Due to the focus on risk modeling and treatment planning in this thesis, many recent developments in breast cancer treatment have not been addressed, e.g., oncoplastic surgery, chemoprevention, scintimammography, or targeted therapies. In fact, the absolute risk associated with a mutation in a genetic susceptibility gene is commonly calculated by use of pedigrees of families with many affected members [39,40]. Geneticists often correct for ascertainment by controlling for the family phenotypes or disease history. BRCA1 and/or BRCA2 mutation carriers and their families (e.g., age at diagnosis, cancer occurrence, tumor site, and prognosis) may contribute to the

Discussion

heterogeneity of the disease. Factors, such as smoking, reproductive history, other genotypes unlinked to BRCA gene status, and interactions among these factors, may also modify cancer risk.

In this thesis, we also made some simplifications in modeling the treatment, e.g., the microscopic disease distribution model, the surgical model and dose delivery which all are subject to geometric uncertainties. The microscopic disease distribution was taken as a one-dimensional half-Gaussian model due to the limitation of data sample number in the pathology data. We assumed an ellipsoid volume is removed with tumor and margins but in practice the surgeons might remove a half-elliptical cylinder volume in breast-conserving surgery. Moreover, in building prediction models, we assumed that the planned dose was delivered. In Chapter 6, we used a theoretical dose distribution instead a deliverable dose distributions. Caution is therefore needed for interpreting the findings. We expect more and more relevant data becoming available in future and the limitations in the current analysis can be addressed.

Reference

- [1] Ma J, Jemal A. Breast Cancer Statistics. In: Ahmad A, editor. Breast Cancer Metastasis Drug Resist., Springer New York; 2013, p. 1–18.
- [2] Cook NR, Rosner BA, Hankinson SE, Colditz GA. Mammographic screening and risk factors for breast cancer. *Am J Epidemiol* 2009;170:1422–32.
- [3] Bartelink H, Horiot J-C, Poortmans P, Struikmans H, van den Bogaert W, Barillot I, et al. Recurrence rates after treatment of breast cancer with standard radiotherapy with or without additional radiation. *N Engl J Med* 2001;345:1378–87.
- [4] Darby S, McGale P, Correa C, Taylor C, Arriagada R, Clarke M, et al. Effect of radiotherapy after breast-conserving surgery on 10-year recurrence and 15-year breast cancer death: meta-analysis of individual patient data for 10,801 women in 17 randomised trials. *Lancet* 2011;378:1707–16.
- [5] Bartelink H, Horiot J-C, Poortmans PM, Struikmans H, Van den Bogaert W, Fourquet A, et al. Impact of a higher radiation dose on local control and survival in breast-conserving therapy of early breast cancer: 10-year results of the randomized boost versus no boost EORTC 22881-10882 trial. *J Clin Oncol* 2007;25:3259–65.
- [6] Smith BD, Arthur DW, Buchholz TA, Haffty BG, Hahn CA, Hardenbergh PH, et al. Accelerated Partial Breast Irradiation Consensus Statement From the American Society for Radiation Oncology (ASTRO). *Int J Radiat Oncol* 2009;74:987–1001.

Chapter 7

- [7] Witte MG, van der Geer J, Schneider C, Lebesque J V, Alber M, van Herk M. IMRT optimization including random and systematic geometric errors based on the expectation of TCP and NTCP. *Med Phys* 2007;34:3544–55.
- [8] Jin J-Y, Kong F-M, Liu D, Ren L, Li H, Zhong H, et al. A TCP model incorporating setup uncertainty and tumor cell density variation in microscopic extension to guide treatment planning. *Med Phys* 2011;38:439.
- [9] Freedman AN, Seminara D, Gail MH, Hartge P, Colditz GA, Ballard-Barbash R, et al. Cancer Risk Prediction Models: A Workshop on Development, Evaluation, and Application. *JNCI J Natl Cancer Inst* 2005;97:715–23.
- [10] Walker JG, Licqurish S, Chiang PPC, Pirota M, Emery JD. Cancer risk assessment tools in primary care: a systematic review of randomized controlled trials. *Ann Fam Med* 2015;13:480–9.
- [11] Lee S-M, Park J-H, Park H-J. Implications of Systematic Review for Breast Cancer Prediction. *Cancer Nurs* 2008;31:E40–6.
- [12] National Cancer Institute. The nation's investment in cancer research. A plan and budget proposal for the fiscal year 2006. n.d.
- [13] Darabi H, Czene K, Zhao W, Liu J, Hall P, Humphreys K. Breast cancer risk prediction and individualised screening based on common genetic variation and breast density measurement. *Breast Cancer Res* 2012;14:R25.
- [14] Hüsing A, Canzian F, Beckmann L, Garcia-Closas M, Diver WR, Thun MJ, et al. Prediction of breast cancer risk by genetic risk factors, overall and by hormone receptor status. *J Med Genet* 2012;49:601–8.
- [15] van Zitteren M, van der Net JB, Kundu S, Freedman AN, van Duijn CM, Janssens ACJW. Genome-based prediction of breast cancer risk in the general population: a modeling study based on meta-analyses of genetic associations. *Cancer Epidemiol Biomarkers Prev* 2011;20:9–22.
- [16] Crooke PS, Justenhoven C, Brauch H, Dawling S, Roodi N, Higginbotham KSP, et al. Estrogen metabolism and exposure in a genotypic-phenotypic model for breast cancer risk prediction. *Cancer Epidemiol Biomarkers Prev* 2011;20:1502–15.
- [17] Lee E-O, Ahn S-H, You C, Lee D-S, Han W, Choe K-J, et al. Determining the main risk factors and high-risk groups of breast cancer using a predictive model for breast cancer risk assessment in South Korea. *Cancer Nurs* 27:400–6.
- [18] Dai J, Hu Z, Jiang Y, Shen H, Dong J, Ma H, et al. Breast cancer risk assessment with five independent genetic variants and two risk factors in Chinese women. *Breast Cancer Res* 2012;14:R17.
- [19] Ueda K, Tsukuma H, Tanaka H, Ajiki W, Oshima A. Estimation of individualized probabilities of developing breast cancer for Japanese women. *Breast Cancer* 2003;10:54–62.
- [20] Boyle P, Mezzetti M, La Vecchia C, Franceschi S, Decarli A, Robertson C. Contribution of three components to individual cancer risk predicting breast cancer risk in Italy. *Eur J Cancer Prev* 2004;13:183–91.

Discussion

- [21] Greenland S. Model-based estimation of relative risks and other epidemiologic measures in studies of common outcomes and in case-control studies. *Am J Epidemiol* 2004;160:301–5.
- [22] Pfeiffer RM, Park Y, Kreimer AR, Lacey J V., Pee D, Greenlee RT, et al. Risk Prediction for Breast, Endometrial, and Ovarian Cancer in White Women Aged 50 y or Older: Derivation and Validation from Population-Based Cohort Studies. *PLoS Med* 2013;10:e1001492.
- [23] van der Leij F, Elkhuizen PHM, Bartelink H, van de Vijver MJ. Predictive factors for local recurrence in breast cancer. *Semin Radiat Oncol* 2012;22:100–7.
- [24] Fisher B, Anderson S. Twenty-year follow-up of a randomized trial comparing total mastectomy, lumpectomy, and lumpectomy plus irradiation for the treatment of invasive breast cancer. *N Engl J Med* 2002;347:1233–41.
- [25] Litière S, Werutsky G, Fentiman IS, Rutgers E, Christiaens M-R, Van Limbergen E, et al. Breast conserving therapy versus mastectomy for stage I-II breast cancer: 20 year follow-up of the EORTC 10801 phase 3 randomised trial. *Lancet Oncol* 2012;13:412–9.
- [26] Werkhoven E Van, Hart G, Tinteren H Van, Elkhuizen P, Collette L, Poortmans P, et al. Nomogram to predict ipsilateral breast relapse based on pathology review from the EORTC 22881-10882 boost versus no boost trial. *Radiother Oncol* 2011;100:101–7.
- [27] Begg CB, Zabor EC, Bernstein JL, Bernstein L, Press MF, Seshan VE. A conceptual and methodological framework for investigating etiologic heterogeneity. *Stat Med* 2013;32:5039–52.
- [28] Darby SC, McGale P, Taylor CW, Peto R. Long-term mortality from heart disease and lung cancer after radiotherapy for early breast cancer: prospective cohort study of about 300,000 women in US SEER cancer registries. *Lancet Oncol* 2005;6:557–65.
- [29] Collette S, Collette L, Budiharto T, Horiot J-C, Poortmans PM, Struikmans H, et al. Predictors of the risk of fibrosis at 10 years after breast conserving therapy for early breast cancer: a study based on the EORTC Trial 22881-10882 “boost versus no boost”. *Eur J Cancer* 2008;44:2587–99.
- [30] Offersen B V., Overgaard M, Kroman N, Overgaard J. Accelerated partial breast irradiation as part of breast conserving therapy of early breast carcinoma: a systematic review. *Radiother Oncol* 2009;90:1–13.
- [31] Kawamoto K, Houlihan CA, Balas EA, Lobach DF. Improving clinical practice using clinical decision support systems: a systematic review of trials to identify features critical to success. *BMJ* 2005;330:765.
- [32] Salem H, Attiya G, El-Fishawy N. A Survey of Multi-Agent based Intelligent Decision Support System for Medical Classification Problems. *Int J Comput Appl* n.d.;123:20–5.
- [33] Kohn MS, Sun J, Knoop S, Shabo A, Carmeli B, Sow D, et al. IBM’s Health Analytics and Clinical Decision Support. *Yearb Med Inform* 2014;9:154–62.

Chapter 7

- [34] Miner G. Practical Text Mining and Statistical Analysis for Non-structured Text Data Applications. Academic Press; 2012.
- [35] Bishop CM. Pattern recognition and machine learning. springer; 2006.
- [36] Han J, Kamber M, Pei J. Data Mining: Concepts and Techniques: Concepts and Techniques. Elsevier; 2011.
- [37] Kirkwood BR. Essentials of medical statistics. 1988.
- [38] Manning CD, Schütze H. Foundations of Statistical Natural Language Processing. MIT Press; 1999.
- [39] Tyrer J, Duffy SW, Cuzick J. A breast cancer prediction model incorporating familial and personal risk factors. Stat Med 2004;23:1111–30.
- [40] Anderson DE, Badzioch MD. Risk of familial breast cancer. Cancer 1985;56:383–7.

Discussion

Summary

Predicting the outcome of the treatment is important, however, difficult. Especially, a typical randomized control trial takes about 10 years in order to compare the long-term outcome of different treatments. In this thesis, I demonstrated a risk modeling framework which predict the treatment outcome and has added value to the current practice of breast conserving therapy. Further, I applied the analytics framework in planning new type of treatments.

Specifically in this thesis, I explained why surgical resection margin is not recognized as a prognostic factor in breast-conserving therapy and why doctors reported different results in Chapter 3. The reason is that the impact of a negative margin width on local recurrence is limited due to the large variation of microscopic disease across patient population. Chapter 2 contains a complementary experiment to testify an important assumption in Chapter 3 that the distribution of *in-vivo* microscopic disease can be reliably estimated through *ex-vivo* breast specimen tissue. Unlike lung tissue, limited deformation of breast tissue was observed in our study. In Chapter 4, I built an analytical framework to estimate the outcome of breast-conserving therapy through simulations. I applied this framework to estimate the difference between younger and older patients in Chapter 5, and found that the higher local recurrence rate in younger patients could be explained by larger clonogenic tumor cell quantity, even though the tumor cells were found to be more radiosensitive. I also predicted the outcome of the Young-Boost trial as tumor control probability of 92% at 10 years using the same framework. In Chapter 6, I further developed this concept and estimated the benefit of switching to 'dose-painting' strategy from the current practice of using homogeneous dose. The overall tumor control probability of a patient population is significantly improved under the dose-painting plan compared to the homogeneous dose plan with the same mean dose. However, the adoption of dose-painting plan should depend on

target TCP and setup error in practice. Finally, I discussed state of the art of risk modeling and treatment planning methods, limitations of my thesis and future direction of research (decision support analytics) in Chapter 7.

List of Abbreviations

APBI	Accelerated partial-breast irradiation
BCS	Breast-conserving surgery
BCT	Breast-conserving therapy
CCF	Clonogenic cell fraction
CI	Confidence Interval
CTV	Clinical target volume
EBCTCG	Early Breast Cancer Trialists' Collaborative Group
EORTC	European Organization for Research and Treatment of Cancer
GTV	Gross tumor volume
ICRU	International Commission on Radiation Units and Measurements
LR	Local recurrence
MARGINS	Multi-modality Analysis and Radiological Guidance IN breast conServing therapy
MinSRM	Minimal surgical resection margin
MSD	Microscopic disease
NTCP	Normal tissue complication probability
PA-Grade	Histopathology grading
PTV	Planning target volume
RT	Radiation Therapy / Radiotherapy
RCTs	Randomized Controlled Trials
SD	Standard deviation
SRM	Surgical resection margin
TCP	Tumor control probability
WBI	Whole breast irradiation
WLE	Wide-local excision

List of Publications

PhD Study

Chen, Wei, Joep Stroom, Jan-Jakob Sonke, Harry Bartelink, Annemarie C. Schmitz, and Kenneth G. Gilhuijs. " Analysis of deformations between in-vivo and ex-vivo tissue around invasive breast cancer." *XVI International Conference on the Use of Computers in Radiation Therapy*, Amsterdam, 2010.

Chen, Wei, Joep Stroom, Jan-Jakob Sonke, Harry Bartelink, Annemarie C. Schmitz, and Kenneth G. Gilhuijs. "Impact of negative margin width on local recurrence in breast conserving therapy." *Radiotherapy and Oncology* 104, no. 2 (2012): 148-154.

Chen, Wei, Kenneth Gilhuijs, Joep Stroom, Harry Bartelink, and Jan-Jakob Sonke. "A simulation framework for modeling tumor control probability in breast conserving therapy." *Radiotherapy and Oncology* 111, no. 2 (2014): 289-295.

Stroom, Joep, Kenneth Gilhuijs, Sandra Vieira, **Wei Chen,** Javier Salguero, Elizabeth Moser, and Jan-Jakob Sonke. "Combined recipe for clinical target volume and planning target volume margins." *International Journal of Radiation Oncology* Biology* Physics* 88, no. 3 (2014): 708-714.

Chen, Wei, Jan-Jakob Sonke, Joep Stroom, Harry Bartelink, Marcel Verheij, and Kenneth Gilhuijs. "The effect of age in breast conserving therapy: A retrospective analysis on pathology and clinical outcome data." *Radiotherapy and Oncology* 114, no. 3 (2015): 314-321.

Chen, Wei, Joep Stroom, Kenneth Gilhuijs, Harry Bartelink, Marcel Verheij, and Jan-Jakob Sonke. "Towards dose-painting for microscopic disease: application to breast-conserving therapy." submitted to *Radiotherapy and Oncology*.

Master Study

Chen, Wei, Caifeng Shan, and Gerard De Haan. "Optimal regularization parameter estimation for spectral regression discriminant analysis." *Circuits and Systems for Video Technology, IEEE Transactions on* 19, no. 12 (2009): 1921-1926.

Shan, Caifeng, and **Wei Chen**. "Head pose estimation using spectral regression discriminant analysis." *In Computer Vision and Pattern Recognition Workshops, 2009. CVPR Workshops 2009*. IEEE Computer Society Conference on, pp. 116-123. IEEE, 2009.

Acknowledgement

The decision of embarking on a Ph.D. journey is definitely a pivotal point in my life. While the destination may at first seem to be a distant and vague dot on the horizon, the journey itself is full of adventures and discoveries, which also lead to much joy and excitement. Many people have helped shape the destination of my Ph.D. journey, to whom I will always feel grateful.

First and foremost, I would like to thank my promoters Prof.dr. Harry Bartelink and Prof.dr. Marcel Verheij, as well as my co-promoters Dr. Jan-Jakob Sonke and Dr. Kenneth Gilhuijs for their continuous support and guidance through my Ph.D. trajectory. Harry, thank you for introducing me to the field. I always enjoyed our discussions, which not only offered me valuable knowledge but also triggered my critical thinking. Thank you for teaching me the three research principles: “Is it new?”, “Is it true?”, and “So what?”. I will keep them in mind for my future academic journey. Marcel, thank you for allowing me to follow my own path and encouraging me to set up my own research agenda. Also, thanks for creating such great working environment where people can grow and learn from each other. I truly enjoyed working in your department. Jan-Jakob, you have constantly amazed me with your insightful feedback despite your own hectic schedule. Thanks for all the challenging questions that pushed me thinking forward. Kenneth, thank you for helping me initiate the PhD project and offering me a systematic way to conduct research. I am so grateful that you stay on board with me, despite the physical distance between Amsterdam and Utrecht.

I would also like to express my gratitude towards the members of my doctoral committee. Thank you for taking the time to review my thesis and providing feedback. I am honored to have you as my opponents.

This thesis would have not reached the current level of quality without the involvement of the larger scientific community. I am thankful for the conference participants at ICCR2010, AAPM2012, as well as review teams of Radiotherapy and Oncology that have provided valuable feedback on my research. To this point, I would like to express my special thanks to one of my favorite co-authors, Dr. Joep Stroom. Joep, thanks for your spot-on feedback and thanking you for sending us the sunshine from Lisbon whenever needed.

Another crucial enabler for this thesis has been the generous support of various organizations. I would like to express my gratitude to the Center for Translational Molecular Medicine (CTMM), the Netherlands Cancer Institute (NKI), VU University Medical Center (VUmc), and the Onderzoekschool Oncologie Amsterdam oncology graduate program (OOA).

An inspiring and pleasant working environment has helped me to grow over the years of the PhD trajectory. In this respect, I have been fortunate to work with a bunch of amazing fellow PhDs and Postdocs: Hua, Chun, Alize, Ale, Angelo, Anja, Barbara, Hanno, Igor, Jasper, Javier, Johan, Lennert, Maddalena, Marcel, Marnix, Matthijs, Natascha, Peter, Roel, Sander, Simon, Suzanne, Uros, Wilma, Xiangfei and Yenny. Without you, my PhD journey would be much of a solitary ride. Diedie, Patricia, Vera, and Lissy, thank you for the continuous administrative support.

My family deserves the deepest gratitude for their unconditional love and support in over the years. I am thankful to my parents-in-law for their constant help. Thank you for taking care of our small family during the busy seasons. My little boy, Julian, you have brought so much fun and joy to our family. Finally, I would like to express my great gratitude to my beloved wife. Yixin, you are the smartest girl I have ever met and I have learned a lot from you. Thanks for all the inspiring conversations and your endless patience. I look forward to our wonderful journey ahead.

Wei Chen

Eindhoven, December 2015

Curriculum Vitae



Wei Chen, born in 1987, investigated the causal factors that predict the treatment outcome for breast cancer patients with statistical modeling methods. He also optimized treatment planning strategy to improve the performance of plan under patient/system uncertainties. He developed a 3D/2D image registration framework with Python and created a manifold method (Machine Learning) to improve the efficiency of the compressed-sensing based inverse planning technique.

Prior to NKI, Wei was a research assistant in Philips Research Europe and Microsoft Zhejiang University Lab. His work was closely related to data mining and image analysis for computer vision tasks. Prior to that, he was selected in Young Talent Class and entered Zhejiang University at the age of 15.

Wei has a deep knowledge of optimization, statistics, mathematical modeling and image analysis in both consumer electronics domain and healthcare domain. Since May 2014, Wei joined Philips as a scientist and participated in various projects related to patient monitoring, mobile digital solution and personal health. He published 4 research papers in top journals of Radiation Oncology, 1 paper in *Circuits and Systems for Video Technology*, and 1 full paper and 1 extended abstract on the leading conferences. He also filed 4 patent applications in the area of consumer / healthcare electronics.